Precambrian Research 358 (2021) 106138

Contents lists available at ScienceDirect

Precambrian Research

journal homepage: www.elsevier.com/locate/precamres

Neoproterozoic stratigraphy of the Southwestern Basement Province, Svalbard (Norway): Constraints on the Proterozoic-Paleozoic evolution of the North Atlantic-Arctic Caledonides

Virginia T. Wala [a], Grzegorz Ziemniak [b], Jaroslaw Majka [b,c], Karol Faehnrich [a], William C. McClelland [d], Edward E. Meyer [a], Maciej Manecki [b], Jakub Bazarnik [e], Justin V. Strauss [a,*]

[a] Department of Earth Sciences, Dartmouth College, HB6105 Fairchild Hall, Hanover, NH 03755, USA
[b] Faculty of Geology, Geophysics and Environmental Protection, AGH – University of Science and Technology, al. Mickiewicza 30, 30 059 Kraków, Poland
[c] Department of Earth Sciences, Uppsala University, Villavägen 16, 752 36 Uppsala, Sweden
[d] Department of Earth and Environmental Sciences, University of Iowa, Iowa City, IA 52242, USA
[e] Polish Geological Institute-National Research Institute, Carpathian Branch, Skrzatów 1, 31 560 Kraków, Poland

ARTICLE INFO

Keywords:
Svalbard
Southwestern Basement Province
Wedel Jarlsberg Land
Oscar II Land
Caledonian Orogeny
Neoproterozoic
Terrane
Detrital zircon geochronology

ABSTRACT

The Arctic archipelago of Svalbard, Norway, plays an important role in tectonic reconstructions of the Cambrian–Devonian Caledonian orogen in the North Atlantic and circum-Arctic regions. To elucidate the Proterozoic geological history of the Southwestern Basement Province of Svalbard and place its origin and displacement history in the context of regional tectono-stratigraphic events, we present new geological mapping, stratigraphic assignments, carbonate carbon ($\delta^{13}C_{carb}$) and strontium ($^{87}Sr/^{86}Sr$) isotope chemostratigraphy, and detrital/igneous zircon U-Pb geochronology coupled with Hf isotope geochemistry from Neoproterozoic rocks exposed in southwestern Spitsbergen. The examined metasedimentary successions include a Tonian mixed carbonate-siliciclastic succession (the Nordbukta/Deilegga groups) that is regionally truncated by a Cryogenian (<650 Ma) angular unconformity (the Torellian unconformity), the age of which is confirmed herein by field relationships and re-analysis of previously reported detrital monazite data. New detrital zircon U-Pb data from the Nordbukta Group yield ca. 1030–1170, 1280–1400, 1430–1510, and 1580–1680 Ma age populations that are typical of North Atlantic (e.g., North and East Greenland, Scotland, and the Scandinavian Caledonides) Mesoproterozoic-Neoproterozoic sedimentary successions. Overlying Cryogenian–Ediacaran strata of the Sofiebogen, Dunderbukta, and Kapp Lyell (Bellsund) groups record rift-related sedimentation and host chemostratigraphic data that provide ties to the ca. 640(?)–635 Ma Marinoan snowball Earth glaciation. Detrital zircon U-Pb data from the Cryogenian Slyngfjellet, Jens Erikfjellet, and Konglomeratfjellet formations yield similar age spectra to the underlying Nordbukta and Deilegga groups, while younger Ediacaran strata of the Höferpynten and Gåshamna formations record a prominent shift to bimodal ca. 1850 and 2850 Ma U-Pb age populations. Integrating these data with previously published geochemical and geochronological datasets from Svalbard and other circum-Arctic Mesoproterozoic–Neoproterozoic successions, we propose that the Southwestern Basement Province represents a composite terrane composed of multiple peri-Baltican (Wedel Jarlsberg-Oscar II, Berzeliuseggene-Eimfjellet, and Prins Karls Forland terranes) and peri-Laurentian (Hornsund terrane) crustal fragments that were likely initially juxtaposed and/or amalgamated during the Caledonian orogeny. These terranes were subsequently complexly deformed and modified during the younger Devonian-Carboniferous Ellesmerian and Paleogene-Eocene Eurekan orogenic events that affected western Svalbard.

1. Introduction

Neoproterozoic sedimentary and volcanic successions in the North Atlantic region provide a fragmented record of the assembly and breakup of the supercontinent Rodinia (Fig. 1; e.g., Gee et al., 1995; Cawood et al., 2001, 2007, 2010, 2016; Gee and Pease, 2004; Nystuen et al., 2008; Pease et al., 2008; Lorenz et al., 2012; Corfu et al., 2014; Kjøll et al., 2019; Gee and Stephens, 2020; Gumsley et al., 2020). These

* Corresponding author.
E-mail address: justin.v.strauss@dartmouth.edu (J.V. Strauss).

https://doi.org/10.1016/j.precamres.2021.106138
Received 29 September 2020; Received in revised form 1 February 2021; Accepted 4 February 2021

successions were variably metamorphosed during the Cambrian–Devonian Caledonian orogeny, which deformed the Neoproterozoic–early Paleozoic continental margins of northeastern Laurentia and western Baltica (present coordinates) and both collated and dispersed continental and arc crustal fragments within the North Atlantic and circum-Arctic regions (e.g., Harland, 1997; Gee and Teben'kov, 2004; Gee and Pease, 2004; Gee et al., 2008; Colpron and Nelson, 2009; Miller et al., 2011, 2018; Pease, 2011; Corfu et al., 2014; Beranek et al., 2015; Strauss et al., 2017; Slagstad et al., 2020). Uncertainties in the tectonic evolution and displacement histories of these peri-Laurentian and peri-Baltican crustal fragments have hindered regional tectonic and paleogeographic reconstructions of the circum-Arctic (e.g., Cawood et al., 2010; Pease, 2011; Lorenz et al., 2012; McClelland et al., 2019).

Svalbard's position at the northernmost exposed extent of the Caledonian orogen makes it important for elucidating Proterozoic-Paleozoic tectonic reconstructions of the North Atlantic-Arctic Caledonides (Fig. 1). Differences in the geological character of Svalbard's pre-Devonian basement led previous workers to define three general regions – the Western, Central, and Eastern terranes (e.g., Harland, 1971; Harland and Wright, 1979) or the Southwestern, Northwestern, and Northeastern basement provinces (e.g., Gee et al., 2008; Dallmann, 2015a) – that are juxtaposed along major N-S-trending fault zones (e.g., Harland, 1997). Based on gross stratigraphic, geochronological, geochemical, and paleontological constraints, most of Svalbard's pre-Devonian bedrock has Laurentian affinities (see review in Harland, 1997); yet, some units, particularly within the Southwestern Basement Province (SBP), appear to be linked to Baltica based on recent geochronological and metamorphic datasets (Gee and Teben'kov, 2004; Gasser and Andresen, 2013; Majka et al., 2014, 2015). For example, some of these recent studies (Majka et al., 2008, 2010, 2014, 2015; Mazur et al., 2009; Majka and Kośmińska, 2017) have emphasized magmatic and metamorphic linkages between Neoproterozoic igneous and metamorphic rocks of the SBP and the ca. 700–550 Ma Timanide orogen (*sensu lato*) of northern Baltica and northwestern Russia (Andreichev, 1998; Gee et al., 2000; Gee and Pease, 2004; Gee and Teben'kov, 2004; Larionov et al., 2004; Kuznetsov et al., 2007). Far fewer studies have focused on the depositional history and sedimentary provenance of Neoproterozoic metasedimentary successions in the SBP (Bjørnerud, 2010; Gasser and Andresen, 2013; Ziemniak et al., 2019), partially due to their complex stratigraphic relationships and pervasive metamorphic overprint. The main objectives of this contribution are to: (1) refine the age and tectonic setting of Neoproterozoic strata in the SBP; (2) determine the provenance of these metasedimentary units; and (3) evaluate the origin and displacement history of the SBP. Specifically, we place new detrital zircon U-Pb geochronology and Hf isotope geochemistry and carbonate carbon ($\delta^{13}C_{carb}$) and strontium ($^{87}Sr/^{86}Sr$) isotope chemostratigraphy into a revised tectono-stratigraphic framework for the SBP and propose a new model for its role in the tectonic evolution of the North Atlantic and circum-Arctic regions.

2. Geologic setting

Proterozoic and early Paleozoic metasedimentary and metaigneous basement of the SBP is exposed along the western coast of Spitsbergen and Prins Karls Forland, Svalbard, from Kongsfjorden to Sørkapp Land (Fig. 2). These units were complexly deformed in the early Paleozoic Caledonian orogeny as a result of closure of the Ediacaran–Cambrian Iapetus Ocean and far field deformation associated with terminal collision between Laurentia and Baltica (e.g., Harland, 1971, 1997; Bjørnerud et al., 1991; Manecki et al., 1998). The Caledonian Orogeny in Svalbard is polyphase in nature and includes both Middle-Late Ordovician to early Silurian metamorphism and deformation and late Silurian to Early Devonian ductile strike-slip displacement (see reviews in Harland, 1997, and Dallmann, 2015a). In the SBP, Caledonian deformation is manifest in the emplacement of high pressure metamorphic rocks and oceanic fragments, widespread greenschist-facies metamorphism of pre-Caledonian basement rocks, the development of a northwards-

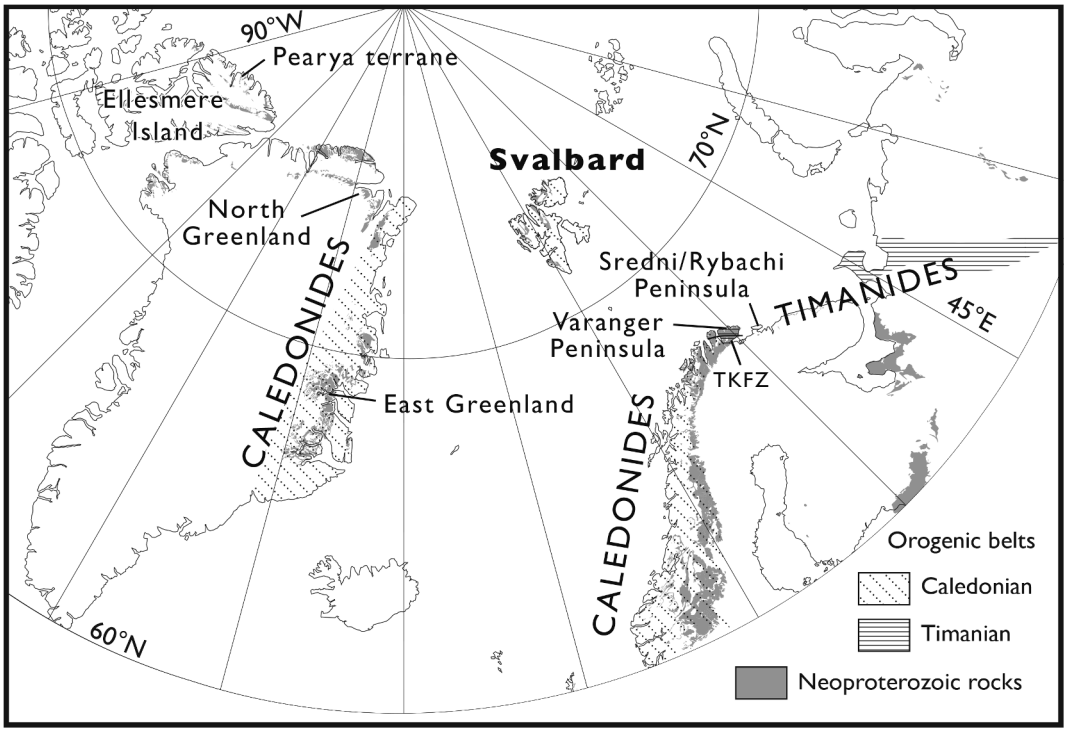

Fig. 1. Map of Neoproterozoic sedimentary and volcanic successions in the North Atlantic region adapted from Harrison et al. (2011). The accretionary Timanian orogen is exposed along the Varanger Peninsula of Scandinavia and the White Sea region of northwestern Russia. The Cambrian–Devonian Caledonian orogen formed by closure of the Iapetus Ocean and terminal collision between Laurentia and Baltica. Location of the Caledonian orogenic belt is adapted from Henriksen and Higgins (2008). TKFZ–Trollfjorden-Komagelva fault zone.

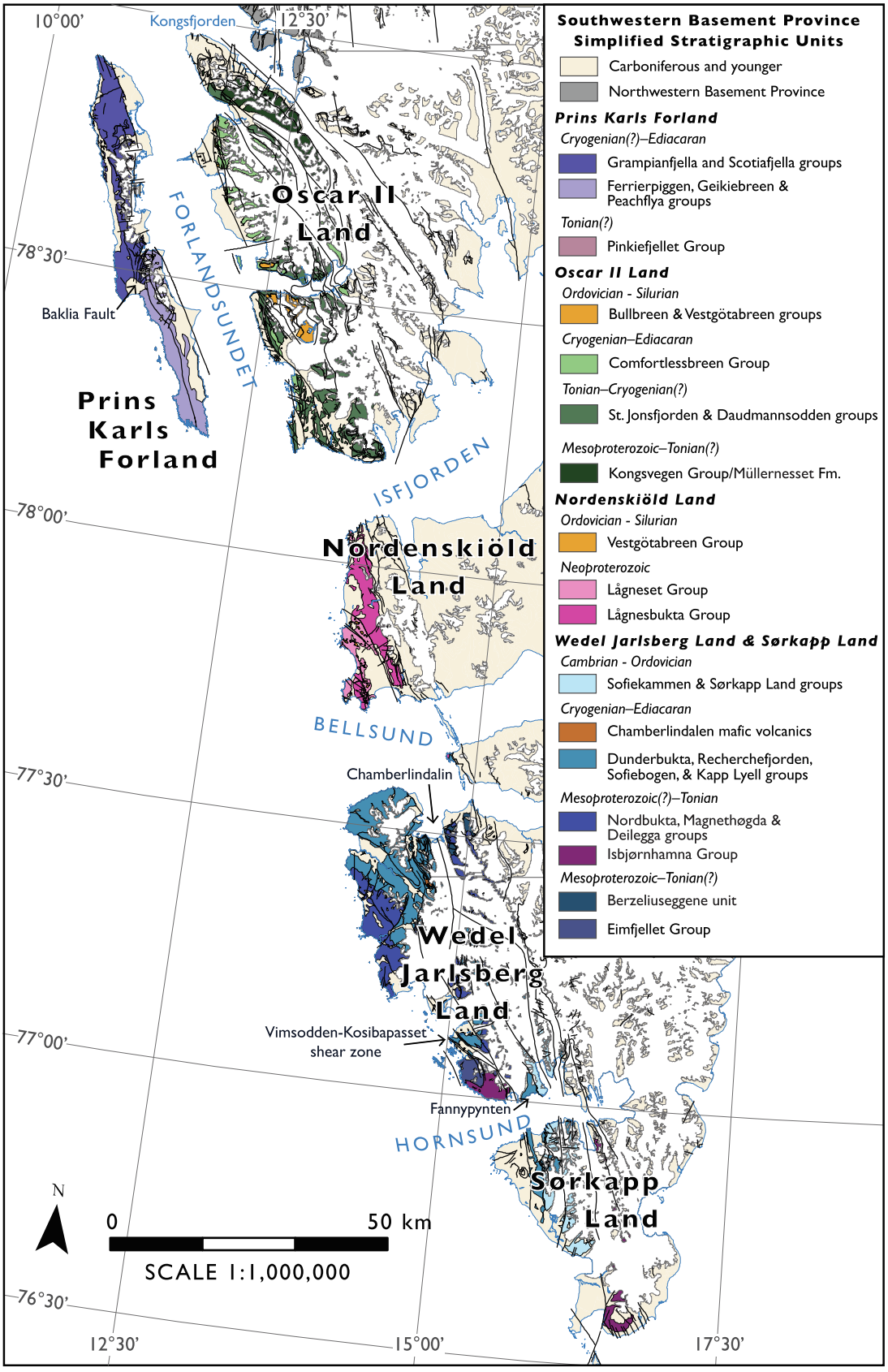

Fig. 2. Simplified geological map of the Southwestern Basement Province (SBP) of Svalbard, Norway, adapted from Dallmann (2015a). Frame indicates location of Fig. 5.

propagating (modern coordinates) fold-thrust belt, and late-stage displacement along sub-vertical ductile strike-slip shear zones (e.g., Harland et al., 1974; Hirajima et al., 1988; Czerny et al., 1993; Manecki et al., 1998; Agard et al., 2005; Labrousse et al., 2008; Mazur et al., 2009; Kośmińska et al., 2014; Majka et al., 2015; Faehnrich et al., 2020). Portions of the SBP were also affected by deformation and localized metamorphism associated with the Devonian–Carboniferous Ellesmerian orogeny (Piepjohn, 2000; Tessensohn, 2001; Kośmińska et al., 2014, 2020; Dallmann and Piepjohn, 2020). In addition, Paleogene-Eocene contractional and transpressional deformation associated with formation of the Eurekan West Spitsbergen Fold-and-Thrust Belt reactivated and overprinted these Caledonian and Ellesmerian structures (e.g., Birkenmajer, 1981; Dallmann et al., 1993a; Braathen et al., 1995; Hjelle et al., 1999; Bergh et al., 1997, 2000; Piepjohn et al., 2000; Dallmann, 2015b; Majka et al., 2015; Schneider et al., 2019), further complicating the underlying stratigraphic architecture of the SBP.

Due to this region's complex tectonic history, the general paucity of isotopically dateable lithologies, the significance of local sedimentary facies changes, and the bewildering array of nomenclatural schemes (e.g., Harland, 1997), stratigraphic correlations across different regions of the SBP remain complex and poorly understood (Dallmann, 2015a; Majka and Kośmińska, 2017; Ziemniak et al., 2019). The most fundamental and outstanding question is whether age-equivalent metasedimentary and metavolcanic units in the SBP belong to the same pre-Devonian continental basement or whether they represent independent terranes, or crustal fragments, that were juxtaposed during the Caledonian orogeny or younger deformational events (e.g., Dallmann, 2015a). Here, we summarize our recent field and analytical efforts that focused on the least deformed and well characterized portion of the SBP, which is exposed in Wedel Jarlsberg Land in southwestern Spitsbergen (Fig. 2). All of the Proterozoic rocks in this region have been affected by Ordovician–Silurian Caledonian greenschist facies metamorphism (e.g., Harland, 1997; Manecki et al., 1998; Mazur et al., 2009; Faehnrich et al., 2020).

2.1. Northern Wedel Jarlsberg Land and Nordenskiöld Land

Mesoproterozoic(?)–Neoproterozoic metasedimentary rocks are widely exposed in northwestern Wedel Jarlsberg Land and western Nordenskiöld Land (Figs. 2–5, S1; Krasil'ščikov and Kovaleva, 1979; Birkenmajer, 1981; Hjelle et al., 1986; Bjørnerud, 1990; Dallmann et al., 1990, 1993a; Harland et al., 1993; Dallmann, 2015a). The oldest succession in northern Wedel Jarlsberg Land, the Stenian(?)–Tonian Nordbukta Group (Kapp Berg, Evafjellet, Peder Kokkfjellet, Seljehaugfjellet, Trinutane, Thiisdalen, and Dordalen formations), consists of ~ 4 km of polydeformed quartzite, phyllite, and metacarbonate (Figs. 3, 4, S1; Bjørnerud, 1990; *see* Birkenmajer, 2010 for slightly different nomenclature). These strata were folded, uplifted, and eroded during the Cryogenian Torellian orogeny (Majka et al., 2014), which resulted in the development of a regional angular unconformity (Birkenmajer, 1975; Bjørnerud et al., 1990, 1991; Czerny et al., 1993). A minimum age constraint for the Torellian unconformity is provided by unpublished ca. 650 Ma detrital monazite grains in units overlying the unconformity (originally reported in Mazur et al., 2009; Czerny et al., 2010), as well as correlation to other Cryogenian metamorphic events in adjacent regions of Wedel Jarlsberg Land (Manecki et al., 1998; Majka et al., 2008, 2014, 2015).

Cryogenian–Ediacaran strata above the Torellian unconformity in northern Wedel Jarlsberg Land are exposed in a broad NW-trending syncline and separated into the western Dunderbukta and eastern Recherchefjorden groups and structurally overlying Kapp Lyell (or Bellsund) Group (Figs. 2, 3, 5, S1; Dallmann et al, 1990; Bjørnerud, 1990; Dallmann, 2015a). In the west, the basal Thiisfjellet Formation of the Dunderbukta Group is a highly localized gray- to orange-weathering sandy metadolostone interbedded with black pyritic metalimestone and quartz pebble metaconglomerate (Fig. 4; Bjørnerud, 1990). Where the Thiisfjellet Formation is absent, ~700–1600 m of matrix-supported metaconglomerate (Konglomeratfjellet Formation) outcrop directly above the Torellian unconformity and are dominated by pebble- to cobble-sized clasts of quartzite and doloboundstone (Bjørnerud, 1990). These rocks are sharply overlain by ~50–300 m of metacarbonate (Slettfjelldalen Formation) and ~1–2 km of phyllite (Dunderdalen Formation) that are locally interbedded with quartzite and metadolostone lenses (Bjørnerud, 1990).

To the east in the Chambelindalen region (Figs. 2, 5), poorly exposed phyllite of the Cryogenian–Ediacaran Recherchefjorden Group is locally intercalated with greenstone and intruded by alkaline mafic plutonic rocks (Fig. 3; Harland, 1978; Bjørnerud, 1990; Birkenmajer, 2010; Gołuchowska et al., 2016). These phyllitic rocks are locally associated with fault-bounded packages of the older Dunderbukta and Nordbukta groups (Dallmann et al, 1990; Birkenmajer, 2010; Dallmann, 2015a). Further east, these metasedimentary units of the Recherchefjorden and Nordbukta groups are complexly juxtaposed with early Neoproterozoic (ca. 950 Ma) felsic augen gneiss and metasedimentary rocks of the Berzeliuseggene unit (Metaigneous Unit) and Magnethøgda sequence (the latter was recently assigned to the Deilegga and Sofiebogen groups by Majka et al., 2015) along a poorly understood Caledonian and/or Eurekan(?) strike-slip fault beneath Recherchebreen glacier (Figs. 2, 3; Harland, 1978; Dallmann et al., 1993b; Majka et al., 2014, 2015; Dallmann, 2015a). The Berzeliuseggene unit was metamorphosed during both Torellian and early Caledonian events and subsequently affected by Eurekan contraction and strike-slip deformation (Majka et al., 2014, 2015).

The boundary between the uppermost Dunderbukta and Recherchefjorden groups and the structurally overlying Cryogenian(?)–Ediacaran Kapp Lyell Group (also referred to as the Kapp Lyell Sequence or Kapp Lyell Formation by Bjørnerud, 2010; Birkenmajer, 2010, or the Bellsund Group of Krasil'ščikov and Kovaleva, 1979; Dallmann, 2015a) is controversial. It has been mapped as a prominent folded Caledonian or Eurekan thrust (Figs. 2, 5; Dallmann et al, 1990; Dallmann, 2015a), a complex series of Caledonian or Eurekan faults of variable kinematics (Birkenmajer, 2010), or as a primary depositional contact (Bjørnerud, 2010). The Kapp Lyell Group comprises an ~3 km thick package of matrix-supported metaconglomerate (or diamictite) with minor phyllite and quartzite, and it has been previously subdivided into the Dundrabeisen, Logna, and Lyellstranda formations (Figs. 4, S1; Harland et al., 1993; Harland, 1997; see simple two-fold subdivision of the "Bellsund Group" in Dallmann, 2015a).

Cryogenian–Ediacaran phyllite, quartzite, metacarbonate, and matrix-supported metaconglomerate of the Lågnesbukta and Lågneset groups are exposed on both the northern and southern shores of Nordenskiöld Land (Figs. 2, 3, S2; Dallmann, 2015a) and have been loosely correlated with similar age rocks further south in Wedel Jarlsberg Land (Hjelle et al., 1986; Harland et al., 1993; Dallmann, 2015a). The depositional and structural relationships between these units on Nordenskiöld Land are poorly understood due to limited exposure in coastal strandflats (e.g., Harland et al., 1993), which has led to significant uncertainties in the stratigraphic architecture of this region (Fig. S3; Hjelle, 1962, 1969; Hjelle et al., 1986; Turchenko et al., 1983; Harland et al., 1993). Zircon analyzed from a granite clast in matrix-supported conglomerate of the Kapp Linné Formation (mapped as part of the Lågneset Group by Hjelle et al., 1986; Dallmann, 2015a) in northern Nordenskiöld Land yielded a U-Pb crystallization age of 973 ± 10 Ma with a 656 ± 5 Ma metamorphic rim (Larionov and Teben'kov, 2004). It is unclear if this unit is correlative with similar matrix-supported metaconglomerate of the Kapp Martin Formation (mapped as part of the Lågneset group by Dallmann, 2015a) in southern Nordenskiöld Land. In northern Nordenskiöld Land, these Cryogenian-Ediacaran rocks are in fault or depositional contact with units mapped as the Tonian St. Johnsfjorden and Daudmannsodden groups of Oscar II Land (Figs. 2, S3; Hjelle et al., 1986; Dallmann, 2015a). Both the Lågnesbukta and Lågneset groups are intruded by metabasite lenses that were

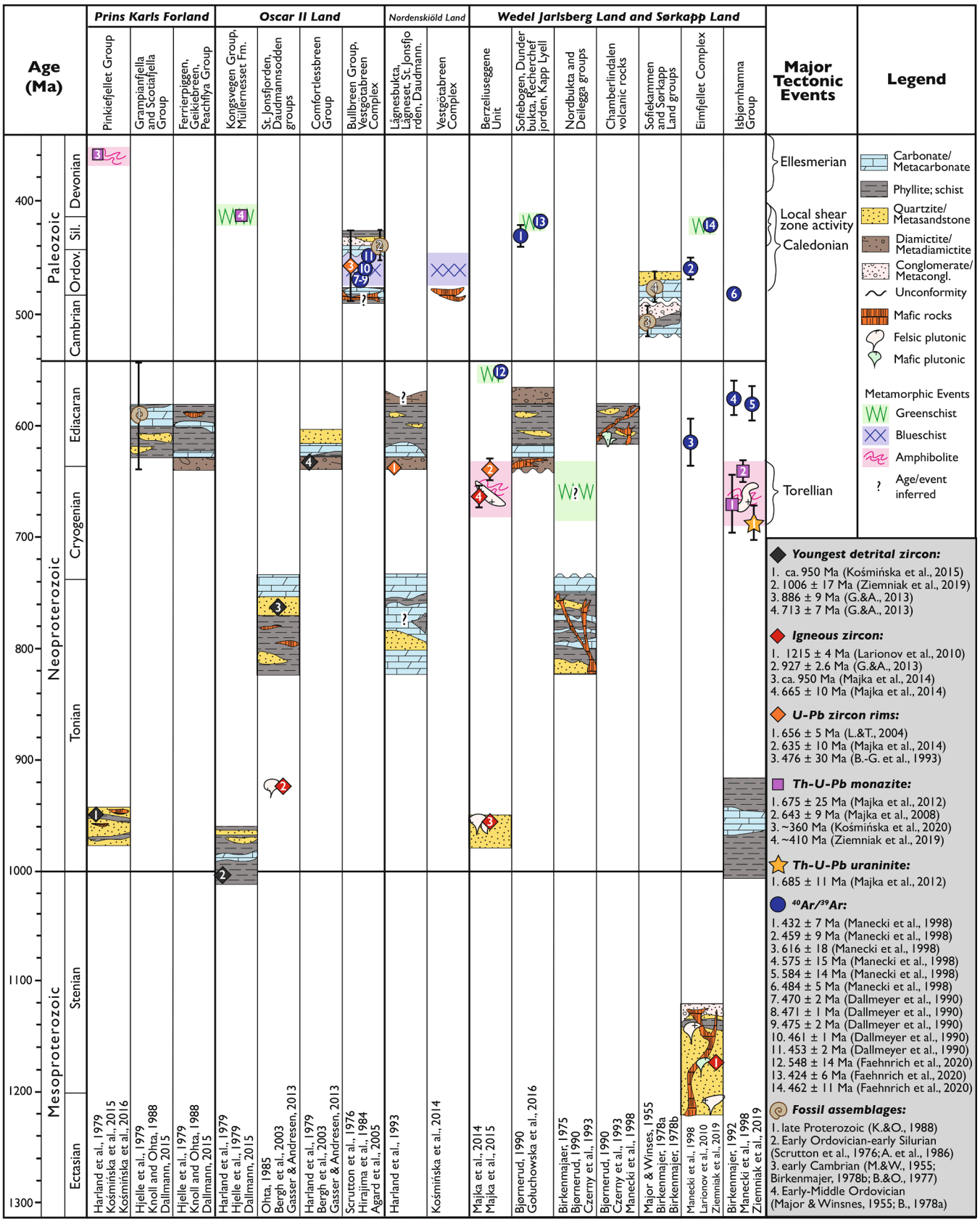

Fig. 3. Tectono-stratigraphy and published age constraints of the Southwestern Basement Province (SPB) of Svalbard, Norway. Map distribution of these units are shown in Figs. 2 and 5, and detailed unit descriptions are provided in the text. Note that many of these units have poorly constrained age ranges, so the boundaries shown here are schematic. Gp.–Group; Ordov.–Ordovician; Sil.–Silurian; Ect.–Ectasian; G.&A.–Gasser and Andresen; B.-G; Bernard-Griffiths; K.&O.–Knoll and Ohta; A.–Armstrong; M.&W.–Major and Winsnes; B.&O.–Birkenmajer and Orlowski; B.–Birkenmajer.

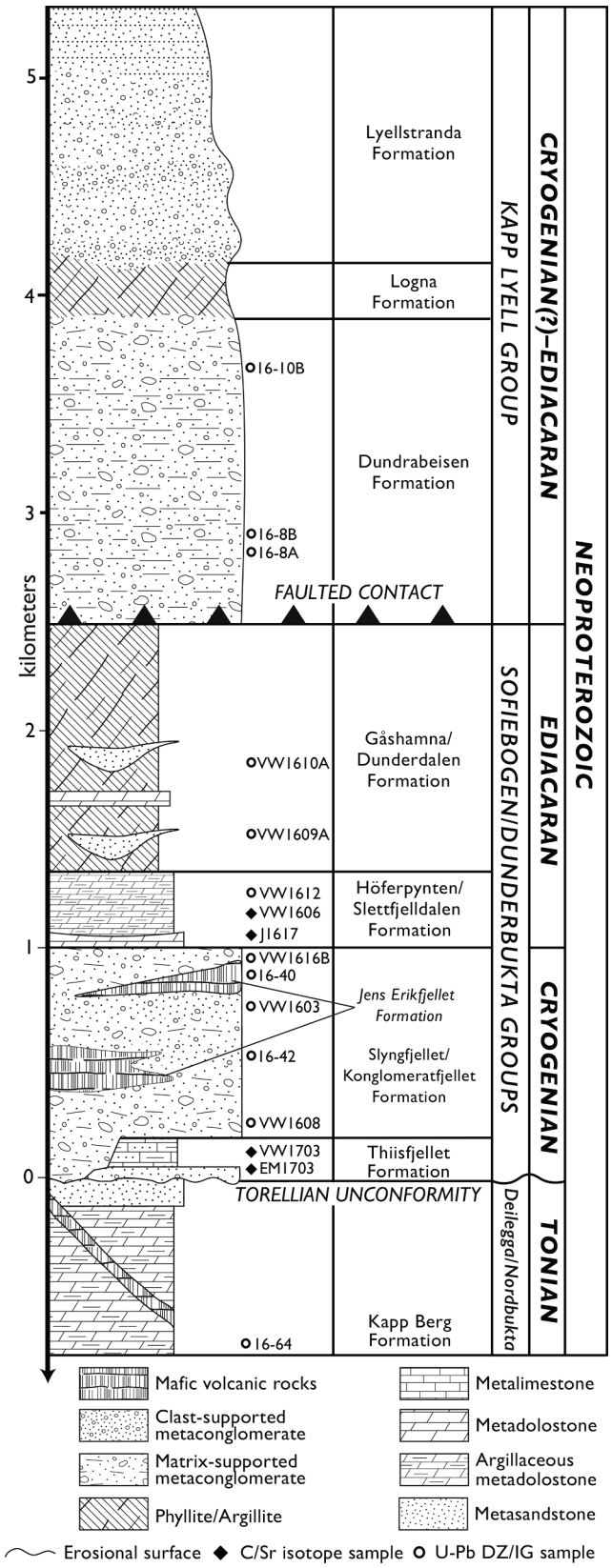

Fig. 4. Generalized stratigraphy of Neoproterozoic metasedimentary and metavolcanic rocks in northern and southern Wedel Jarlsberg Land, Svalbard. Sample locations are shown as approximate locations within the stratigraphy. Adapted from previous work by Birkenmajer (1975), Bjørnerud (1990), and Czerny et al. (1993), as well as our own field observations. DZ/IG–detrital zircon/igneous zircon.

metamorphosed under greenschist to blueschist conditions (Kosminska et al., 2014), similar to the Ordovician Vestgötabreen Complex of Oscar II Land (Barnes et al., 2020, and references therein).

2.2. Southern Wedel Jarlsberg Land and Sørkapp Land

The oldest known rocks of the SBP belong to the Mesoproterozoic Eimfjellet Complex and Neoproterozoic Isbjørnhamna Group, which are exposed in a fault-bounded region in southern Wedel Jarlsberg Land (Figs. 2, 3, 5, S3; Birkenmajer, 1992; Czerny et al., 1993; Balašov et al., 1995, 1996; Larionov et al., 2010; Ziemniak et al., 2019). The Eimfjellet Complex (Skjerstranda, Eimfjellbreane, Brattegdalen, Skålfjellet, Gullichsenfjellet, and Pyttholmen formations) consists of ca. 1200 Ma polydeformed metagabbro and metagranite with associated quartzite and schist that are intercalated with or cut by mafic dikes. The early Neoproterozoic (Tonian) Isbjørnhamna Group consists of schist, quartzite, and metacarbonate of the Skoddefjellet, Ariekammen, and Revdalen formations (Birkenmajer, 1992; Czerny et al., 1993; Ziemniak et al., 2019), which were also recently recognized on the southernmost tip of Sørkapp Land (Ziemniak et al., 2019). The Eimfjellet Complex and Isbjørnhamna Group were metamorphosed to amphibolite grade at ca. 640 Ma during the Torellian orogeny (Manecki et al., 1998; Majka et al., 2008, 2010, 2012; Larionov et al., 2010). The contact between the two units is mapped as a Caledonian thrust fault, although the detailed kinematics and timing of their juxtaposition is currently unknown and could be related to the Torellian event (Ziemniak et al., 2019). Both the Eimfjellet Complex and Isbjørnhamna Group are considered part of an independent crustal fragment separated on its eastern margin from the rest of the SBP by the Caledonian sinistral ductile Vimsodden-Kosibapasset shear zone (VKSZ) (Figs. 2, 5; Mazur et al., 2009; Ziemniak et al., 2019; Faehnrich et al., 2020).

Younger Neoproterozoic metasedimentary successions are widely exposed in central and southern Wedel Jarlsberg Land and across Hornsund in Sørkapp Land (Figs. 2–5, S1, S3; Czerny et al., 1993). Here, the Stenian(?)–Tonian Nordbukta Group equivalent is referred to as the Deilegga Group and is locally dominated by siliciclastic metasedimentary rocks of the Strypegga, Skilryggbreen, and Deilggbreen formations (Fig. S1; Czerny et al., 1993; see slightly different nomenclature summarized in Harland, 1997). In this region, the polydeformed Deilegga Group is overlain by the Cryogenian–Ediacaran Sofiebogen Group, which consists of a basal ~15–500 m thick unit of clast- and matrix-supported conglomerate (Slyngfjellet Formation) that directly overlies the Torellian unconformity (Fig. 4; Birkenmajer, 1992; Czerny et al., 1993). The Cryogenian Slyngfjellet Formation is locally overlain by or intercalated with ~30–120 m of schist, aphanitic metabasalt, and greenschist of the Jens Erikfjellet Formation, which has continental tholeiitic geochemical signatures and is locally fed by dikes and sills within the underlying Deilegga Group (Czerny et al., 1993; Czerny, 1999; Gołuchowska et al., 2012). Metaconglomerate of the Slyngfjellet Formation and local metavolcanic rocks of the Jens Erikfjellet Formation are sharply overlain by an ~5–100 m thick succession of metacarbonate referred to as the Höferpynten Formation (Birkenmajer, 1975; Czerny et al., 1993), the base of which commonly consists of a several m-thick yellow-weathering laminated metadolostone unit (Czerny et al., 1993). These metacarbonate rocks are overlain by the Gåshamna Formation, which consists of an ~2–2.5 km thick succession of black, green, and maroon phyllite with centimeter- to decameter-thick lenses of quartzite and metacarbonate (Fig. 4; Birkenmajer, 1992). In southwestern Wedel Jarlsberg Land and on northwestern Sørkapp Land, these units are overlain by or structurally juxtaposed with Cambrian–Ordovician carbonate rocks of the Sofiekammen and Sørkapp Land groups (Figs. 2, 3, S1, S3; Major and Winsnes, 1955; Birkenmajer, 1978a, 1978b; Harland, 1997). The contact between these early Paleozoic carbonate rocks and the Neoproterozoic Sofiebogen and Deilegga groups has been interpreted as both a profound unconformity ("Jarlsbergian unconformity" of Birkenmajer, 1991) and as a prominent Caledonian thrust fault (e.g.,

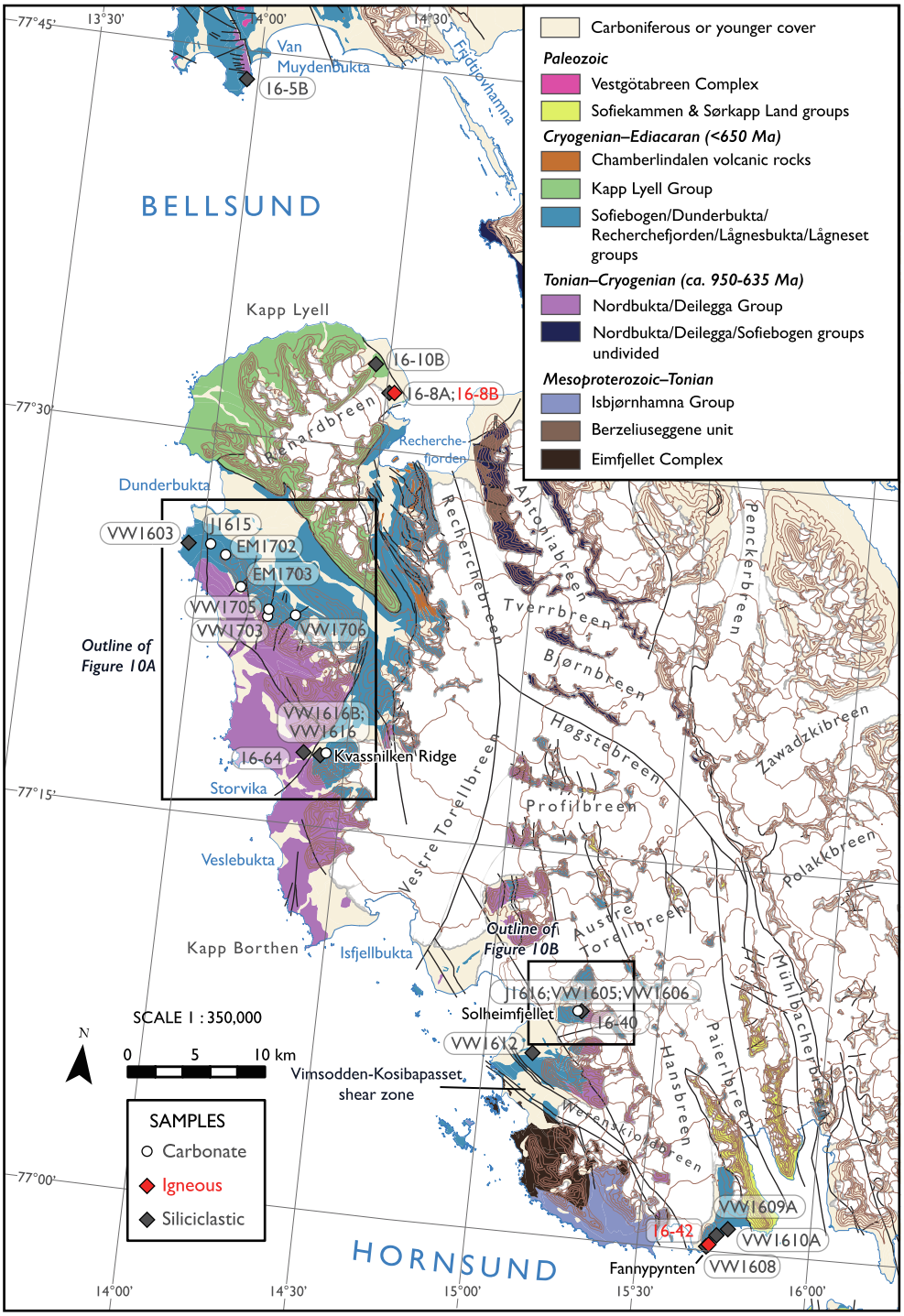

Fig. 5. Simplified geologic map of southernmost Nordenskiöld Land and Wedel Jarlsberg Land, Southwestern Basement Province (SBP), Svalbard. Mapping based on Dallmann et al. (1993b), Czerny et al. (1993), and our own field observations. Samples localities are shown on the map and listed in Table 1. Location of this figure is shown on Fig. 2 and frames indicate locations in Fig. 10. Gp–Group.

Mazur et al., 2009).

3. Methods

Geological mapping, sample collection, and measured stratigraphic sections were performed in Wedel Jarlsberg Land over three- to four-week field seasons in 2016 and 2017 and in Oscar II Land in 2017 (Fig. 5). Measured stratigraphic sections were logged at cm- to m-scale and sampled for isotopic analyses at m-scale. Carbonate carbon and oxygen ($\delta^{13}C_{carb}$, $\delta^{18}O_{carb}$) isotopic measurements were obtained at Dartmouth College on 176 samples from measured sections of the Dunderbukta and Sofiebogen groups (Table 1, S1). Major and trace element analyses and $^{87}Sr/^{86}Sr$ isotopic analysis were performed at the Yale Metal Geochemistry Center on 16 carbonate samples from three stratigraphic sections in Wedel Jarlsberg Land, two from the Thiisfjellet Formation (VW1703, EM1703) and one from the Höferpynten Formation (VW1606) (Table 1, S1). Detailed analytical methodologies are provided in the Supplementary Information.

To better constrain the provenance of metasedimentary rocks of the SBP, one sample from the Nordbukta Group (16-64), two samples from the Dunderbukta Group (VW1603, VW1616B), five samples from the Sofiebogen Group (VW1608, 16-40, VW1612, VW1610A, VW1609A), two samples from the Kapp Lyell Group (16-8A, 16-10B), and one sample from the Lågneset Group (16-5B) were collected and analyzed for detrital zircon U-Pb geochronology (Figs. 5, 6, 7, 8, 9; Table 1) via laser ablation-inductively coupled plasma mass spectrometry (LA-ICPMS) at the University of Arizona LaserChron Center in Tucson, Arizona, following methods outlined in Gehrels et al. (2006, 2008) and Gehrels and Pecha (2014). Two metaigneous clasts, one from the Slyngfjellet Formation (16–42; Sofiebogen Group) and one from the Dundrabeisen Formation (16-8B; Kapp Lyell Group), were also analyzed for igneous zircon U-Pb geochronology via secondary ion mass spectrometry (SIMS) at the Micro-Analyses Laboratory of the Polish Geological Institute – National Research Institute in Warsaw, Poland, following methods outlined in Williams and Claesson (1987) and Williams (1998). Hafnium isotopic data were acquired on a subset of detrital and igneous zircons (Table 1) at the University of Arizona LaserChron Center from the Nordbukta (16–64), Dunderbukta (VW1603), Sofiebogen (VW1608, VW1610A, VW1609A), and Kapp Lyell (16-8A) groups, as well as from both of the metaigneous clasts (16–42, 16-8B), following methods outlined in Gehrels and Pecha (2014). Detailed information and methodologies for these analytical sessions are provided in the Supplementary Information.

During filtering of acquired U-Pb data, we used the $^{206}Pb/^{238}U$ ratio to calculate an age for analyses younger than 1200 Ma and the $^{207}Pb/^{206}Pb$ result for analyses older than 1200 Ma following Strauss et al. (2019). Discordance in zircon has long been recognized (Wetherill, 1956) and presents a constant challenge for interpretation of detrital zircon data (Mezger and Krogstad, 1997). Reverse discordance ($^{206}Pb/^{238}U$ date > $^{207}Pb/^{206}Pb$ date) is typically an artifact of analytical procedure since Pb diffusion occurs at sub-micron scales (Mattinson et al., 1996) and Pb-gain through intragrain diffusion is rare (Corfu et al., 1994) but present in Archean grains (Kusiak et al., 2015; Valley et al., 2014; Wiemer et al., 2017). Normal discordance ($^{207}Pb/^{206}Pb$ > $^{206}Pb/^{238}U$ date) is much more common due the natural process of Pb-loss through metamictization, recrystallization, and fluid interaction during metamorphism and hydrothermal alteration (e.g., Rubatto, 2017). The effects of discordance can be pronounced in detrital zircon populations sourced from metamorphic terranes (e.g., McClelland et al., 2016) and samples that experienced post-depositional metamorphism (e.g., Gilotti et al., 2017). Nevertheless, there is useful information in normally discordant data; thus, for detrital samples we apply different filters of >5% reverse discordance and >10% normal discordance. Since discussion of the data below focuses on identification of reliable proportions of age groups to characterize the detrital zircon signature of regional sedimentary units rather than specific age groups to evaluate depositional ties with particular source regions, the 10% concordance filter is an appropriate tradeoff between compromised age interpretation and excessive data rejection (Gehrels, 2014). Comparison of 5%, 10%, and 15% normal discordance cutoffs (Fig. S4) demonstrates that the choice of this normal discordance filter in this particular dataset does not alter the position of the dominant age peaks discussed below. In addition, analyses that had >10% 2σ uncertainty in $^{206}Pb/^{238}U$ and $^{207}Pb/^{206}Pb$ ages are excluded following Gibson et al. (2021). Nevertheless, all analyses are reported in the Supplementary Information so changes in filtering criteria can be employed for future studies.

The peak age of the youngest detrital U-Pb age population that has greater than three zircon grains is considered herein as a conservative estimate for the maximum depositional age of the sample (Dickinson and Gehrels, 2009), although in many cases this overestimates the age based on other stratigraphic constraints. Zircon grains obtained from individual igneous clasts define a cogenetic population that is fundamentally different than detrital populations where individual grains have no demonstrable or justifiably assumed protolith relationship with other detrital grains. Thus, the concordance and uncertainty filters applied to the detrital zircon samples described above are not necessary in evaluation and interpretation of multiple analyses from a single magmatic sample. Data from the igneous samples were evaluated on the basis of mutually overlapping concordant analyses interpreted to best reflect the crystallization age of the igneous clasts (section 4.2.9).

Table 1
Sample Information.

Sample/Section Number	Stratigraphic Unit	Lithology	Latitude (N)*	Longitude (E)*	Types of Analyses	IGSN
Nordbukta Group						
16–64	Kapp Berg Formation	metasandstone	77.29800903	14.37492798	U-Pb, Hf	IEJVS000N
Dunderbukta/Sofiebogen Group						
EM1703	Thiisfjellet Formation	metalimestone	77.41518	14.41518	$\delta^{13}C$, $\delta^{18}O$, $^{87}Sr/^{86}Sr$	
VW1703	Thiisfjellet Formation	metalimestone	77.426089	13.961383	$\delta^{13}C$, $\delta^{18}O$, $^{87}Sr/^{86}Sr$	
VW1603	Konglomeratfjellet Formation	metasandstone	77.14864201	15.26787702	U-Pb, Hf	IEJVS000O
VW1616B	Konglomeratfjellet Formation	metasandstone	77.29792496	14.42391199	U-Pb	IEJVS000P
VW1608	Slyngfjellet Formation	metasandstone	77.00576099	15.70925203	U-Pb, Hf	IEJVS000Q
16–42	Slyngfjellet Formation	orthogneiss clast	77.00576099	15.70925203	U-Pb, Hf	IEJVS000R
16–40	Jens Erikfjellet Formation	metasandstone	77.14867101	15.27422396	U-Pb	IEJVS000S
J1615	Slettfjelldalen Formation	metadolostone	77.426357	14.025739	$\delta^{13}C$, $\delta^{18}O$	
EM1702	Slettfjelldalen Formation	metadolostone	77.4215	14.07246	$\delta^{13}C$, $\delta^{18}O$	
VW1705	Slettfjelldalen Formation	metadolostone	77.387218	14.221457	$\delta^{13}C$, $\delta^{18}O$	
VW1706	Slettfjelldalen Formation	metadolostone	77.387321	14.299952	$\delta^{13}C$, $\delta^{18}O$	
J1616	Höferpynten Formation	metadolostone	77.149169	15.255567	$\delta^{13}C$, $\delta^{18}O$	
J1617	Höferpynten Formation	metalimestone	77.149167	15.255567	$^{87}Sr/^{86}Sr$	
VW1605	Höferpynten Formation	metadolostone	77.148671	15.274224	$\delta^{13}C$, $\delta^{18}O$	
VW1606	Höferpynten Formation	metalimestone	77.149167	15.255567	$\delta^{13}C$, $\delta^{18}O$, $^{87}Sr/^{86}Sr$	
VW1612	Höferpynten Formation	metasandstone	77.11653303	15.15162497	U-Pb	IEJVS000T
VW1616	Höferpynten Formation	metadolostone	77.297925	14.423912	$\delta^{13}C$, $\delta^{18}O$	
VW1609A	Gåshamna Formation	metasandstone	77.00686798	15.71513697	U-Pb, Hf	IEJVS000U
VW1610A	Gåshamna Formation	metasandstone	77.01569396	15.75941999	U-Pb, Hf	IEJVS000V
Lågneset Group						
16-5B	Kapp Martin Formation	metasandstone	77.73196396	13.966074	U-Pb	IEJVS000W
Kapp Lyell Group						
16-8A	Dundrabeisen Formation	metasandstone	77.53870603	14.50319901	U-Pb, Hf	IEJVS000X
16-8B	Dundrabeisen Formation	metagabbro clast	77.53870603	14.50319901	U-Pb, Hf	IEJVS000Y
16-10B	Dundrabeisen Formation	metasandstone	77.55446501	14.460327	U-Pb	IEJVS000Z

Note: Abbreviations for types of analyses: U-Pb–U-Pb zircon geochronology; Hf–Lu-Hf isotopes on zircon; $^{87}Sr/^{86}Sr$–carbonate strontium isotopes
$\delta^{13}C$–carbonate carbon isotopes; $\delta^{18}O$–carbonate oxygen isotopes; *Datum: WGS84

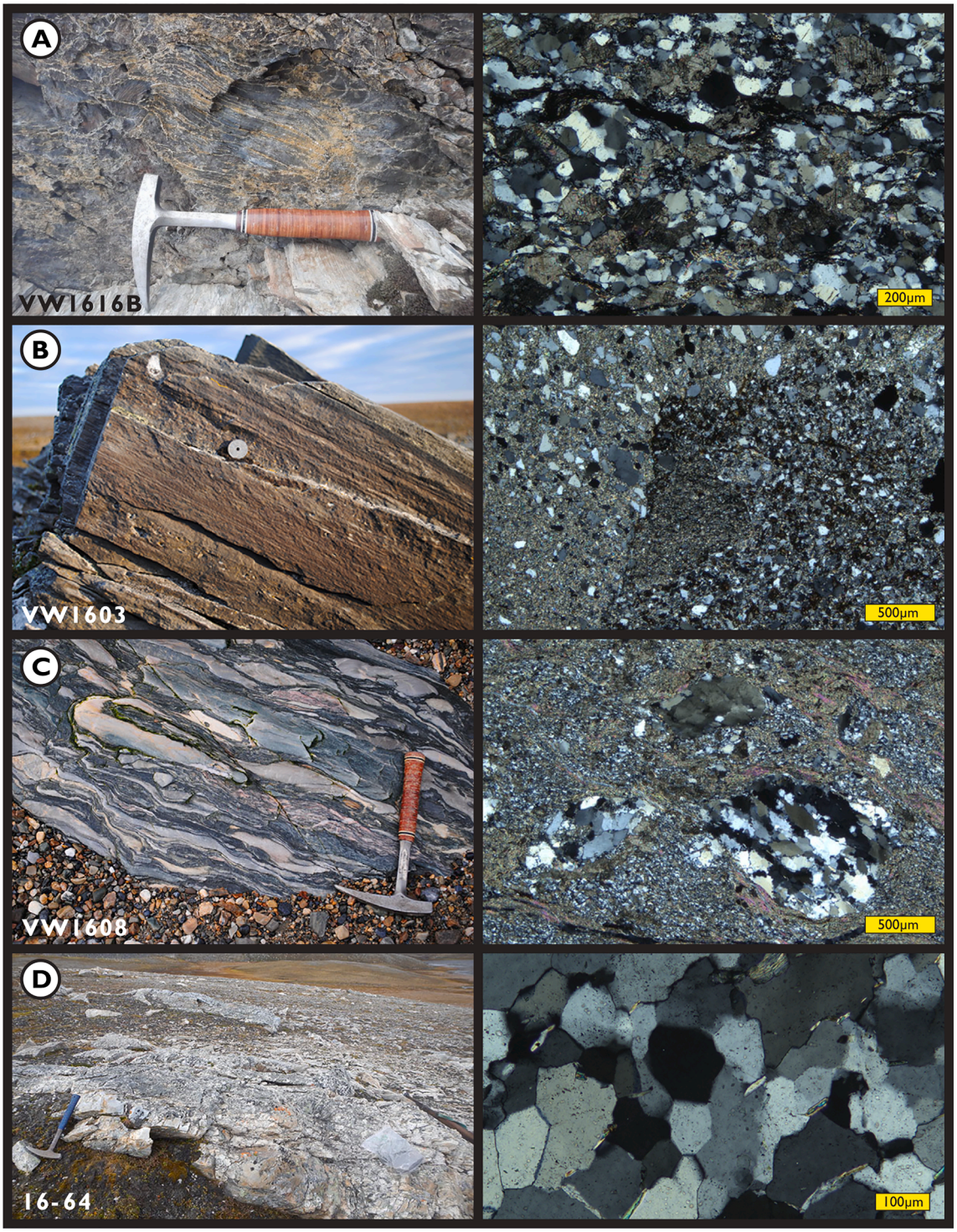

Fig. 6. Photographs of sample horizons (left) and photomicrographs (right) of detrital zircon geochronological samples. **A)** Sample VW1616B of the upper Konglomeratfjellet Formation, taken from a horizon of cleaved fine-grained metasandstone composed of mono- and poly-crystalline quartz, plagioclase feldspar, white mica, graphite, and sericite in a dolomite cement. The white mica, quartz, and graphite define a crude metamorphic foliation. Hammer is 33 cm long. **B)** Brown-weathering quartz wacke of sample VW1603 of the Konglomeratfjellet Formation (left) with poorly sorted and subangular grains of monocrystalline quartz and opaques in a fine-grained matrix of dolomite, siderite, sericite, calcite, and quartz (right). Coin is 2.1 cm in diameter. **C)** Highly sheared matrix-supported metaconglomerate of the Slyngfjellet Formation (sample VW1608) from southernmost Wedel Jarlsberg Land with strained clasts of orthogneiss, quartzite, and marble. Hammer is 33 cm long. Photomicrograph on right shows the sampled finer-grained matrix, which is dominated by sutured lithic fragments, polycrystalline quartz, dolomite, and sericite with rare plagioclase and orthoclase. **D)** Light gray metasandstone horizon (sample 16–64) of the uppermost Kapp Berg Formation (Nordbukta Group). Hammer is 33 cm long. Photomicrograph on right dominated by sutured monocrystalline quartz grains with rare aligned white mica, and opaque minerals.

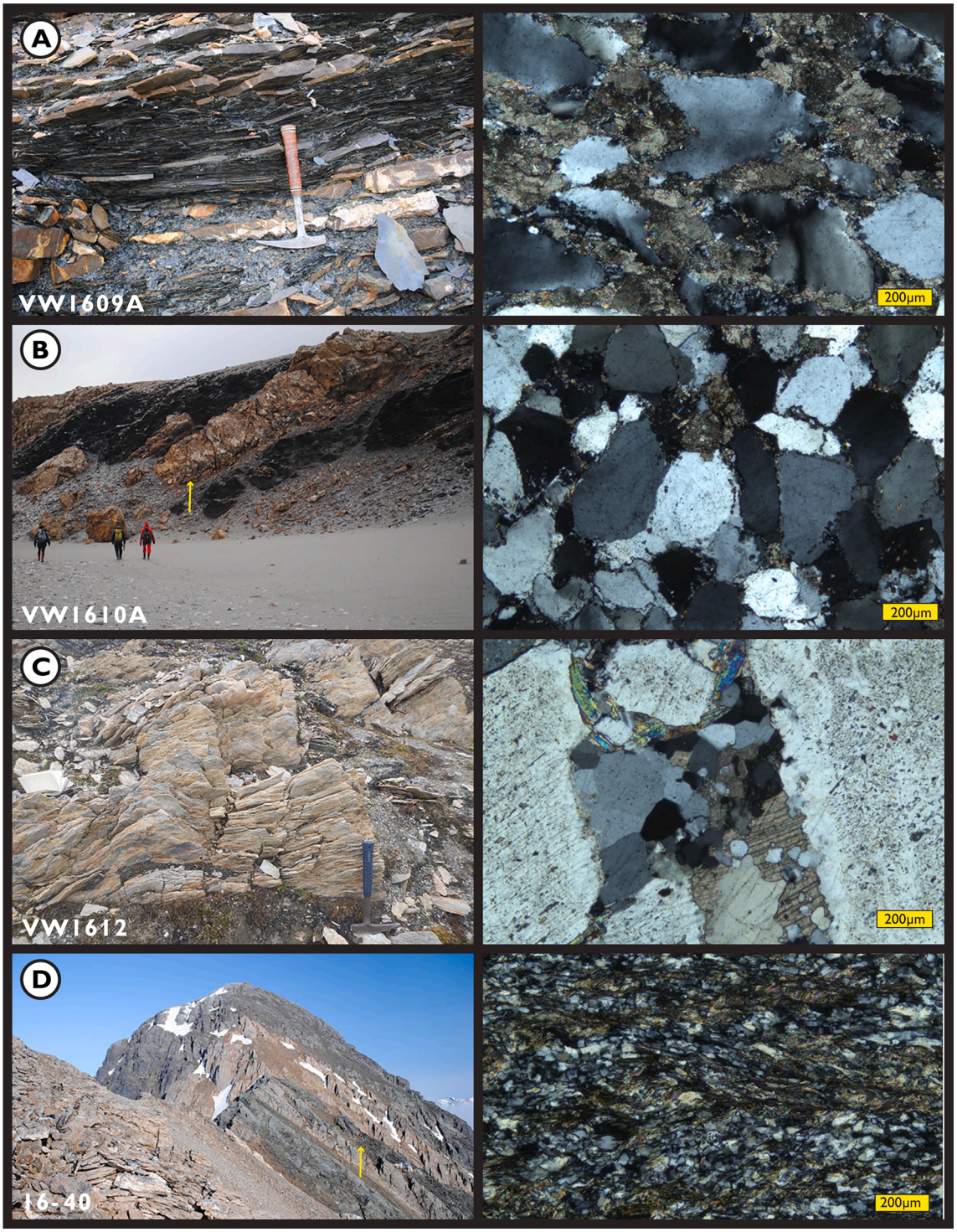

Fig. 7. Photographs of sample horizons (left) and photomicrographs (right) of detrital zircon geochronological samples. **A)** Interbedded black phyllite and calcareous metasandstone (sample VW1609A) from the Gåshamna Formation. Hammer is 33 cm long. Photomicrograph on right displays subrounded and locally sutured quartz grains in a fine-grained recrystallized carbonate matrix. **B)** Horizon of medium- to coarse-grained calcareous metasandstone in dark grey to black phyllite of the Gåshamna Formation (arrowed location is where sample VW1610A was taken). Photomicrograph on right displays coarse-grained and subrounded quartz grains in a fine-grained recrystallized carbonate matrix. **C)** Medium-grained metasandstone of the Höferpynten Formation (sample VW1612) from central Wedel Jarlsberg Land. Hammer is 33 cm long. Photomicrograph on right displays monocrystalline and polycrystalline quartz, dolomite, sericitized orthoclase and plagioclase feldspar, microcline, and white mica. **D)** View looking northeast on Solheimfjellet Ridge, central Wedel Jarlsberg Land, at green-weathering volcaniclastic lithic arenite of the Jens Erikfjellet Formation interbedded within metaconglomerate of the Slyngfjellet Formation (arrow points to 16–40 sample location and outcrop is approximately 20 m tall). Photomicrograph on right shows fine-grained recrystallized monocrystalline quartz and opaque grains surrounded by foliated white mica, chlorite, and sericite.

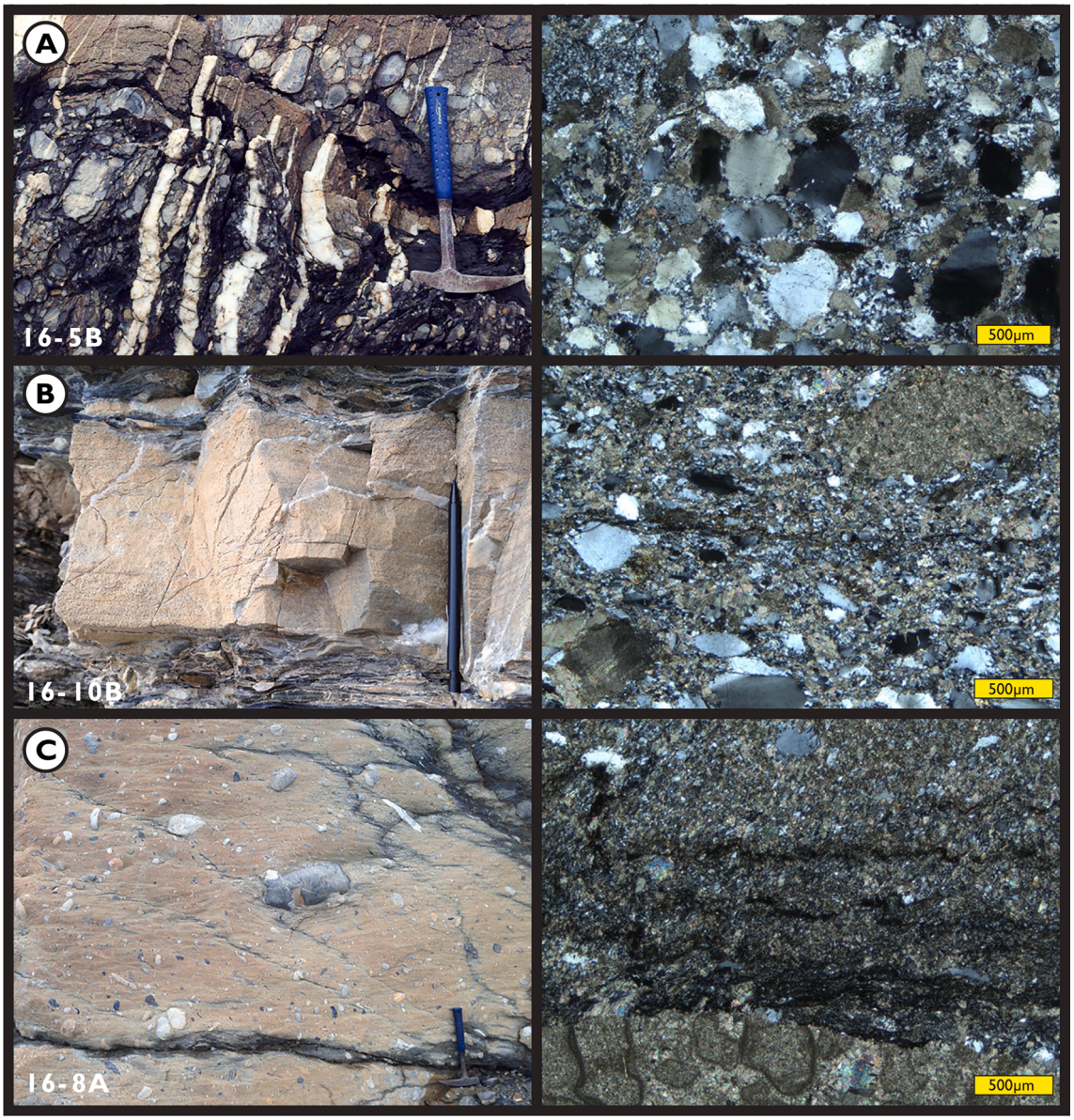

Fig. 8. Photographs of sample horizons (left) and photomicrographs (right) of detrital zircon geochronological samples. **A)** Interbedded medium- to fine-grained calcareous quartz arenite (sample 16-5B) and matrix-supported conglomerate cut with subvertical quartz veins of the Kapp Martin Formation on southern Nordenskiöld Land. Hammer is 33 cm tall. Photomicrograph on right displays subrounded dolomite and quartz grains in a recrystallized carbonate and silica cement. **B)** Fine-grained calcareous metasandstone (sample 16-10B) interbedded with matrix-supported metaconglomerate of the Dundrabeisen Formation (Kapp Lyell Group), northern Wedel Jarlsberg Land. Pencil is 12 cm tall. Photomicrograph of subangular to subrounded fine-grained quartz and dolomite grains in a carbonate matrix (right). **C)** Matrix-supported metaconglomerate of the Dundrabeisen Formation (Kapp Lyell Group), northern Wedel Jarlsberg Land. Hammer is 33 cm long. Sample 16-8A was taken from the matrix and consists of medium- to coarse-grained poorly sorted quartz and carbonate grains in a carbonate matrix. Bands of graphite define a crenulation foliation within sample 16-8A, and the lower carbonate clast has distinct cortoids.

Geochronological data were plotted using Isoplot (Ludwig, 2003) and IsoplotR (Vermeesch, 2018), and all the raw data are reported in Tables S3, S4, and S5 of the Supplementary Information.

4. Results

4.1. Carbonate carbon/oxygen and strontium isotope chemostratigraphy

$\delta^{13}C_{carb}$ data from black metalimestone of the Cryogenian Thiisfjellet Formation (Figs. 5, 10) are highly enriched, with values ranging from +3.2‰ to +10.8‰, and $\delta^{18}O_{carb}$ data range from −11.2‰ to −7.7‰ (Table S1). Samples from two parallel sections of the Thiisfjellet Formation, sections EM1703 and VW1703, yield contrasting $^{87}Sr/^{86}Sr$ values (Figs. 10, 11, Table S2): section EM1703 records Sr concentrations < 500 ppm and $^{87}Sr/^{86}Sr$ values that range from 0.70923 to 0.71407 (average = 0.71074; n = 4); and samples from section VW1703 have higher Sr concentrations with $^{87}Sr/^{86}Sr$ values ranging from 0.70787 to 0.70806 (average = 0.70799, n = 5). Only two samples from section VW1703 pass our 1000 ppm minimum Sr concentration criteria (Fig. 11), yielding $^{87}Sr/^{86}Sr$ values of 0.70787 and 0.70804.

In northwestern Wedel Jarlsberg Land, the basal Slettfjelldalen Formation consists of orange-weathering finely laminated metadolostone that locally becomes more argillaceous up-section (Fig. 9e, f; Dallmann et al, 1990). Five sections within the same stratigraphic unit across northwestern Wedel Jarlsberg Land (J1615, EM1702, VW1705, VW1706, VW1616) record $\delta^{13}C_{carb}$ values that range from −5.5‰ to

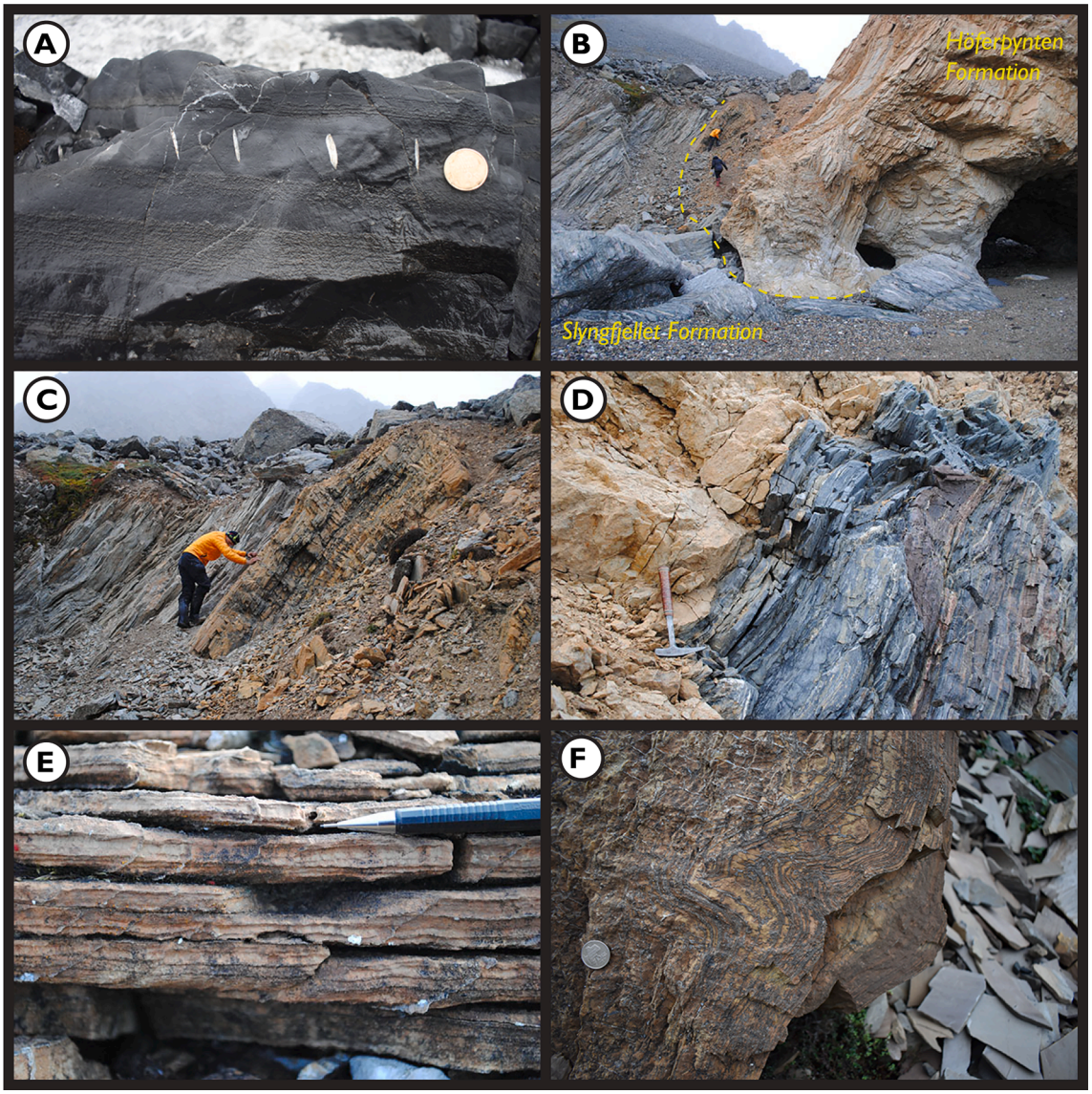

Fig. 9. Selected photographs of metacarbonate strata from Wedel Jarlsberg Land, Southwestern Basement Province (SBP), Svalbard. **A)** Close-up view looking northeast of thin-bedded metalimestone of the Cryogenian Thiisfjellet Formation. Coin is 2.75 cm in diameter. **B)** Overturned and folded contact facing south between the Slyngfjellet and Höferpynten formations in southernmost Wedel Jarlsberg Land (Fannypynten). Geologists for scale. **C)** Close-up of orange-weathering cap metadolostone strata in the basal Höferpynten Formation at the same locality as B). Beds are overturned and geologist is standing on matrix-supported conglomerate sampled for samples VW1608 and 16–42. **D)** Overturned abrupt contact between cap metadolostone and black metalimestone of the basal Höferpynten Formation just out of frame to right in B). This stratigraphic relationship between the basal cap metadolostone and overlying black metalimestone is common throughout southern Wedel Jarlsberg Land. **E)** Very fine lamination of cap metadolostone strata in section J1615 of the Slettfjelldalen Formation looking NNE. **F)** Intrastratal folds and bedding-parallel sheet-crack cements in finely laminated metadolostone of the basal Slettfjelldalen Formation looking SSW.

−3.1‰ (Fig. 10). $\delta^{18}O_{carb}$ data from these sections are consistently depleted and range from −11.6‰ to −13.4‰ (Table S1). In central Wedel Jarlsberg Land, the equivalent Höferpynten Formation consists of ~80–180 m of buff-yellow metadolostone and black metalimestone with local chert and sedimentary breccia (Fig. 9b, c, d). The lower ~35 m commonly consists of laminated dolograinstone with $\delta^{13}C_{carb}$ values that record a gradual rise from −5.8‰ to around 2.4‰ (Fig. 10). The overlying ~10 m of black metalimestone records $\delta^{13}C_{carb}$ values that are enriched, ranging from +4.1‰ to +5.8‰. These strata have $^{87}Sr/^{86}Sr$ ratios ranging from 0.70839 to 0.71164 (Fig. 11, Table S2), although the more radiogenic values above ~ 0.708 all come from samples below the Sr ≥ 1000 ppm cutoff. Section VW1606 records three samples with Sr concentrations above 1000 ppm (Fig. 11); these samples record a narrow range of $^{87}Sr/^{86}Sr$ values between 0.7084 and 0.70843.

4.2. Sample descriptions and U-Pb/Hf isotopic results

4.2.1. Kapp Berg Formation, Nordbukta Group

Sample 16–64 of the Kapp Berg Formation (base of the Nordbukta Group; Bjørnerud, 1990) was collected west of Kvassnilken Ridge from a thick-bedded light gray quartzite horizon (Table 1, Figs. 4, 5, 6). In thin section, this sample is dominated by monocrystalline quartz grains within a very fine-grained matrix of white mica and quartz. The quartz grains are commonly recrystallized and locally display undulose extinction. Colorless zircon from sample 16–64 are relatively small (~50–100 μm) and anhedral to subhedral. Major U-Pb age populations from this sample range from ca. 1170–1030 (19%), 1400–1280 (13%), 1510–1430 (15%), and 1680–1580 (21%) Ma (Fig. 12). The youngest zircon is 915 ± 11 Ma (1σ, 6% discordant; $^{206}Pb/^{238}U$), and the peak of the youngest age population is ca. 970 Ma.

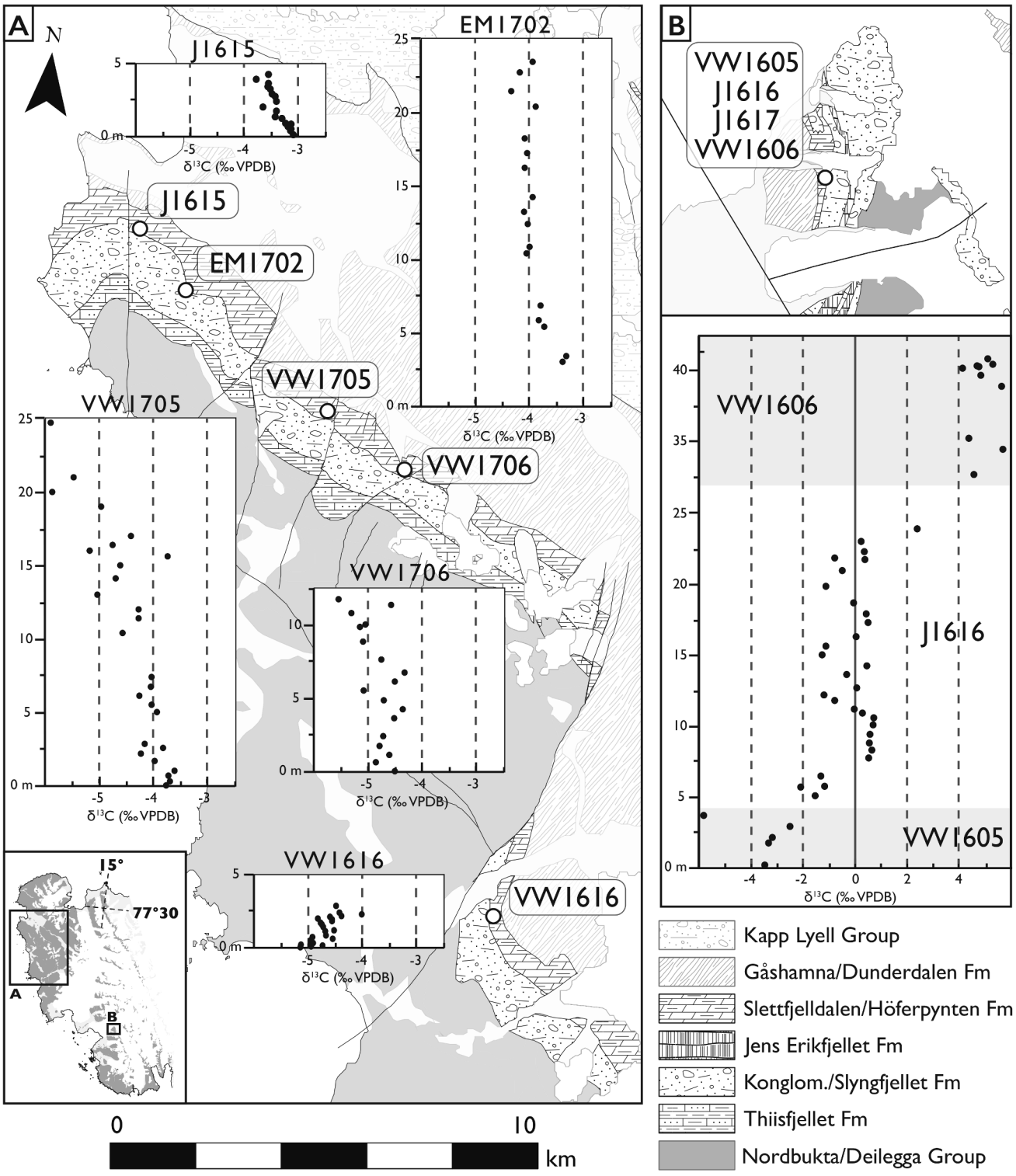

Fig. 10. Carbon isotope chemostratigraphy from measured sections of the Slettfjelldalen and Höferpynten formations in northern (A) and southern (B) Wedel Jarlsberg Land, Southwestern Basement Province (SBP), Svalbard. The inset map in the lower left outlines the locations on Wedel Jarlsberg Land with dark grey units representing all of the Mesoproterozoic(?)–Neoproterozoic stratigraphy; see Fig. 5 for locations as well. Scale bar is the same for both inset maps. Note how the basal Ediacaran Slettfjelldalen and Höferpynten formations record a negative $\delta^{13}C_{carb}$ excursion up to ~ -5‰ (equivalent to the global Meiberg excursion) up to ~ -5‰ before returning to enriched values in sections J1616 and VW1606.

Hafnium isotopic measurements were performed on 20 zircon crystals from sample 16–64 of the Kapp Berg Formation (Fig. 12). Zircon with U-Pb ages of ca. 1480–1090 Ma have positive $\varepsilon Hf_{(t)}$ values that range from +1 to +10. One Neoproterozoic analysis is an outlier and records an $\varepsilon Hf_{(t)}$ value of −7.4. Zircon from the ca. 1680–1580 Ma U-Pb age peak have $\varepsilon Hf_{(t)}$ values that are moderately juvenile to intermediate from −2 to +6. Other Paleoproterozoic and Neoarchean grains have moderately negative $\varepsilon Hf_{(t)}$ values that range from 0 to −3.

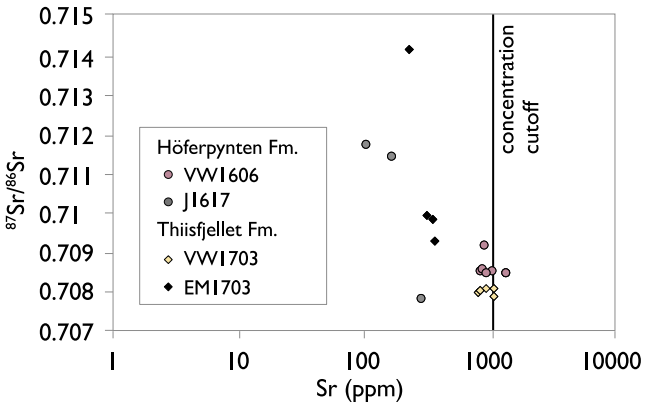

Fig. 11. Cross-plot showing $^{87}Sr/^{86}Sr$ isotopic ratios versus Sr concentrations (ppm) for limestone samples from the Höferpynten and Thiisfjellet formations in Wedel Jarlsberg Land, Southwestern Basement Province (SBP), Svalbard. We employ a rigorous concentration cutoff of 1000 ppm after Halverson et al. (2007).

4.2.2. *Konglomeratfjellet Formation, Dunderbukta Group*

Sample VW1603 was collected from an outcrop of fine-grained medium-bedded quartz wacke of the upper Konglomeratfjellet Formation in northwestern Wedel Jarlsberg Land (Table 1, Figs. 4, 5, 6b). In thin section, the matrix is dominated by very fine-grained dolomite, siderite, sericite, calcite, and quartz with subangular poorly sorted clasts of quartz (Fig. 6b). Zircon from sample VW1603 are ~100–300 μm and mostly subhedral; approximately half of the grains have dark cores and bright rims. This sample yields a U-Pb age distribution with dominant age populations from ca. 1210–990 (34%), 1470–1340 (17%), and 1750–1580 (26%) Ma, and subordinate populations around 1330–1250 (8%), 1540–1490 (4%), 1860–1800 (3%), and 2900–2790 (3%) Ma (Fig. 12). The youngest zircon is 962 ± 21 Ma (1σ, 1% discordant; $^{206}Pb/^{238}U$), and the peak of the youngest age population is ca. 1080 Ma.

Sample VW1616B was collected from the uppermost Konglomeratfjellet Formation, approximately 1 m below the contact with the overlying Slettfjelldalen Formation on Kvassnilken Ridge (Table 1; Figs. 4, 5, 6a). This sample, collected from an ~2 m thick fine-grained quartzite horizon, contains monocrystalline and polycrystalline quartz, dolomite, plagioclase, white mica, graphite, and sericite (Fig. 6a). Pink to yellow zircon range from subrounded to subangular and are ~50–200 μm. Zircons from VW1616B contain similar U-Pb age populations to sample VW1603 with dominant peaks of ca. 1180–990 (24%), 1310–1210 (8%), 1390–1320 (12%), 1470–1400 (10%), 1780–1590 (25%), and 1920–1810 (3%) Ma (Fig. 12). The youngest zircon is 950 ± 9 Ma (1σ, 2% discordant, $^{206}Pb/^{238}U$), and the peak of the youngest age population is ca. 1010 Ma.

Hafnium isotopic data from 19 zircon grains in sample VW1603 cover a broad range of ages from ca. 2800–960 Ma (Fig. 12). Most zircon analyses have juvenile $\varepsilon Hf_{(t)}$ values that cluster from +2 to +7 (79% of the analyses). Outliers include a ca. 1011 Ma grain with an evolved $\varepsilon Hf_{(t)}$ value of −10, a ca. 1540 Ma grain with an evolved $\varepsilon Hf_{(t)}$ value of −6, and a ca. 2802 Ma grain that records an intermediate +0.5 $\varepsilon Hf_{(t)}$ value.

4.2.3. *Slyngfjellet Formation, Sofiebogen Group*

Sample VW1608 was collected from the matrix of a highly sheared, dark green to pink matrix-supported metaconglomerate from the type locality (Fannypynten) of the Slyngfjellet Formation in southern Wedel Jarlsberg Land (Table 1; Figs. 4, 5, 6c). The majority of the pebble- to boulder-sized clasts in this diamictite are composed of quartzite and dolostone with rare orthogneiss boulders that are all flattened within the main foliation plane (Fig. 6c). In thin section, the sample matrix is dominated by fine-grained quartz, dolomite, and sericite. Zircon are

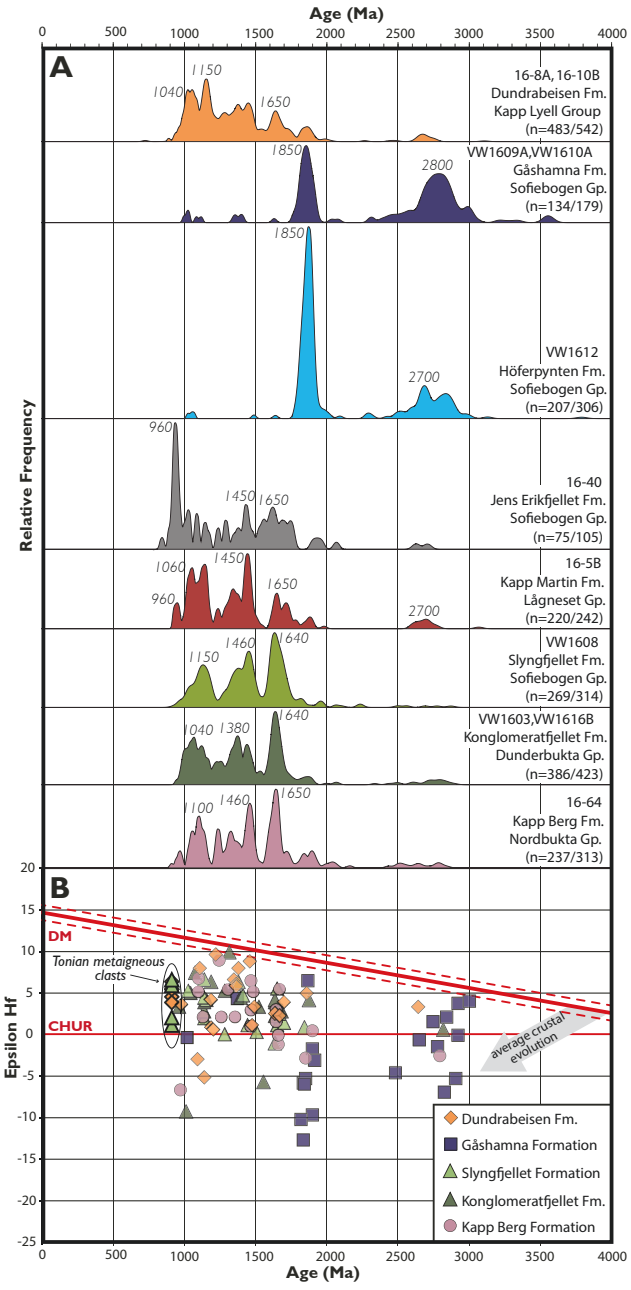

Fig. 12. A) Normalized probability density plots for detrital zircon U-Pb data from samples described herein in the Southwestern Basement Province of Svalbard. Sample locations and descriptions are provided in the text and on Fig. 5, and Table 1. **B)** Hafnium isotopic analyses of detrital zircon from samples in the Nordbukta Group (pink circles), Konglomeratfjellet and Slyngfjellet formations (green triangles), Kapp Lyell Group (orange diamonds), and Gåshamna Formation (purple squares). Bold outlined triangles represent data from metaigneous clasts. CHUR – chondritic uniform reservoir (Vervoort and Blichert-Toft, 1999). DM-depleted mantle (Bouvier et al., 2008). The gray arrow was calculated based on average crustal evolution trajectories assuming present-day $^{176}Lu/^{177}Hf$ = 0.0115 (Vervoort and Patchett, 1996; Vervoort et al., 1999). Gp.–Group; Fm.–Formation.

subhedral to euhedral, vary from ~ 50–300 μm, and are clear to pink. U-Pb zircon data yield four dominant age populations at ca. 1200–970 (25%), 1400–1270 (14%), 1410–1510 (18%), and 1750–1570 (31%) Ma (Fig. 12). The youngest grain is 935 ± 28 Ma (1σ, 6% discordant, $^{206}Pb/^{238}U$), and the age of the youngest peak is ca. 1140 Ma.

Hafnium isotopic data from 18 zircon grains in sample VW1608 yield intermediate to juvenile $\varepsilon Hf_{(t)}$ values that range from −1 to + 7, with a

general trend of being slightly more evolved through time (Fig. 12). Each of the dominant age populations discussed above record a similar range of $\varepsilon Hf_{(t)}$ values, except for the ca. 1200–970 Ma population which yields dominant juvenile $\varepsilon Hf_{(t)}$ values between +3 and +7.

4.2.4. Jens Erikfjellet Formation, Sofiebogen Group

Sample 16–40 was collected on Solheimfjellet, a prominent E-W-striking ridge in south-central Wedel Jarlsberg Land, from the lower of two volcaniclastic horizons in the Jens Erikfjellet Formation (Table 1; Figs. 4, 5, 7). The sample is from a green-weathering horizon of fine-grained lithic arenite that consists of monocrystalline quartz, white mica, chlorite, and various opaque minerals. Zircon from sample 16–40 are relatively small (~50–100 μm) and range from subhedral to euhedral. Dominant zircon age populations include ca. 970–900 (21%), 1490–1340 (15%), and 1770–1530 (28%) Ma age peaks (Fig. 12). The youngest zircon is 849 ± 13 Ma (1σ, 6% discordant; $^{206}Pb/^{238}U$), and the peak of the youngest age population is ca. 950 Ma.

4.2.5. Höferpynten Formation, Sofiebogen Group

Sample VW1612 was collected from a sheared dolomitic quartzite horizon in the Höferpynten Formation adjacent to the VKSZ in southwestern Wedel Jarlsberg Land (Table 1; Figs. 4, 5, 7c). This sample is from a light gray-weathering, medium-grained subarkosic quartzite that contains recrystallized monocrystalline quartz, dolomite, sericitized orthoclase, plagioclase, microcline, and secondary muscovite (Fig. 7c). Light pink to colorless zircon grains are subrounded to angular and range from ~50–150 μm. Zircon U-Pb age populations consist of one major peak at ca. 1920–1790 (58%) Ma with subordinate age populations at ca. 2720–2650 (10%) and 2900–2760 (13%) Ma (Fig. 12). The youngest zircon is 1032 ± 8 Ma (1σ, 4% discordant, $^{206}Pb/^{238}U$), and the peak of the youngest age population is ca. 1880 Ma.

4.2.6. Gåshamna Formation, Sofiebogen Group

Two samples from coarse-grained siliciclastic intervals in the lower (VW1609A) and middle (VW1610A) Gåshamna Formation were collected from the type locality (Fannypynten) in southernmost Wedel Jarlsberg Land (Table 1; Figs. 4, 5, 7a, b). Sample VW1609A was collected from a thin horizon of medium-grained calcareous quartzite in the lower Gåshamna Formation and consists of subrounded fine- to medium-grained quartz and dolomite grains within a fine-grained calcareous matrix (Fig. 7a). Dark yellow to pink subhedral zircon from this sample range between ~50–150 μm with metamict textures and oscillatory zonation. The zircon U-Pb age distributions for sample VW1609A show two dominant populations at ca. 1920–1800 (29%) and 3010–2680 (44%) Ma (Fig. 12). The youngest zircon is 1033 ± 12 Ma (1σ, 2% discordant, $^{206}Pb/^{238}U$), and the peak of the youngest age population is ca. 1850 Ma.

Sample VW1610A was collected from a >3 m thick lens-shaped body of coarse-grained calcareous quartzite from the middle Gåshamna Formation (Table 1; Figs. 4, 5, 7b). This sample is compositionally similar to sample VW1609A, but it contains a higher proportion of quartz framework grains. Zircon are subrounded, dark yellow to pink, and range from ~50–150 μm. Zircon U-Pb age distributions consist of two dominant populations at ca. 1920–1770 (38%) and 2880–2720 (33%) Ma, with subordinate populations of Neoarchean and Mesoarchean grains (Fig. 12). The youngest zircon is 1005 ± 9 Ma (1σ, 2% discordant, $^{206}Pb/^{238}U$), and the peak of the youngest age population is ca. 1860 Ma.

Twenty-one Hf isotopic measurements were performed on zircon grains from the samples of the Gåshamna Formation (Fig. 12). The dominant Paleoproterozoic U-Pb age population (ca. 1920–1820 Ma) has zircon with $\varepsilon Hf_{(t)}$ values that are all intermediate to evolved, ranging from −2 to −14, except for one positive outlier at +7. The latest Paleoproterozoic to Archean age populations (ca. 2990 – 2480 Ma) display a scattered range of $\varepsilon Hf_{(t)}$ values from −8 to +4 (Fig. 12).

4.2.7. Dundrabeisen Formation, Kapp Lyell Group

Two samples were collected from the Dundrabeisen Formation of the Kapp Lyell Group on northern Wedel Jarlsberg Land (16-8A and 16-10B; Table 1; Figs. 4, 5, 8b, c). Sample 16-8A was collected from the matrix of a yellow-weathering metaconglomerate horizon with subrounded to subangular quartzite and dolostone pebbles and boulders. The matrix is composed of very fine-grained quartz and dolomite, and in thin section, the quartz displays recrystallization textures with diffuse grain boundaries and bands of graphite defining a prominent foliation (Fig. 8c). Zircon U-Pb age distributions from this sample show three dominant age populations at ca. 1220–980 (34%), 1500–1330 (25%), and 1730–1600 (15%) Ma, with subordinate Paleoproterozoic and Neoarchean grains (Fig. 12). The age of the youngest zircon is 730 ± 19 Ma (1σ, 5% discordant, $^{206}Pb/^{238}U$), and the peak of the youngest age population is ca. 1056 Ma.

Sample 16-10B was collected from a medium-bedded calcareous metasandstone horizon near the top of the Dundrabeisen Formation (Table 1; Fig. 4, 5, 8b). Zircon from this sample are subhedral to euhedral, range from 50 to 200 μm, and display occasional bright metamorphic rims. This sample yields U-Pb age populations at ca. 1080–1000 (19%), 1190–1090 (21%), 1350–1200 (13%) Ma, and 1490–1370 (15%) Ma with subordinate groups at ca. 1700–1600 (6%), 1890–1800 (7%), and 2760–2650 (5%) Ma (Fig. 12). The age of the youngest zircon is 895 ± 8 Ma (1σ, 5% discordant, $^{206}Pb/^{238}U$), and the peak of the youngest age population is ca. 1030 Ma.

Hafnium isotopic measurements were performed on 20 zircon crystals from sample 16-8A of the Dundrabeisen Formation (Fig. 12). These grains have intermediate to juvenile $\varepsilon Hf_{(t)}$ values, with only two moderately evolved $\varepsilon Hf_{(t)}$ values that are −3 to −6. Mesoproterozoic-Neoproterozoic zircon crystals (ca. 1480–970 Ma) are mostly juvenile with $\varepsilon Hf_{(t)}$ values of 0 to + 10, whereas the Archean-Paleoproterozoic zircon populations have a smaller, yet still juvenile, range with $\varepsilon Hf_{(t)}$ values of +2 to +5.

4.2.8. Kapp Martin Formation, Lågneset Group

Sample 16-5B was collected from a gray-weathering, medium- to fine-grained quartzite horizon within matrix-supported metaconglomerate of the Kapp Martin Formation of the Lågneset Group on southern Nordenskiöld Land (Table 1; Figs. 5, 8a). Subrounded quartz grains within the metasandstone range from ~200–500 μm and commonly display undulatory extinction (Fig. 8a). Zircon from this sample are anhedral to subhedral, range from 75 to 200 μm, and have occasional bright metamorphic rims. These grains yield dominant U-Pb age populations at ca. 1080–1020 (12%), 1170–1090 (17%), 1390–1290 (13%), and 1480–1400 (16%) Ma with subordinate peaks at ca. 1680–1620 (7%) and 1750–1690 (6%) Ma (Fig. 12). The age of the youngest zircon is 933 ± 10 Ma (1σ, 3% discordant, $^{206}Pb/^{238}U$), and the peak of the youngest age population is ca. 950 Ma.

4.2.9. Metaigneous Clasts in the Slyngfjellet and Dundrabeisen Formations

Sample 16–42 consists of an ~30 cm orthogneiss clast collected within matrix-supported metaconglomerate of the Slyngfjellet Formation on southernmost Wedel Jarlsberg Land (Table 1; Figs. 5, 13A). This sample yielded 54 pink prismatic zircons that range from ~100–250 μm and show clear oscillatory zonation with bright metamorphic rims (Fig. 13a). These zircons yielded a large portion of discordant LA-ICPMS analyses (n = 34/54) with $^{207}Pb/^{206}Pb$ ages ranging from 291 ± 15 to 2994 ± 53 Ma (Table S4). With the exception of a much older grain with a $^{207}Pb/^{206}Pb$ date of 1768 ± 10 Ma, ten selected concordant grains give $^{206}Pb/^{238}U$ dates that range from 953 ± 11 to 998 ± 10 Ma and define a weighted mean $^{206}Pb/^{238}U$ age of 978 ± 3 Ma (Fig. 13a; mean square of weighted deviates (MSWD) = 2.5, 95% confidence). The older Paleoproterozoic concordant grain is interpreted as a xenocrystic core, and the complex systematics and high degree of discordance is interpreted to reflect the combined effects of Pb-loss and inheritance. The SIMS data from sample 16–42 defines a Pb-loss trajectory consistent with the LA-

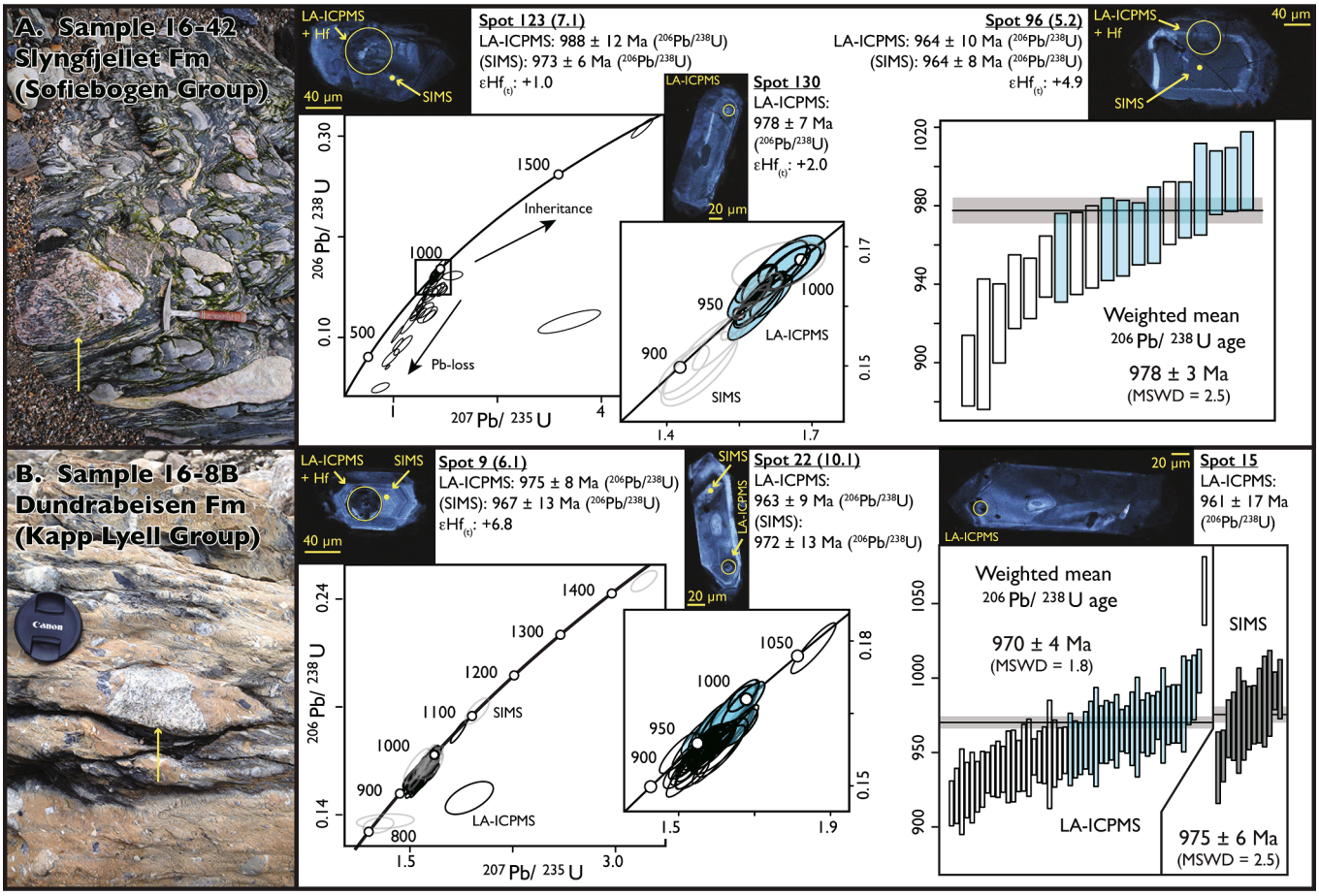

Fig. 13. U-Pb isotopic data for igneous clasts in the **A)** Slyngfjellet Formation of the Sofiebogen Group (Sample 16–42) and the **B)** Dundrabeisen Formation of the Kapp Lyell Group (Sample 16-8B). Arrows in photographs show sampled clasts, and blue ellipses show selected grains in calculated weighted means. See text for further explanation.

ICPMS weighted mean $^{206}Pb/^{238}U$ age of 978 ± 3 Ma that is interpreted as the best age estimate for the clast (Fig. 13a). Hafnium isotopic measurements on five concordant zircon crystals from sample 16–42 revealed juvenile $\varepsilon Hf_{(t)}$ values that range from +1 to +7 (Fig. 12).

Sample 16-8B consists of an ~10 cm metagabbro clast collected from matrix-supported metaconglomerate of the Dundrabeisen Formation near the nose of the Renardbreen Glacier in northern Wedel Jarlsberg Land (Table 1; Figs. 5, 13b). This sample yielded 54 prismatic dark pink zircon crystals that were ~50–300 µm, and nearly all of these zircons display oscillatory zonation, many with very thin bright metamorphic rims (Fig. 13b). Fifty LA-ICPMS analyses from sample 16-8B that are concordant to near concordant yielded $^{206}Pb/^{238}U$ dates ranging from 916 ± 7 to 1059 ± 12 Ma (Table S4). SIMS analyses of cores yielded a population of older dates that are interpreted as xenocrystic components (Fig. 13b) but also define a coherent cluster that yields a weighted mean $^{206}Pb/^{238}U$ age of 975 ± 6 Ma (MSWD = 2.5, 1σ). Excluding the oldest date that is clearly an outlier, the LA-ICPMS data define a weighted mean $^{206}Pb/^{238}U$ age of 954 ± 3 Ma (Fig. 13b; 1σ, n = 49/50, MSWD = 4.3). The large spread in LA-ICPMS $^{206}Pb/^{238}U$ dates is interpreted to reflect Pb-loss. Removing the younger age group, the remaining analyses define a weighted mean $^{206}Pb/^{238}U$ age of 970 ± 4 Ma (Fig. 13a; n = 26/50, MSWD = 1.8, 95% confidence) that is consistent with the observed SIMS age and therefore interpreted as the best estimate for the crystallization age of the igneous clast. Hafnium isotopic measurements from five concordant grains in sample 16-8B are juvenile, with values that range from +4 to +7 (Fig. 12).

5. Discussion

5.1. Tectono-stratigraphy of the Southwestern Basement Province (SBP)

Mesoproterozoic–early Paleozoic rocks of the SBP define a complex assemblage of crustal fragments that were most likely partially to fully amalgamated during the polyphase Caledonian orogeny (e.g., Gee and Page, 1994; Harland, 1997; Manecki et al., 1998; Gee and Teben'kov, 2004; Labrousse et al., 2008; Mazur et al., 2009; Kośmińska et al., 2014; Majka et al., 2015; Ziemniak et al., 2019; Barnes et al., 2020; Faehnrich et al., 2020). As highlighted previously, these fault-bounded regions were subsequently deformed and translated during the Devonian-Carboniferous Ellesmerian and Paleogene-Eocene Eurekan orogenies, which not only complicated their primary structural relationships, but also reset local thermochronometers that may have once elucidated their primary juxtaposition histories (e.g., Kośmińska et al., 2014; Barnes and Schneider, 2019; Dörr et al., 2019; Schneider et al., 2019; Dallmann and Piepjohn, 2020; Faehnrich et al., 2020). Despite this, pre-Caledonian metasedimentary rocks across the SBP have been previously correlated based on lithological and stratigraphic similarities (e.g., Harland, 1997), as well as preliminary detrital zircon-based provenance studies (Gasser and Andresen, 2013; Ziemniak et al., 2019).

Here, we propose to subdivide the SBP into four discrete Caledonian terranes that are based upon modifications to the original terrane subdivisions outlined in Harland (1997) and subsequent tectono-stratigraphic subdivisions of Dallmann (2015a); these include the

Wedel Jarlsberg-Oscar II, Prins Karls Forland, Berzeliuseggene-Eimfjellet, and Hornsund terranes (Fig. 14). Harland (1997) used the term "terrane" for both "a series, system or group of rocks" as well as for rock packages that "were postulated to be allochthonous, or suspected to be so" – we are strictly using the terrane terminology in the latter framework (*sensu* Coney et al., 1980) with a focus on the origins of SBP crustal fragments prior to the Caledonian orogeny. In order to provide important context and justification for the proposed tectonic subdivisions, we provide an abbreviated regional stratigraphic overview of each SBP terrane starting with a synthesis of new data presented herein from Wedel Jarlsberg Land. The Wedel Jarlsberg-Oscar II terrane is the largest of the SBP terranes and hosts the most coherent metasedimentary successions; as a result, it forms the backbone of our tectonostratigraphic correlations within the SBP and to other regions in the North Atlantic and circum-Arctic.

5.1.1. *Wedel Jarlsberg-Oscar II terrane (new name)*

The Wedel Jarlsberg-Oscar II terrane, the southern half of which is the focus of this study, extends from northern Sørkapp Land to northern Oscar II Land (Figs. 2, 14). This terrane is exposed as a series of narrow anastomosing tectonic slivers and more significant fault-bounded blocks in presumed tectonic contact with all of the newly defined SBP terranes, as well as the Northwestern Basement Province. The Wedel Jarlsberg-Oscar II terrane was originally separated into four separate entities (NW Wedel Jarlsberg Land–North of Torellbreen Terrane, SW Wedel Jarlsberg Land–South of Torellbreen Terrane, Oscar II Land Terrane, and Nordenskiöldkysten [Nordenskiöld Land] Terrane) by Harland (1997). While its boundaries are mostly covered by glaciers, coastal strandflats, and younger sedimentary cover, the eastern terrane boundary may be roughly outlined by Harland's (1997) postulated Kongsfjorden-Hansbreen or Western marginal fault zones (Fig. 14), which today roughly parallels the boundary between thick- and thin-skinned deformation in the West Spitsbergen Fold-and-Thrust Belt (e.g., Dallmann, 2015a). Its western boundary with the Prins Karls Forland terrane is not exposed, but it may be broadly marked by a series of high-angle Eurekan extensional structures bounding or within the Forlandsundet Graben (Fig. 14; e.g., Kleinspehn and Teyssier, 1992; von Gosen and Paech, 2001; Bergh et al., 2003; Harland, 1997; Dallmann, 2015a, 2015b). Its northern boundary with the Northwestern Basement Province is marked by the NW-SE-trending frontal thrust of the West Spitsbergen Fold-and-Thrust Belt (Fig. 14; or Kongsfjorden graben of Harland, 1997; Piepjohn et al., 2001; Saalmann and Thiedig, 2002; Dallmann, 2015a), which also locally marks the intersection of Harland's (1997) Kongsfjorden-Hansbreen fault zone with a series of NW-SE-trending structures in the Kongsfjorden region (Figs. 2, 14). The southwestern boundary with the Berzeliuseggene-Eimfjellet terrane is locally well exposed along the Caledonian VKSZ (Figs. 5, 14; Czerny et al., 1993, 2010; Mazur et al., 2009; Faehnrich et al., 2020). Near Antoniabreen in northeastern Wedel Jarlsberg Land (Fig. 5), it is complexly juxtaposed by Caledonian and Eurekan structures with portions of the Berzeliuseggene-Eimfjellet terrane (Majka et al., 2015). The southern and southeastern boundaries of the Wedel Jarlsberg-Oscar II terrane are complicated by anastomosing and glacially covered structures with the Hornsund terrane.

5.1.1.1. *Stenian(?)–Tonian units and correlations.*

The basal ~3–4 km thick Nordbukta Group, exposed on northwestern Wedel Jarlsberg Land, and the equivalent Deilegga Group of southern Wedel Jarlsberg Land, consist of a diverse succession of metacarbonate, phyllite, and quartzite that reflect the progressive development of a thick early Neoproterozoic shallow marine carbonate platform (Bjørnerud, 1990; Czerny et al., 1993). The minor population of latest Stenian to early Tonian detrital zircon (ca. 1027–915 Ma) in strata of the basal Kapp Berg Formation of

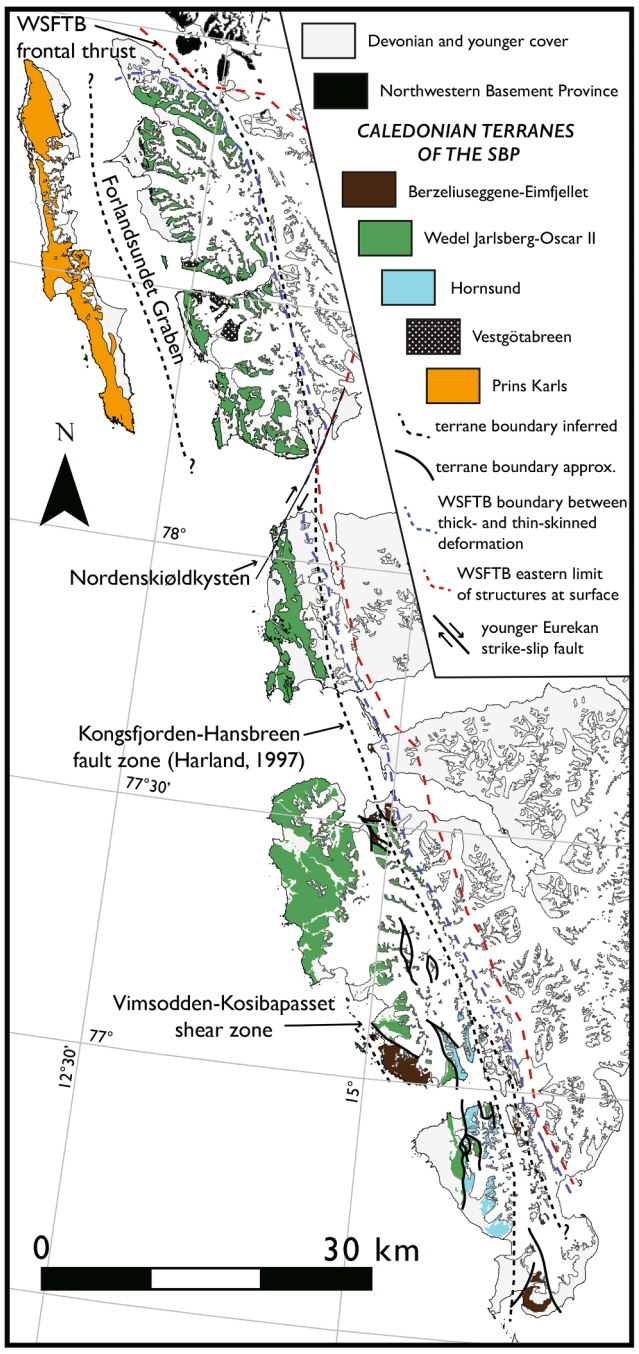

Fig. 14. Schematic map of Caledonian terranes in the composite Southwestern Basement Province of Svalbard, Norway. Note that many, if not all, of the proposed terrane boundaries have been reactivated during younger Devonian–Carboniferous Ellesmerian and Paleogene–Eocene Eurekan deformation. For example, the boundary between thick- and thin-skinned deformation in the West Spitsbergen Fold-and-Thrust Belt (WSFTB; e.g., Birkenmajer, 1981; Dallmann et al., 1993a; Braathen et al., 1995; Bergh et al., 1997; Saalmann and Thiedig, 2002; Dallmann, 2015a) may approximate the eastern boundary of the Wedel Jarlsberg-Oscar II terrane boundary or the boundary of the SBP itself (e.g., Harland, 1997). See text for further explanation of the boundaries and their significance, but note that the early Paleozoic Vestgötabreen Complex is separated out on the map despite its current inclusion with the Wedel Jarlsberg-Oscar II terrane.

the Nordbukta Group (Fig. 12) confirms a Tonian or younger depositional age for these strata and is consistent with the ca. 850 Ma maximum depositional age proposed by Ziemniak et al. (2019) from the Deilegga Group.

The new detrital zircon U-Pb data presented here from the Nordbukta Group (Fig. 12) are also consistent with zircon U-Pb age populations from the Stenian(?)–Tonian St. Jonsfjorden and Daudmannsodden groups of Oscar II Land and Nordenskiöld Land (Fig. 15; Gasser and Andresen, 2013; Dallmann, 2015a). These mixed siliciclastic and carbonate metasedimentary rocks (Hjelle et al., 1999; Bergh et al., 2003) have previously been correlated with the Deilegga and Nordbukta groups based on gross stratigraphic descriptions and preliminary U-Pb detrital zircon data (Fig. 15; Gasser and Andresen, 2013; Ziemniak et al., 2019), although minor alkaline to subalkaline mafic pyroclastic tuff and lava in the St. Jonsfjorden Group (Ohta, 1985; Burzyński et al., 2017) have no known stratigraphic equivalents in the Deilegga or Nordbukta groups. In addition, the oldest exposed strata in Oscar II Land, which comprise amphibolite-grade schist, quartzite, and marble of the Stenian–Tonian(?) Kongsvegen Group in the north (Harland et al., 1966, 1993), and the presumed equivalent Müllerneset Formation in the south (Figs. 2, 3; Harland et al., 1979), have no exposed equivalent in Wedel Jarlsberg Land (unless they are simply fault-bounded stratigraphic equivalents of the St. Jonsfjorden and/or Daudmannsodden groups). Despite these minor differences, we propose these Stenian(?)–Tonian mixed siliciclastic and carbonate metasedimentary successions in Oscar II Land, Nordenskiöld Land, and Wedel Jarlsberg Land comprise the oldest exposed Proterozoic basement to the Wedel Jarlsberg-Oscar II terrane.

5.1.1.2. Torellian unconformity. Argillaceous quartzites of the upper Deilegga and Nordbukta groups are truncated by the late Neoproterozoic Torellian unconformity throughout Wedel Jarlsberg Land (Bjørnerud et al., 1991; Birkenmajer, 1992; Czerny et al., 1993; Mazur et al., 2009). This event is represented by a prominent lithological break, with evidence for subaerial exposure, regolith development, and angular truncation of Nordbukta and Deilegga rocks beneath the Cryogenian-Ediacaran Sofiebogen and Dunderbukta groups (Fig. 4; Birkenmajer, 1975; Cochrane, 1984; Kalinec, 1985; Nania, 1987; Bjørnerud, 1990). Our preliminary field observations from the St. Jonsfjorden area of Oscar II Land also reveal the presence of an angular Torellian unconformity at the top of the St. Jonsfjorden Group, where local Stenian(?)–Tonian metacarbonate rocks of the Alkhornet Formation are folded and overlain unconformably by matrix-supported metaconglomerate of the younger Cryogenian Comfortlessbreen Group (see below).

Here, we compile and review unpublished detrital monazite electron microprobe (EMP) data cited in Mazur et al. (2009) and Czerny et al. (2010) that provide the only local age constraint for the Torellian unconformity (Table S6). Detrital monazite cores yield single EMP Th-U-Pb dates of ca. 1730 and 1545 Ma and prominent age clusters between ca. 1875–1820 (n = 3), 1245–940 (n = 15), 835–715 (n = 4), and 705–625 (n = 12) Ma. These detrital cores are overgrown by metamorphic rims that yield a weighted average Th-U-Pb date of 444 ± 15 (MSWD = 0.83, 2σ, n = 20), which is similar to regional Caledonian ^{40}Ar-^{39}Ar thermochronological datasets (e.g., Dallmann et al., 1993b; Manecki et al., 1998; Faehnrich et al., 2020). Critically, the youngest detrital monazite age population in the Slyngfjellet Formation yields a weighted average Th-U-Pb date of 654 ± 19 Ma (MSWD = 0.52, n = 12), which we suggest is a conservative maximum depositional age for the Cryogenian Sofiebogen and Dunderbukta groups and a minimum age for the Torellian unconformity in Wedel Jarlsberg Land. This is consistent with ca. 650–640 Ma metamorphic ages reported from the newly defined Berzeliuseggene-Eimfjellet terrane of the SBP (Majka et al., 2008, 2015).

5.1.1.3. Cryogenian–Ediacaran units and correlations. A Cryogenian age for the Torellian unconformity in the Wedel Jarlsberg-Oscar II terrane is also confirmed herein by the depositional age of the overlying Sofiebogen and Dunderbukta groups. Carbonate carbon isotopic data from the Thiisfjellet Formation range from +3.2‰ to +10.8‰ and are consistent with global Cryogenian strata deposited during the ca. 660–640 Ma interglacial interval between the Sturtian and Marinoan glaciations (Fig. 16; Bold et al., 2016; Cox et al., 2016). The complimentary ^{87}Sr/^{86}Sr values of 0.70787 and 0.70804 from the only presumably unaltered samples of the Thiisfjellet Formation (Fig. 11) are slightly more radiogenic than other latest Cryogenian or interglacial carbonate successions (Fig. 16), which generally yield ^{87}Sr/^{86}Sr data ranging from ~0.70700 to 0.70750 (e.g., Bold et al., 2016). We interpret this as either reflecting diagenetic alteration in these samples or a lack of known interglacial stratigraphic variability in other published Ediacaran ^{87}Sr/^{86}Sr isotopic datasets (e.g., Cui et al., 2015).

Thick packages of matrix-supported metaconglomerate (diamictite) in the overlying Cryogenian Slyngfjellet and Konglomeratfjellet formations have been interpreted as glacial in origin, but their temporal relationships to global Cryogenian glaciations have remained controversial (e.g., Orvin, 1940; Harland et al., 1979, 1993; Bjørnerud, 2010; Majka et al., 2010). Critically, these glacial strata are sharply overlain by metacarbonate of the Höferpynten and Slettfjelldalen formations, the base of which consist of ~0.5–3 m thick finely laminated dolostone units that host distinct sedimentary structures, such as sheet crack cements, m-scale trochoidal bedforms, and finely laminated peloidal dolograinstone (Fig. 9e, f), that are consistent with basal Ediacaran cap carbonates exposed worldwide (e.g., Hoffman, 2011; Lamb et al., 2012; Hoffman et al., 2017). In support of this sedimentological data, depleted $\delta^{13}C_{carb}$ measurements from these cap dolostone units in Wedel Jarlsberg Land are consistent with global Ediacaran datasets that record the post-glacial Maieberg negative carbon isotope excursion (Figs. 10, 16; Hoffman and Schrag, 2002; Hoffman et al., 2017; Ahm et al., 2019). The distinct return to ~0‰ after a nadir of approximately −5‰ in the Höferpynten and Slettfjelldalen formations (Fig. 10) is also recognized in basal Ediacaran successions of Brazil (Misi and Veizer, 1998), Australia (Calver, 2000), Oman (Fike et al., 2006), northwestern Canada (Macdonald et al., 2013), and South China (Zhu et al., 2013). Furthermore, black metalimestone packages that directly overlie these cap dolostone exposures in the Höferpynten Formation record enriched $\delta^{13}C_{carb}$ values between +4.1‰ and +5.7‰ and ^{87}Sr/^{86}Sr values that range from 0.70839 to 0.70909 (Figs. 10, 11), both of which are consistent with other basal Ediacaran carbonate successions (Fig. 16; Bold et al., 2016; Rooney et al., 2020). Thus, we suggest that the Slyngfjellet/Konglomeratfjellet and Höferpynten/Slettfjelldalen formations are correlative to globally distributed deposits of the terminal Cryogenian ca. 640(?)–635 Ma Marinoan snowball Earth glaciation and the associated basal Ediacaran cap carbonate.

The youngest Neoproterozoic unit in Oscar II Land belongs to the Comfortlessbreen Group, which includes an ~2–3 km thick matrix-supported conglomerate unit, an ~20–2,000 m thick quartzite package, and an ~1 km thick succession of laminated green- and cream-colored marble, chloritic schist, and dark-gray calcareous phyllite (Bergh et al., 2003). Detrital zircon U-Pb data from the Comfortlessbreen Group provided a ca. 1070 Ma maximum depositional age, with the youngest grain reported at 711 ± 4 Ma (Fig. 15; 1σ, 1% discordant, ^{206}Pb/^{238}U; Gasser and Andresen, 2013). This glaciogenic unit has been previously correlated with the Kapp Lyell Group of Wedel Jarlsberg Land based on its thickness and lithological similarities (Bergh et al., 2003); however, unnamed dolostone units directly overlying the Comfortlessbreen diamictite in the St. Jonsfjorden region reveal sedimentological attributes that are more consistent with basal Ediacaran cap carbonates described above in the Höferpynten and Slettfjelldalen formations. Thus, we suggest the diamictite-bearing strata of the Comfortlessbreen Group of Oscar II Land records the Marinoan snowball Earth glaciation and is more likely correlative with the Konglomeratfjellet and Slyngfjellet formations of Wedel Jarlsberg Land. It is unclear if the overlying quartzite, marble, schist, and phyllite of the Comfortlessbreen

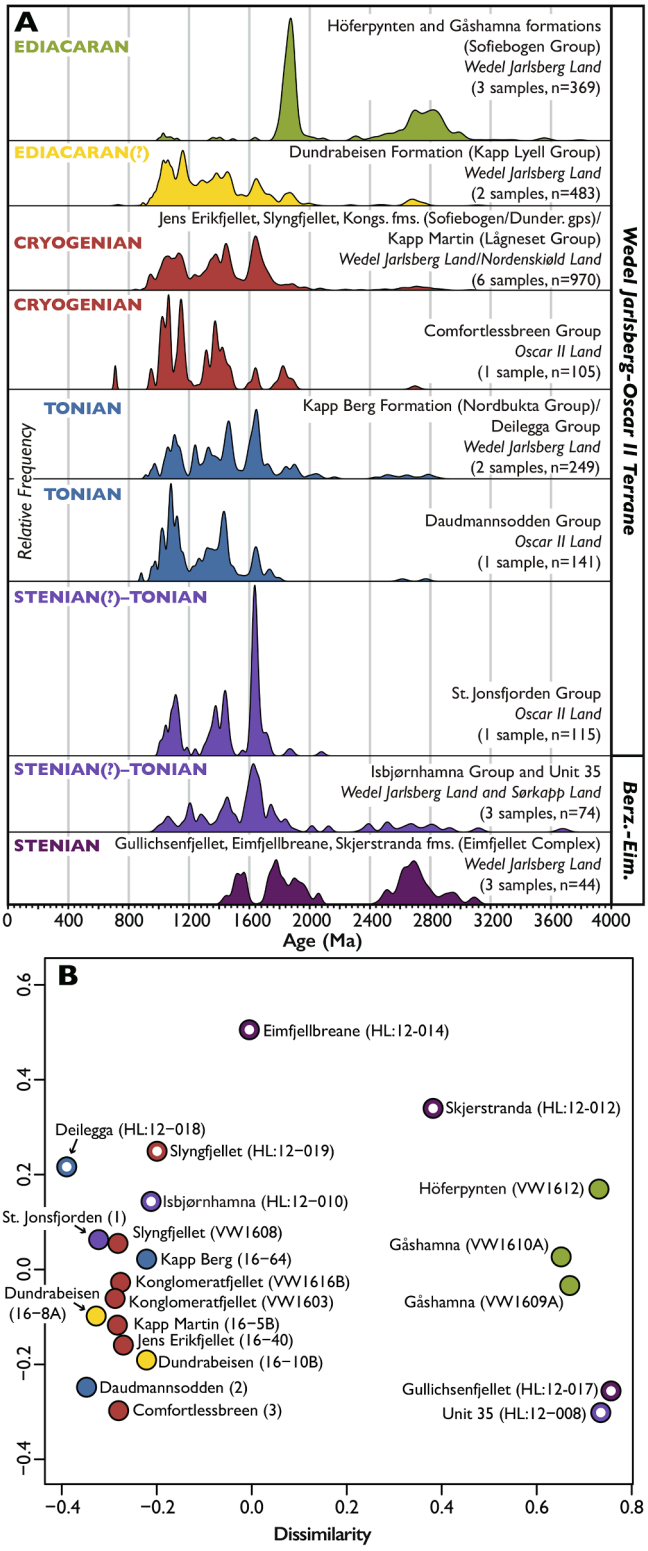

Fig. 15. A) Normalized probability density plots for detrital zircon U-Pb data from previously published samples in the Southwestern Basement Province and new samples presented herein from the Wedel Jarlsberg-Oscar II and Berzeliuseggene-Eimfjellet terranes. Prior to making this comparison plot, all data were filtered for >10% discordance, >5% reverse discordance, and >10% 2σ uncertainty in $^{206}Pb/^{238}U$ or $^{207}Pb/^{206}Pb$ ages. Errors were converted to 1σ and then the $^{206}Pb/^{238}U$ ratio was used to calculate an age for analyses younger than 1200 Ma and the $^{207}Pb/^{206}Pb$ result for analyses older than 1200 Ma. Published U-Pb data are from the following datasets: Deilegga Group (Sample HL:12–018; Ziemniak et al., 2019); Slyngfjellet Formation (Sample HL:12–019, Ziemniak et al., 2019); Isbjørnhamna Group (Samples HL:12–008, HL:12–010, and Sp21/08; Ziemniak et al., 2019); Eimfjellet Complex (Samples HL:12–012, HL:12–014, HL:12–017; Ziemniak et al., 2019); St. Jonsfjorden Group (Sample 1; Gasser and Andresen, 2013); Daudmannsodden Group (Sample 2; Gasser and Andresen, 2013); Comfortlessbreen Group (Sample 3; Gasser and Andresen, 2013). **B)** Multi-dimensional scaling (MDS) plot (Vermeesch, 2013) of the same data presented in A) except all samples are plotted individually. Samples with <50 individual zircon U-Pb analyses are shown as partially filled circles to highlight ambiguity for provenance comparison. Data were plotted using IsoplotR (Vermeesch, 2018). Kongs.–Konglomeratfjellet Formation; Dunder.–Dunderbukta Group; gps–groups; fms.–formations.

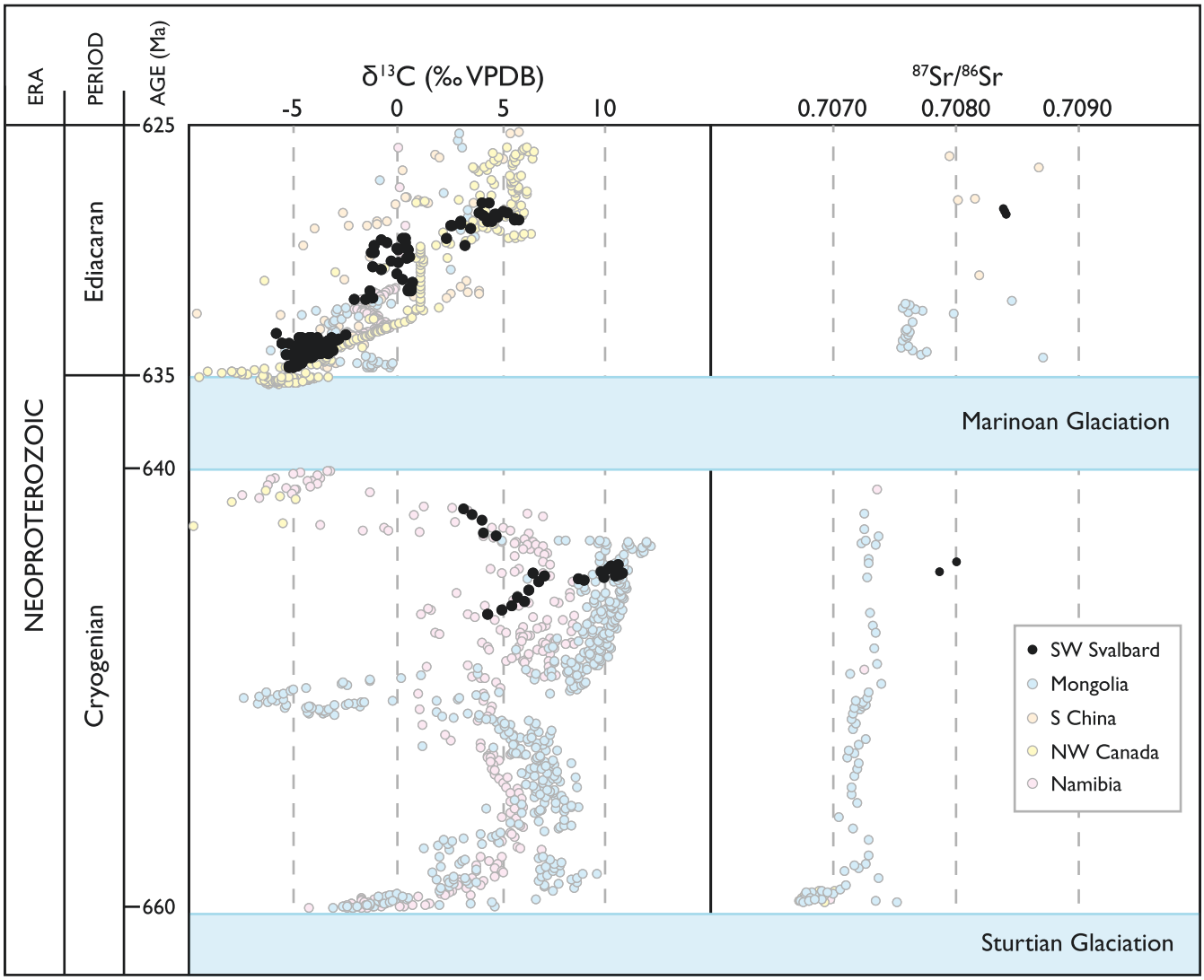

Fig. 16. Global correlations of Cryogenian and basal Ediacaran strata after Bold et al. (2016). Data are color coded with geographic information: Black = Wedel Jarlsberg-Oscar II terrane of southwestern Svalbard (this paper), Blue = Mongolia (Bold et al., 2016), Orange = South China (Sawaki et al., 2010; Zhu et al., 2013), Yellow = NW Canada (Kaufman et al., 1993; Macdonald et al., 2013; Narbonne et al., 1994; Rooney et al., 2014, 2015), Pink = Namibia (Halverson et al., 2005). The $^{87}Sr/^{86}Sr$ data is from SW Svalbard (this paper), Mongolia (Brasier et al., 1996; Shields et al., 2002; Bold et al., 2016), South China (Sawaki et al., 2010; Cui et al., 2019), NW Canada (Kaufman et al., 1993; Narbonne et al., 1994; Rooney et al., 2014), and Namibia (Kaufman et al., 1993; Yoshioka et al., 2003; Halverson et al., 2007).

Group are Cryogenian or Ediacaran in age, although we propose they are most likely equivalent with the Ediacaran Gåshamna and Dunderdalen formations (see below).

Poorly understood Neoproterozoic phyllite, metacarbonate, and matrix-supported conglomerate of the Lågneset and Lågnesbukta groups are also exposed on both the northern and southern shorelines of Nordenskiöld Land (Figs. 3, 5, S2; Harland et al., 1993; Hjelle et al., 1986; Dallmann, 2015a). As highlighted previously, zircon analyzed from a granite clast in glaciogenic diamictite of the Kapp Linné Formation (Lågnesbukta Group) yielded a U-Pb crystallization age of 973 ± 10 Ma with a 656 ± 5 Ma metamorphic rim (Figs. 2, 3, 14; Larionov and Teben'kov, 2004). This U-Pb age is similar to Tonian basement clasts described herein from the Slyngfjellet and Dundrabeisen formations (Fig. 13), and the metamorphic rim age is consistent with metamorphic and geochronological ages on the Torellian unconformity. Based on these preliminary data, we suggest the Kapp Linné Formation records the Marinoan snowball Earth glaciation and is therefore correlative with the Comfortlessbreen Group within Oscar II Land and the Konglomeratfjellet and Slyngfjellet formations of Wedel Jarlsberg Land. The documentation of an angular unconformity beneath the Comfortlessbreen Group and the presence of the ca. 656 Ma metamorphic rim on zircon in the Kapp Linné Formation provide evidence for the Torellian event outside of Wedel Jarlsberg Land, most likely as a characteristic feature of the Wedel Jarlsberg-Oscar II terrane.

5.1.1.4. Ediacaran units and correlations. The Höferpynten and Slettfjelldalen formations of Wedel Jarlsberg Land are sharply overlain by ~2 km of poorly exposed black to green slate and phyllite that are interbedded with minor quartzite and metacarbonate of the Gåshamna and Dunderdalen formations (Figs. 3, 4; Bjørnerud, 1990; Birkenmajer, 1992; Czerny et al., 1993; Dallmann et al., 1993b). These units record deep-water sedimentation dominated by sediment-gravity flows (Birkenmajer, 1992; Harland et al., 1993), while rare deformed dolostone horizons have been interpreted as olistostrome (Bjørnerud, 1990). Notably, this prominent shift in depositional environment is accompanied by a profound change in provenance that apparently manifests itself first in the basal Ediacaran Höferpynten Formation (Figs. 12, 15); both the Höferpynten and Gåshamna formations record bimodal

Paleoproterozoic and Neo- to Meso-archean zircon age populations, which stand in stark contrast to the diverse Mesoproterozoic age populations that dominate most other metasedimentary units in the SBP (Fig. 12).

The contact between the Gåshamna/Dunderdalen formations and structurally overlying strata of the glaciogenic Kapp Lyell Group (Fig. 4; or Bellsund Group of Dallmann, 2015a) in northern Wedel Jarlsberg Land was previously interpreted as conformable due to the presence of transitional "dropstones" in the uppermost Dunderdalen Formation (Bjørnerud, 2010). Instead, we agree with previous mapping studies that considered the contact structural in nature (e.g., Dallmann et al, 1990; Birkenmajer, 2010; Dallmann, 2015a) and hypothesize that these clasts represent isolated tectonic boudins in previously mapped younger fault zones between the two map units.

Bjørnerud (2010) correlated glacial deposits of the Kapp Lyell Group ("Sequence") with the Cryogenian Marinoan glaciation based on the assumption that the stratigraphically underlying Konglomeratfjellet Formation represented deposits of the ca. 717–660 Ma Sturtian glaciation. Our new stratigraphic, sedimentological, and geochemical results indicate a Marinoan age for the Konglomeratfjellet Formation, so it follows that the Kapp Lyell Group may instead record the ca. 580–579 Ma Gaskiers glaciation (Pu et al., 2016). Since the contact between the basal Dundrabeisen Formation of the Kapp Lyell Group and underlying Ediacaran stata is faulted, it is also plausible the Kapp Lyell Group represents a tectonic repetition of the Konglomeratfjellet Formation or an older thrust sheet of hitherto unknown Sturtian glacial deposits; however, we suggest the most parsimonious interpretation is that the Kapp Lyell Group records the Gaskiers glaciation because: 1) it is lithologically distinct from the Slyngfjellet Formation, 2) it contains clasts of the underlying basal Ediacaran Slettfjelldalen Formation (Bjørnerud, 2010), 3) it appears to lack an associated cap carbonate unit.

Metagabbro, metadolerite, and greenstone exposures in the Chamberlindalin region of northern Wedel Jarlsberg Land and southern Nordenskiöld Land (Figs. 3, 5) were originally mapped as volcanic and plutonic equivalents to the Cryogenian Jens Erikfjellet Formation (Dallmann et al., 1993b). More recent geochemical investigations indicate these units in Wedel Jarlsberg Land are geochemically distinct from the Jens Erikfjellet Formation and instead record an alkali cumulate magma plumbing system that developed at a depth of ~30–50 km (Czerny, 1999; Gołuchowska et al., 2016). Importantly, these mafic volcanic and plutonic rocks are mapped as Ediacaran(?) bodies intruding phyllite and quartzite of the Ediacaran Dunderdalen Formation (Dallmann, 2015a; Gołuchowska et al., 2016); however, no geochronological, geochemical, or petrographic data exist to support this age relationship, and both the Dunderdalen and Gåshamna units have no known mafic intrusive rocks outside of the Chamberlindalin region in Wedel Jarlsberg Land. Despite this, the Stenian(?)–Tonian St. Jonsfjorden Group of Oscar II Land is locally intruded by abundant mafic dikes and sills (Harland et al., 1979; Ohta, 1985; Burzyński et al., 2017), one of which recently yielded an isotope dilution-thermal ionization mass spectrometry (ID-TIMS) age on baddeleyite of 560 ± 12 Ma (2σ; Gumsley et al., 2020). Therefore, it is possible that the pre-Caledonian mafic dikes and sills of southern Nordenskiöld Land and Chamberlindalen are a southern continuation of these unnamed ca. 560 Ma intrusive rocks (Gumsley et al., 2020). This relationship may highlight a much more extensive Ediacaran magmatic event that affected the Wedel Jarlsberg-Oscar II terrane following the Cryogenian Torellian orogeny.

5.1.1.5. Early Paleozoic High-Pressure and ophiolitic rocks. The Wedel Jarlsberg-Oscar II terrane hosts an allochthonous belt of early Paleozoic (Caledonian) high-pressure rocks and small ophiolitic slivers (the Vestgötabreen Complex) that are discontinuously exposed from Kongsvegen to central Nordenskiöld Land (Figs. 2, 3; Horsfield, 1972; Ohta, 1979; Hirajima et al., 1984; Dallmeyer et al., 1990; Bernard-Griffiths et al., 1993; Ohta et al., 1995; Agard et al., 2005; Labrousse et al., 2008; Kośmińska et al., 2014; Barnes et al., 2020). In the Vestgötabreen Complex of the St. Jonsfjorden region of Oscar II Land, these high-pressure rocks include blueschist, eclogite, garnet-phengite schist, carpholite schist, marble, serpentinite, greenstone, and magnesite (Hirajima et al., 1984; Agard et al., 2005; Labrousse et al., 2008; Barnes et al., 2020) that are unconformably overlain by Middle Ordovician to early–middle Silurian carbonate and siliciclastic rocks of the Bullbreen Group (Fig. 3; Scrutton et al., 1976; Harland et al., 1979; Armstrong et al., 1986). Retrograde garnet-bearing blueschists were also identified in central Nordenskiöld Land (Kośmińska et al., 2014). Although it may be prudent to eventually separate out these allochthonous rocks of the Vestgötabreen Complex as an independent terrane or subterrane, their local juxtaposition with Wedel Jarlsberg-Oscar II terrane rocks, as well as their linked metamorphic history, provides an important constraint on the position and setting of this terrane during the Caledonian orogen.

5.1.2. Prins Karls Forland terrane

The Prins Karls Forland terrane (Harland, 1997) is only exposed on Prins Karls Forland, a narrow ~80 km long island off the west coast of Spitsbergen (Figs. 2, 14), and it is separated from the remainder of the SBP by the N-S-trending Eurekan Forlandsundet Graben (e.g., Kleinspehn and Teyssier, 1992; von Gosen and Paech, 2001; Bergh et al., 2003; Dallmann, 2015a, 2015b). Mesoproterozoic(?)–Neoproterozoic metasedimentary rocks of the Prins Karls Forland terrane are broadly separated into two regions by the N-S-trending Eurekan Baklia Fault (Fig. 2; Dallmann, 2015a, 2015b). West of this fault, a >4 km thick package of Cryogenian(?)–Ediacaran microfossil-bearing slate, phyllite, quartzite, metaconglomerate, greenstone, and metacarbonate of the Grampianfjella and Scotiafjellet groups is faulted against amphibolite facies metasedimentary rocks of the <950 Ma Pinkiefjellet Group, which consists of mylonitized and garnet-bearing metapelite, quartzite, and minor metacarbonate (Figs. 3, S5; Knoll and Ohta, 1988; Harland et al., 1979; Hjelle et al., 1979, 1999; Manby, 1986; Dallmann, 2015a; Kośmińska et al., 2020). The Grampianfjella and Scotiafjellet Group metasedimentary rocks are also locally fault-bounded with the polydeformed early Paleozoic Macnairrabbane unit, which consists of quartz-carbonate schist, phyllite, and metaconglomerate with rare Cambrian or younger fossiliferous debris (Hjelle et al., 1999; Piepjohn et al., 2000). Neoproterozoic successions east of the Baklia Fault (Figs. 3, S5) include >600 m of matrix-supported conglomerate (Ferrierpiggen Group), ~750 m of calcareous phyllite and metacarbonate (Geikiebreen Group), and ~1.3 km of predominantly green phyllite that is interbedded with metasandstone, marble, and mafic metavolcanic rocks (Peachflya Group; Harland et al., 1993; Dallmann, 2015a, 2015b).

The Pinkiefjellet Group of the Prins Karls Forland terrane experienced Ellesmerian (ca. 375–355 Ma) amphibolite facies metamorphism (Kośmińska et al., 2020). Although unpublished detrital zircon U-Pb data from quartzites in the Pinkiefjellet Group appear to be similar to Neoproterozoic samples presented herein from the other SBP terranes (Kośmińska et al., 2015), this Late Devonian–early Carboniferous metamorphic history is unique within the SBP. As discussed by Kośmińska et al. (2020), this raises the possibility that widespread "Caledonian" deformation in metasedimentary rocks of the Prins Karls Forland terrane may instead be Ellesmerian; however, another possibility is that the Prins Karls Forland terrane is itself composite in nature, with the local juxtaposition of different crustal fragments recording unique sedimentary and metamorphic histories. Either way, at least three distinct phases of pre-Eurekan ductile and brittle deformation, as well as widespread Eurekan brittle thrusting and strike-slip displacement, have affected the Proterozoic and early Paleozoic basement rocks throughout the Prins Karls Forland terrane (e.g., Harland et al., 1979; Hjelle et al., 1979, 1999; Morris, 1982; Manby, 1986; Piepjohn et al., 2000; Dallmann, 2015a, 2015b; Schneider et al., 2019; Kośmińska et al., 2020); as a result, the internal stratigraphic architecture and detailed correlations of the Proterozoic and early Paleozoic basement rocks remain speculative (Dallmann, 2015b). Given this, we argue this crustal

fragment likely occupied a unique position in the Caledonian and Ellesmerian orogens and should therefore remain distinguished from the other crustal fragments of the SBP (Harland, 1997) until further examination.

5.1.3. Berzeliuseggene-Eimfjellet terrane (new name)

Mesoproterozoic–Tonian metasedimentary and metaigneous rocks of the Berzeliuseggene-Eimfjellet terrane outcrop in two narrow belts along the northeastern and southwestern edges of Wedel Jarlsberg Land (Fig. 14), where they are locally juxtaposed by Caledonian and/or Eurekan fault zones (or widespread glacially covered areas) with rocks of the Wedel Jarlsberg-Oscar II terrane (Czerny et al., 1993; Mazur et al., 2009; Majka et al., 2015; Faehnrich et al., 2020). These rocks were not originally distinguished as a separate terrane by Harland (1997), and correlative metasedimentary rocks of the Stenian(?)–Tonian Isbjørnhamna Group were recently recognized on southern Sørkapp Land (Ziemniak et al., 2019), extending the geographic range of this terrane.

The oldest exposed basement to the Berzeliuseggene-Eimfjellet terrane consists of the ca. 1200 Ma Eimfjellet Complex of southwestern Wedel Jarlsberg Land (Figs. 2, 3, S3), which comprises metamorphosed mafic and felsic flows and tuffs that are intercalated with lenses of metagabbro and metagranite (Balašov et al., 1995, 1996; Czerny, 1999; Larionov et al., 2010). These metaigneous and metasedimentary units are in fault contact with schist, quartzite, and marble of the Stenian(?)–Tonian Isbjørnhamna Group (Ziemniak et al., 2019), the latter of which was distinguished based on provenance from the age-equivalent Nordbukta, Deilegga, St. Jonsfjorden, and Daudmannsodden groups of the Wedel Jarlsberg-Oscar II terrane (Ziemniak et al., 2019). Our new U-Pb detrital zircon data still broadly support this distinction, especially the distinct lack of Tonian detrital zircon in the Isbjørnhamna Group (Fig. 15), although we stress that the published detrital zircon data from the Eimfjellet Complex are low-n. Both the Eimfjellet Complex and Isbjørnhamna Group record ca. 640 Ma (Torellian) metamorphic resetting (Manecki et al., 1998; Majka et al., 2008; Czerny et al., 2010; Larionov et al., 2010); their juxtaposition is assumed to be related to Torellian contraction (e.g., Majka et al., 2010, 2014; Ziemniak et al., 2019), although it is also possible this faulting occurred during Caledonian deformation.

In northwestern Wedel Jarlsberg Land, Tonian (ca. 950 Ma) felsic augen gneiss, pegmatite, amphibolite, schist, and fine-grained metaigneous rocks of the Berzeliuseggene unit are tectonically juxtaposed with metacarbonate, quartzite, and metaconglomerate of the Sofiebogen and Deilegga groups of the Wedel Jarlsberg-Oscar II terrane (Fig. 14; Majka et al., 2015; Magnethøgda sequence of Dallmann et al., 1993b). The Berzeliuseggene metaigneous rocks record amphibolite facies metamorphism at ca. 640 Ma, high-pressure Caledonian metamorphism at ca. 470 Ma, and subsequent polyphase Eurekan deformation (Majka et al., 2015), locally complicating the original tectonic boundaries between the Berzeliuseggene-Eimfjellet and Wedel Jarlsberg-Oscar II terranes (Fig. 14).

The Torellian amphibolite facies metamorphic event provides a strong link between the Berzeliuseggene and Eimfjellet/Isbjørnhamna successions that we argue distinguishes these rocks from the other SBP basement terranes; despite this, their primary tectono-stratigraphic relationships to one another remain unknown and the presence of the Torellian unconformity in the adjacent Wedel Jarlsberg-Oscar II terrane suggests these two terranes share a common Cryogenian tectonic history. For example, the Berzeliuseggene metaigneous rocks could be a potential source of Tonian orthogneiss clasts in the Slyngfjellet and Dundrabeisen formations (Fig. 13), as well as the Comfortlessbreen Group and Kapp Linné Formation (Larionov and Teben'kov, 2004; Gasser and Andresen, 2013); however, this is speculative given there are a significant number of potential Tonian basement source regions in the Northeastern and Northwestern basement provinces of Svalbard, as well as in Pearya (Ellesmere Island, Canada), Greenland, Scotland, and the Scandinavian Caledonides (e.g., Kalsbeek et al., 2000, 2008; Cawood et al., 2010; Lorenz et al., 2012; McClelland et al., 2019). Notably, the expression of the Torellian event in the pre-Cryogenian basement rocks of the Berzeliuseggene-Eimfjellet and Wedel Jarlsberg-Oscar II terranes is different – one experienced widespread amphibolite facies metamorphism, while the other only experienced mild folding and cleavage development (Birkenmajer, 1975; Bjørnerud et al., 1990, 1991; Czerny et al., 1993; Majka et al., 2014). As a result, one cannot clearly demonstrate proximity based on the available data, nor can one rule out they were distal fragments in a much more extensive Cryogenian accretionary deformation event, or even that these crustal fragments were potentially juxtaposed during the Torellian orogeny itself. Structural and thermochronological work along the VKSZ documents Caledonian ca. 420–410 Ma sinistral ductile strike-slip juxtaposition of the southwestern segment of the Berzeliuseggene-Eimfjellet terrane with a portion of the Wedel Jarlsberg-Oscar II terrane (Czerny et al., 1993; Manecki et al., 1998; Mazur et al., 2009; Faehnrich et al., 2020); thus, based on the available data, this Caledonian juxtaposition history is consistent with the independent origins of these two terranes.

5.1.4. Hornsund terrane

The Hornsund terrane is exposed from central Wedel Jarlsberg Land through northern Sørkapp Land (Fig. 14) and is dominated by early Paleozoic platformal carbonate rocks of Laurentian affinity. These strata were distinguished as the Hornsund Terrane of the Central basement terrane by Harland (1997), but they are more commonly considered part of the younger Paleozoic cover sequence of the SBP (e.g., Birkenmajer, 1978a, 1978b; Dallmann, 2015a). As highlighted previously, the contact between the early Paleozoic Sofiekammen and Sørkapp Land groups of the Hornsund terrane and the Neoproterozoic Deilegga and Sofiebogen groups of the Wedel Jarlsberg-Oscar II terrane was interpreted as unconformable and sedimentary in origin (the "Jarlsbergian unconformity" of Birkenmajer, 1991; Harland, 1997, and references therein); however, Mazur et al. (2009) later reinterpreted the main exposure between the two successions as a prominent Caledonian thrust fault.

The basal ~935 m thick Sofiekammen Group (Blåstertoppen, Vardepiggen, Slaklidalen, Gnålberget, and Nørdstetinden formations) consists of sandy dolostone, limestone, and marble with thin intervals of sandstone and shale (Figs. 3, S3; Birkenmajer, 1978a; Dallmann et al., 1993b). The basal Blåstertoppen, Vardepiggen, and Slaklidalen formations all contain rare early Cambrian (Terreneuvian) *Bonnia-Olenellus* Zone trilobites and other invertebrate faunas, which provide a strong tie to the Laurentian continental margin (Major and Winsnes, 1955; Cowie, 1974; Birkenmajer and Orłowski, 1976; Harland, 1997). The overlying ~1.4 km thick upper Cambrian–Middle Ordovician Sørkapp Land Group (Wiederfjellet, Luciapynten, Dusken, Nigerbreen, Hornsundtind, and Arkfjellet formations) consists of sandy dolostone, limestone, and marble (Figs. 3, S3; Major and Winsnes, 1955; Birkenmajer, 1978b; Harland, 1997). Major and Winsnes (1955) also described Laurentian gastropods, brachiopods, and nautiloids in the Nigerbreen and Hornsundtind formations. Preliminary detrital zircon U-Pb data from the Blåstertoppen Formation yielded similar bimodal U-Pb age populations to the Höferpynten and Gåshamna formations (Kosteva et al., 2014; data tables are not published), which raises the possibility that either: 1) the Hornsund and Wedel Jarlsberg-Oscar II terranes were independent crustal fragments that shared a common source region in the Ediacaran–Cambrian; or 2) there is no terrane boundary and the early Paleozoic carbonate platform of the Hornsund terrane was built upon the Neoproterozoic basement of the Wedel Jarlsberg-Oscar II terrane. Potentially correlative and less deformed peri-Laurentian Cambrian–Ordovician platformal carbonate strata are also recognized in the Nordaustlandet terrane of the Northeastern Basement Province of Svalbard (Fortey and Bruton, 1973; Swett, 1981; Harland, 1997; Stouge et al., 2013; Dallmann, 2015a), which provides yet another possibility that the Hornsund terrane is simply a fault-bounded fragment of the Northeastern Basement Province. Given the structural relationship documented by Mazur et al. (2009) and the strong lithological, tectonic,

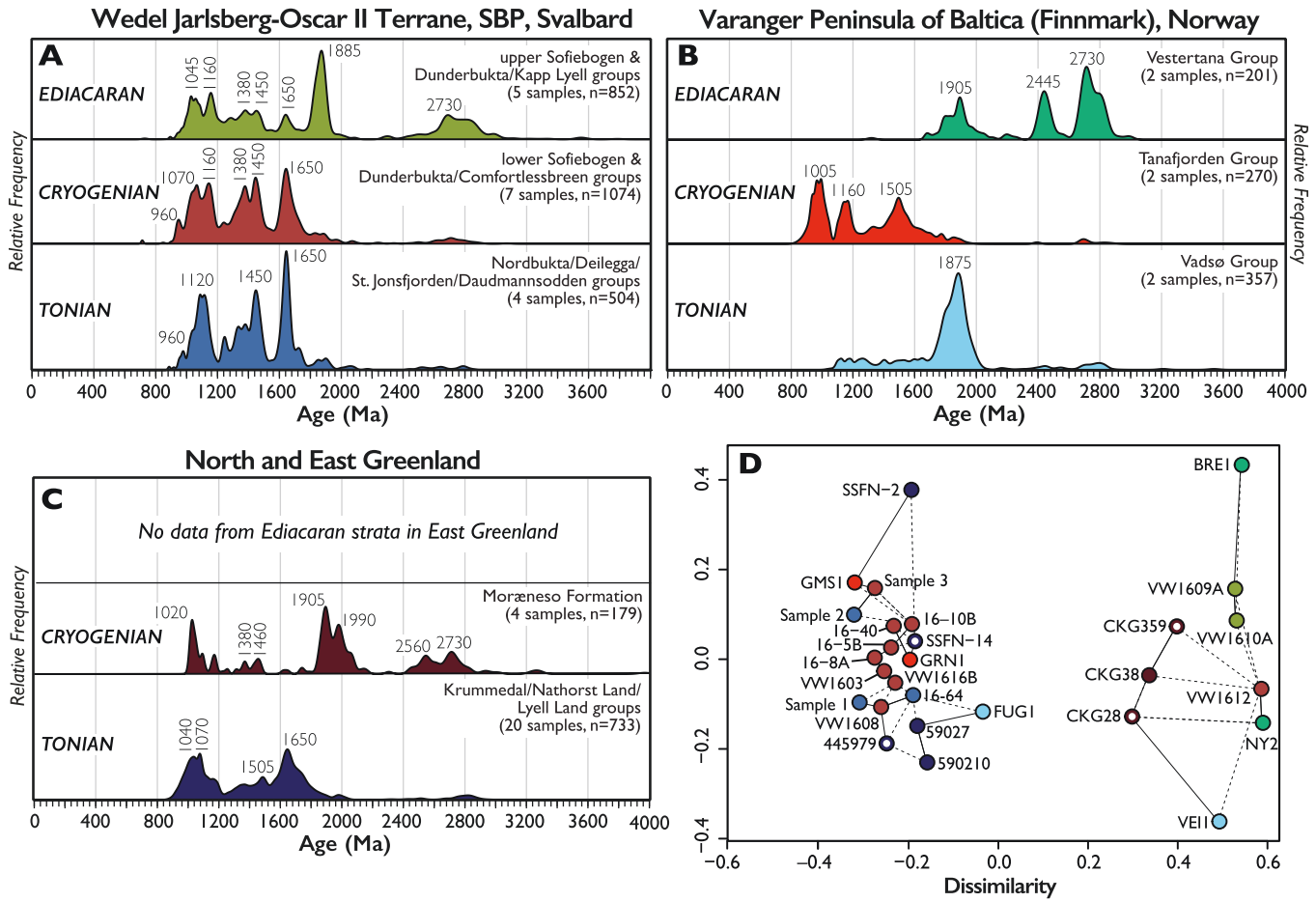

Fig. 17. Normalized probability density plots (PDP) for new and published detrital zircon U-Pb data from Tonian–Ediacaran strata of the **A)** Wedel Jarlsberg-Oscar II terrane of the Southwestern Basement Province of Svalbard, Norway, **B)** Varanger Peninsula region of northern Baltica (Finnmark), Norway, and **C)** North and East Greenland. Prior to making this comparison plot, all data were filtered for >10% discordance, >5% reverse discordance, and >10% 2σ uncertainty in $^{206}Pb/^{238}U$ or $^{207}Pb/^{206}Pb$ ages. Errors were converted to 1σ and then the $^{206}Pb/^{238}U$ ratio was used to calculate an age for analyses younger than 1200 Ma and the $^{207}Pb/^{206}Pb$ result for analyses older than 1200 Ma. In addition to new data presented herein, published U-Pb data are from the following datasets: Deilegga Group (Sample HL:12-018; Ziemniak et al., 2019); Slyngfjellet Formation (Sample HL:12-019, Ziemniak et al., 2019); St. Jonsfjorden Group (Sample 1; Gasser and Andresen, 2013); Daudmannsodden Group (Sample 2; Gasser and Andresen, 2013); Comfortlessbreen Group (Sample 3; Gasser and Andresen, 2013); Krummedal Succession (GGU249933, Strachan et al., 1995; GGU452619, GGU452625, Leslie and Nutman, 2003; 441337, 441341, 441383, Watt et al., 2000); Nathorst Land Group (445935, 445979, Watt et al., 2000; 201728, 201836, 201893, 201991, Dhuime et al., 2007; 590204, 590207, 590210, 590214, 590232, Olierook et al., 2020); Lyell Land Group (SSFN-14, SSFN-2, SSFN-9, Sláma et al., 2011); Moræneso Formation (CKG28, CKG359, CKG38, CKG4, Kirkland et al., 2009); Vadsø Group (FUG1, VEI1, Zhang et al., 2015); Tanafjorden Group (GRN1, GMS1, Zhang et al., 2015); and Vestertana Group (BRE1, Zhang et al., 2015; NY2-07, Roberts and Siedlecka, 2012). **D)** Multi-dimensional scaling (MDS) plot (Vermeesch, 2013) of the same data presented in A), except for samples with <25 zircon grains (following filtering procedures discussed above). Samples with <50 individual zircon U-Pb analyses are shown as partially filled circles to highlight potential ambiguity in their comparisons. Data were plotted using IsoplotR (Vermeesch, 2018); individual units are color-coded to match their respective PDP and then labeled with their primary sample ID. Each sample is connected to its closest neighbor in Kolmogorov-Smirnov space with a solid line and to its second closest neighbor with a dashed line (Vermeesch, 2013, 2018).

and paleobiogeographic contrasts between the Hornsund and other SBP terranes, we suggest the Hornsund terrane should be considered an independent tectonic block (Figs. 3, 14).

5.2. *Regional comparisons within the North Atlantic and Circum-Arctic*

Paleogeographic reconstructions of the North Atlantic and Arctic Caledonides have placed the SBP along both the margins of Laurentia and Baltica prior to the Caledonian orogeny. Harland and Wright (1979) proposed that the SBP originated outboard of the northeastern Greenland margin and was later displaced northwards via sinistral strike-slip faulting during a late stage of the Caledonian Orogeny. This hypothesis was supported by subsequent sedimentological and igneous comparisons between the SBP and East Greenland Caledonides, including the presence of deformed Tonian magmatic rocks overlain by Neoproterozoic glaciogenic diamictite and early Paleozoic platformal carbonate with Laurentian trilobite faunas (Kalsbeek et al., 2000, 2008; Leslie and Nutman, 2003; Larionov and Teben'kov, 2004; Sønderholm et al., 2008; Gasser and Andresen, 2013; Majka et al., 2014).

More recently, correlations between East Greenland and the SBP have been extended through similarities in detrital zircon U-Pb age spectra and associated Hf isotopic data (Olierook et al., 2020). For example, the Tonian Nathorst Land and Lyell Land groups (Eleonore Bay Supergroup) in East Greenland (Fig. 1) and the structurally underlying Stenian–Tonian(?) Krummedal Group have prominent U-Pb age peaks at ca. 1650, broad ca. 1490–1030 Ma age populations, and sparse Paleoproterozoic to Archean grains (Kalsbeek et al., 2000; Watt et al., 2000; Dhuime et al., 2007; Olierook et al., 2020), which are broadly similar to age populations in the Stenian(?)–Tonian St. Jonsfjorden, Nordbukta, and Deilegga groups (Fig. 17; Gasser and Andresen, 2013; Malone et al., 2014; Ziemniak et al., 2019). These Mesoproterozoic, Paleoproterozoic, and Archean zircon age populations in East Greenland are dominated by

intermediate $\varepsilon Hf_{(t)}$ values that range from −8 to +5 (Slama et al., 2011; Olierook et al., 2020), which are broadly similar to our new Hf isotopic data from the Nordbukta Group (Fig. 12).

Previous researchers have also correlated metasedimentary rocks of the SBP with the Hekla Sund area of eastern North Greenland (Fig. 1; Harland, 1997; Gee and Teben'kov, 2004), where Mesoproterozoic(?)–Neoproterozoic syn-rift deposits of the Rivieradal Group are conformably overlain by the Neoproterozoic Hagen Fjord Group (Sønderholm et al., 2008). Marinoan diamictite of the Moræneso Formation (Hagen Fjord Group) contains abundant ca. 2000–1800 Ma zircon grains and subordinate Archean and Mesoproterozoic age populations (Kirkland et al., 2009). This large ca. 2000–1800 Ma peak is missing from the age equivalent Konglomeratfjellet and Slyngfjellet formations of the Wedel Jarlsberg terrane (Fig. 12), but it does appear in the overlying Ediacaran Höferpynten and Gåshamna formations (Fig. 17).

Despite these broad similarities in provenance, our new stratigraphic constraints from the Wedel Jarlsberg-Oscar II terrane reveal fundamental differences with Neoproterozoic sedimentary successions in North and East Greenland. First, evidence for ca. 650–640 Ma Torellian deformation is absent in Greenland, except perhaps in allochthonous Paleozoic thrust sheets in Johannes V. Jensen Land of North Greenland (Rosa et al., 2016). Furthermore, the Tonian sedimentary successions of Greenland are lithologically distinct and considerably thicker (~8.5–14 km thick) than age-equivalent successions in the SBP (e.g., Sønderholm et al., 2008, and references therein). Finally, glacial sedimentation associated with the ca. 580–579 Ma Gaskiers glaciation has not been described in Greenland or autochthonous Laurentia, and the Neoproterozoic successions of Greenland as a whole contain considerably less Ediacaran strata than the Wedel Jarlsberg-Oscar II terrane, where the combined thickness is greater than ~4 km.

The presence of ca. 650–640 Ma Torellian deformation in the SBP supports a stronger link with the earliest phases of the Timanide accretionary orogen of northern Baltica (Fig. 1; Mazur et al., 2009; Majka et al., 2010, 2012, 2014, 2015), which is also supported by preliminary provenance and paleomagnetic studies from the Wedel Jarlsberg-Oscar II and Berzeliuseggene-Eimfjellet terranes (Gasser and Andresen, 2013; Michalski et al., 2017; Ziemniak et al., 2019). Neoproterozoic sedimentary successions associated with the Timanian orogen are exposed on the Varanger, Rybachi, and Sredni peninsulas of northern Norway (Finnmark) and northwestern Russia (Fig. 1; Siedlecka, 1985; Siedlecka and Roberts, 1992; Siedlecka et al., 2004; Roberts and Siedlecka, 2012). South of the prominent Trollfjorden-Komagelva Fault Zone (TKFZ; Siedlecka and Roberts, 1992) on Varanger Peninsula (Fig. 1), Neoproterozoic strata of the Vadsø, Tanafjorden, and Vestertana groups are well exposed (Edwards et al., 1973; Edwards, 1984; Siedlecka, 1985; Rice, 1994; Rice et al., 2011) and provide a potential correlative succession for the Wedel Jarlsberg-Oscar II and other SBP terranes. The Tonian–Cryogenian Vadsø and Tanafjorden groups broadly record a transition from siliciclastic- to carbonate-dominated strata (Edwards et al., 1973; Edwards, 1984; Siedlecka et al., 2004) that are similar to the Nordbukta and Deilegga groups. These rocks are separated by an angular unconformity from the overlying late Cryogenian–Ediacaran Vestertana Group, reflecting the transition from a passive to active margin associated with Timanian arc-continent collision (Siedlecka et al., 2004). We propose this may be equivalent to the Torellian unconformity in the Wedel Jarlsberg-Oscar II terrane of the SBP. The Vestertana Group includes two glaciogenic deposits, the Smalfjord and Mortensnes formations, which have been correlated with the Marinoan and Gaskiers glaciations, respectively (Siedlecka, 1985; Halverson et al., 2005; Rice et al., 2011); these deposits reflect a clear stratigraphic link with the Slyngfjellet/Konglomeratfjellet/Kapp Linné formations (and Comfortlessbreen Group) and the Kapp Lyell Group of the Wedel Jarlsberg-Oscar II terrane. The younger Mortensnes Formation is conformably overlain by deep-water strata of the upper Vestertana Group (Rice et al., 2011), which may be correlative with the Dunderdalen and Gåshamna formations.

Detrital zircon U-Pb age spectra from the Tanafjorden Group include ca. 1600–1400, 1350–1000, and 1000–900 Ma age populations with scattered Paleoproterozoic to Archean grains (Fig. 17; Zhang et al., 2015); these data are similar to the age-equivalent Deilegga and Nordbukta groups. Critically, the Ediacaran Nyborg and Stáhpogieddi formations (Vestertana Group) contain distinct bimodal ca. 1800 and 2850 Ma U-Pb age peaks (Roberts and Siedlecka, 2012; Zhang et al., 2015), which is similar to the provenance shift recorded in the Höferpynten and Gåshamna formations of the Wedel Jarlsberg-Oscar II terrane (Fig. 17). Thus, not only does the general stratigraphy of the Norwegian Varanger Peninsula match the sedimentary successions of Wedel Jarlsberg Land, but so does the timing and significance of its major provenance shifts.

Neoproterozoic and early Paleozoic successions of the SBP have also been correlated with coeval rocks of various circum-Arctic terranes (e.g., Gee and Teben'kov, 2004; Amato et al., 2009; Colpron and Nelson, 2009; Cocks and Torsvik, 2011; Malone et al., 2014; O'Brien et al., 2016; Hoiland et al., 2018). For example, the similar Ordovician tectonic history of the SBP and the Pearya terrane of Ellesmere Island (Fig. 1), Canada, was originally recognized by Harland and Wright (1979), while subsequent authors have expanded on this proposed link through more focused stratigraphic, metamorphic, and geochronological studies (Trettin, 1989; Ohta, 1994; Gee and Page, 1994; Gee and Teben'kov, 2004; Mazur et al., 2009; Kośmińska et al., 2014; Malone et al., 2014). A similar argument can be made for various continental fragments in the Arctic Alaska–Chukotka microplate of northeastern Russia and northern Alaska, which consists of a suite of amalgamated peri-Laurentian and peri-Baltican terranes that were juxtaposed prior to the Carboniferous along the northern margin of Laurentia (Amato et al., 2009; Miller et al., 2011, 2018; Strauss et al., 2013, 2017, 2019; Till et al., 2014; Hoiland et al., 2018). Thick metasedimentary successions of the southwestern subterranes (Strauss et al., 2013) of the Arctic Alaska–Chukotka microplate consist of poorly understood Tonian orthogneiss and mafic intrusive rocks and overlying Neoproterozoic metasedimentary successions with prominent U-Pb detrital zircon populations of ca. 1800–950 Ma with subordinate Archean grains (Hoiland et al., 2018). This is similar to the Wedel Jarlsberg-Oscar II terrane, and these data highlight potential linkages to the SBP across the Arctic Ocean.

5.3. *Implications for the origin and assembly of the SBP*

Neoproterozoic metasedimentary rocks of the Wedel Jarlsberg-Oscar II terrane record a Stenian(?)–Tonian passive margin succession that was deformed prior to ca. 650 Ma and then unconformably overlain by glaciogenic strata related to the Marinoan and Gaskiers glaciations (Fig. 3). Indications of subaerial exposure at the Torellian unconformity surface, along with the presence of reworked clasts of the Deilegga and Nordbukta groups in the Cryogenian Thiisfjellet, Konglomeratfjellet, and Slyngfjellet formations, provides sedimentological evidence for uplift and exposure of the local Tonian basement prior to Sofiebogen, Dunderbukta, Comfortlessbreen, Lågneset, and Kapp Lyell Group sedimentation. The Cryogenian Slyngfjellet Formation of the Sofiebogen Group locally interfingers with mafic flows of the Jens Erikfjellet Formation (Czerny et al., 1993). The geochemical composition of dikes and sills in the Jens Erikfjellet Formation (Czerny, 1999), along with its volcano-stratigraphic characteristics and stratigraphic position, are consistent with the interpretation that regional Cryogenian volcanism in the Wedel Jarlsberg-Oscar II terrane directly overlapped with the end of the Torellian orogeny and the terminal phase of the Marinoan glaciation. Taken together, these data indicate that the Wedel Jarlsberg-Oscar II terrane may either record distal foreland basin sedimentation associated with the Torellian orogeny and/or syn- to post-collisional rift-related sedimentation. Given the similarities discussed above with the northern margin of Baltica, we suggest the Torellian and Timanide orogens are local expressions of the same accretionary system, and we propose that the Wedel Jarlsberg-Oscar II and Berzeliuseggene-Eimfjellet terranes likely originated in proximity to northern Baltica (Fig. 18).

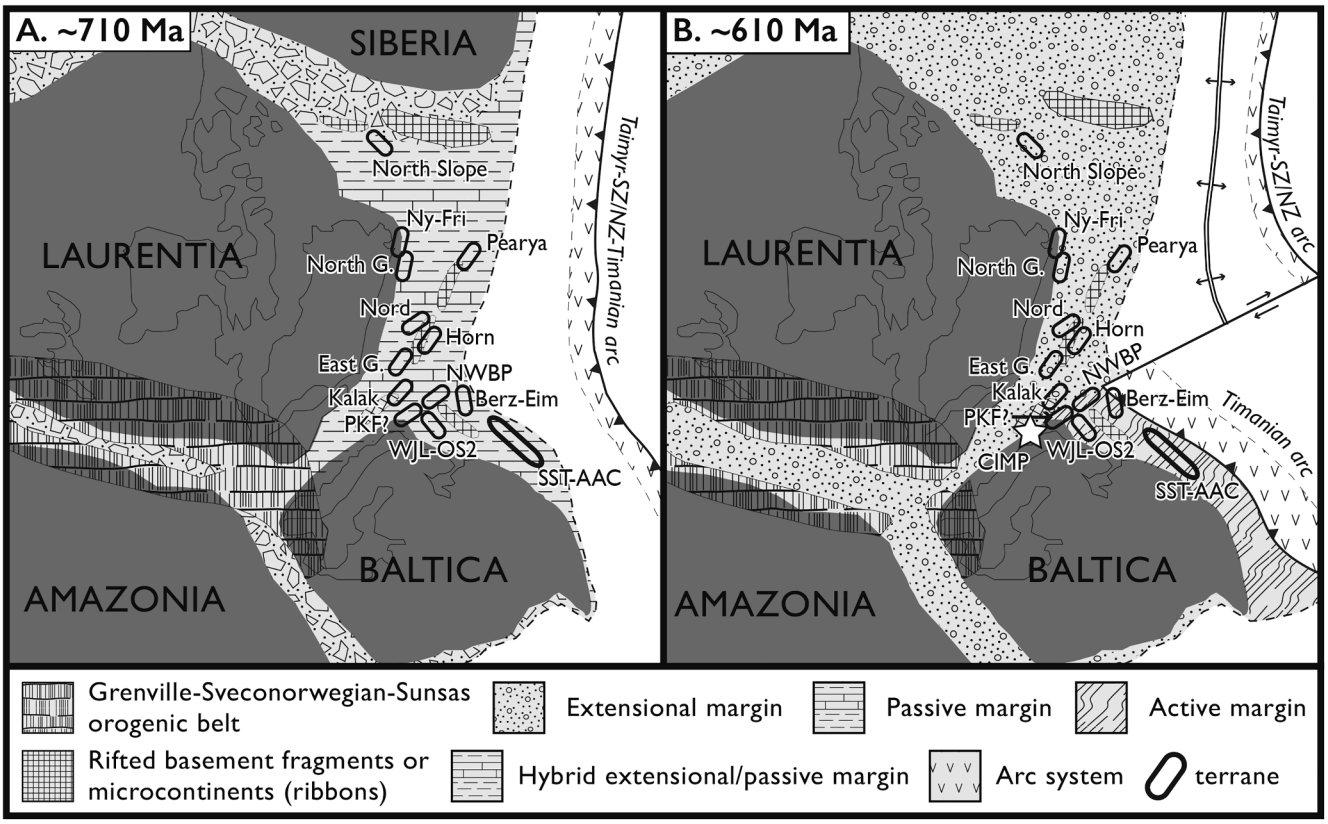

Fig. 18. Schematic Neoproterozoic paleogeographic reconstructions of the North Atlantic-Arctic Caledonides modified after Malone et al. (2014) and Bazarnik et al. (2019). See text for discussion. North G.–North Greenland; Ny-Fri–Ny Friesland terrane, Northeast Basement Province of Svalbard; Nord–Nordaustlandet terrane, Northeastern Basement Province of Svalbard; East G.–East Greenland; Kalak–Kalak Nappe Complex of Norway; NWBP–Northwest Basement Province of Svalbard; Berz-Eim–Berzeliuseggene-Eimfjellet terrane, Southwestern Basement Province of Svalbard; WJL-OS2–Wedel Jarlsberg-Oscar II terrane, Southwestern Basement Province of Svalbard; PKF?–Prins Karls Forland terrane of the Southwestern Basement Province (question marks denotes uncertainty in affinity to Laurentia or Baltica); CIMP–Central Iapetus magmatic province (centralized location denoted by white star); SST-AAC–southwestern subterranes of the Arctic Alaska–Chukotka microplate.

Middle Ediacaran (ca. 560 Ma) magmatism in the Wedel Jarlsberg-Oscar II terrane is geochemically and temporally similar to the Seiland Igneous Province of northwestern Baltica (Gołuchowska et al., 2016; Gumsley et al., 2020), which is an alkaline ultramafic–mafic magmatic complex that was emplaced between ca. 570 and 560 Ma (Roberts et al., 2006; Larsen et al., 2018). Previous researchers have linked the Seiland Igneous Province to geochemically similar dike swarms on the northern margin of Baltica related to the Central Iapetus Magmatic Province (Larsen et al., 2018). This link, together with stratigraphic ties to Tonian–Ediacaran strata of the Varanger Peninsula, further supports restoration of the Wedel Jarlsberg-Oscar II terrane to a position along the northern margin of Baltica during the Neoproterozoic–early Paleozoic break-up of Rodinia (Fig. 18).

Critically, however, the terminal Ediacaran and overlying early Paleozoic stratigraphy of Baltica and the SBP terranes are fundamentally different. For example, the Ediacaran Mortensnes Formation of the Varanger Peninsula, Norway, is conformably overlain by thick packages of latest Ediacaran to early Cambrian siliciclastic strata (Rice et al., 2011; Högström et al., 2013), while rocks of this age and setting are mostly absent from the SBP (perhaps except in the Prins Karls Forland terrane). Moreover, Cambrian-Ordovician carbonate platform strata of the Hornsund terrane, SBP, have strong Laurentian stratigraphic and faunal affinities (Major and Winsnes, 1955; Birkenmajer and Orłowski, 1976; Birkenmajer, 1978b, 1978a); therefore, it is unlikely this terrane has anything to do with the continental margin of Baltica (Fig. 18), and it is more likely it was juxtaposed later with the other terranes of the SBP. In order to rectify these fundamental differences, we suggest the peri-Baltican terranes of the SBP (Wedel Jarlsberg-Oscar II, Berzeliuseggene-Eimfjellet, and maybe Prins Karl Forland) were rifted away from the margin of Baltica during Ediacaran-Cambrian extension in the North Atlantic (Cawood et al., 2001, 2007). Stranded outboard of Baltica and Laurentia during the break-up of Rodinia, the SBP terranes (as well as other terranes in the circum-Arctic) may have been subsequently juxtaposed during protracted closure of the northern tract of the Iapetus Ocean associated with the early development of the Caledonian orogen (e.g., Strauss et al., 2017). The presence of Devonian-Carboniferous Ellesmerian metamorphism in the Prins Karls Forland terrane and localized folding and synorogenic sedimentation in the Wedel Jarlsberg-Oscar II terrane (e.g., Dallmann and Piepjohn, 2020) suggests amalgamation of these disparate terranes may have be protracted over the early to middle Paleozoic.

6. Conclusions

Integrated stratigraphic, chemostratigraphic, and geochronological data presented herein from the SBP provide important new insights into the tectonic evolution of Svalbard with implications for the North Atlantic and Arctic Caledonides. The main conclusions of this study are as follows:

1. Tonian metasedimentary rocks of the Nordbukta and Deilegga groups of Wedel Jarlsberg Land are regionally truncated by a Cryogenian (<650 Ma) angular unconformity (the Torellian unconformity), the age of which is confirmed herein by field relationships and re-analysis of previously unpublished detrital monazite data. New detrital zircon U-Pb data from these strata yield ca. 1030–1170,

1280–1400, 1430–1510, and 1580–1680 Ma age populations that are typical of North Atlantic Mesoproterozoic–Neoproterozoic sedimentary successions.
2. Carbonate carbon and strontium isotopic analyses from the Thiisfjellet Formation of the Sofiebogen Group provide chemostratigraphic ties to Cryogenian interglacial (ca. 659–640 Ma) carbonates. This correlation provides a conservative depositional age constraint for the underlying Cryogenian Torellian unconformity that is consistent with previous datasets (e.g., Majka et al., 2014).
3. Cryogenian–Ediacaran strata of the Sofiebogen, Dunderbukta, and Kapp Lyell groups host carbonate carbon ($\delta^{13}C_{carb}$) and strontium ($^{87}Sr/^{86}Sr$) isotope chemostratigraphic data that provide stratigraphic ties to the ca. 640(?)–635 Ma Marinoan and ca. 580–579 Ma Gaskiers glaciations. New detrital zircon U-Pb data from the Cryogenian Slyngfjellet, Jens Erikfjellet, Kapp Martin, and Konglomeratfjellet formations yield similar age spectra to the underlying Nordbukta and Deilegga groups, while younger Ediacaran strata of the Höferpynten and Gåshamna formations record a prominent shift to bimodal ca. 1850 and 2850 Ma U-Pb age populations.
4. Integrating these new data with previously published geochemical, geochronological, and thermochronological datasets from southwestern Svalbard, we propose the SBP is composite and can be further subdivided into the Wedel Jarlsberg-Oscar II, Berzeliuseggene-Eimfjellet, Prins Karls Forland, and Hornsund terranes.
5. Neoproterozoic metasedimentary rocks of the Wedel Jarlsberg-Oscar II and Berzeliuseggene-Eimfjellet terranes (and perhaps the Prins Karls Forland terrane) record sedimentological, provenance, and metamorphic similarities with age-equivalent successions in northern Baltica. In contrast, the Hornsund terrane has sedimentological and paleontological affinities with the Laurentian margin. Thus, we propose that the SBP is composed of multiple peri-Baltican and peri-Laurentian fragments that were initially amalgamated and translated during the Caledonian orogeny and then subsequently modified in the Ellesmerian and Eurekan orogenies.

CRediT authorship contribution statement

Virginia T. Wala: Funding acquisition, Investigation, Writing - original draft. **Grzegorz Ziemniak:** Investigation, Writing - review & editing. **Jaroslaw Majka:** Conceptualization, Funding acquisition, Writing - review & editing. **Karol Faehnrich:** Investigation, Writing - review & editing. **William C. McClelland:** Investigation, Writing - review & editing. **Edward E. Meyer:** Investigation, Writing - review & editing. **Maciej Manecki:** Investigation. **Jakub Bazarnik:** Investigation. **Justin V. Strauss:** Conceptualization, Funding acquisition, Investigation, Project administration, Visualization, Writing - original draft, Writing - review & editing.

Declaration of Competing Interest

The authors declare that they have no known competing financial interests or personal relationships that could have appeared to influence the work reported in this paper.

Acknowledgements

VTW was supported by a Geological Society of America (GSA) graduate student research grant, a National Geographic Young Explorer's Grant, an Arctic Field Grant from the Research Council of Norway, a Harp Grant from the Institute of Arctic Studies at Dartmouth College, and Dartmouth College's School of Graduate and Advanced Studies Alumni Research Fund. This project was supported by the National Science Foundation (NSF) Tectonics program (EAR-1650152 and EAR-1650022 awarded to JVS and WCM, respectively), as well as a National Geographic Society Grant (C-129R-17) awarded to JVS. Additional support for laboratory and field work was provided by National Science Centre (Poland) research project 2015/17/B/ST10/03114 awarded to JM. Zircon imaging utilized equipment of the University of Iowa Central Microscopy Research Facilities purchased with funding from NSF grant EAR-1038684 and National Institute of Health (NIH) grant S10-RR022498-01. We thank Paweł Słupski, Ula Buszkiewicz, Katarzyna Walczak, Rachel Rubin, and Jerzy Czerny for field support and Jerzy and Krzysztof Różański of the Eltanin for transportation. Jennifer Howley, Tyler Allen, Emma Kroeger, and Iniko Ceaser provided lab support at Dartmouth College and the University of Iowa. Emma Kroeger, Mark Pecha, and Nicky Giesler provided help at the University of Arizona LaserChron Center, which is funded through NSF EAR-1338583 and EAR-1649254. We thank Synnøve Elvevold for supporting our Arctic Field Grant. Finally, Karsten Piepjohn, an anonymous reviewer, and Associate Editor Victoria Pease provided detailed and helpful feedback on an earlier version of this manuscript.

Appendix A. Supplementary data

Supplementary data to this article can be found online at https://doi.org/10.1016/j.precamres.2021.106138.

References

Agard, P., Labrousse, L., Elvevold, S., Lepvrier, C., 2005. Discovery of Paleozoic Fe-Mg carpholite in Motalafjella, Svalbard Caledonides: A milestone for subduction-zone gradients. Geology 33, 761–764.

Ahm, A.S.C., Maloof, A.C., Macdonald, F.A., Hoffman, P.F., Bjerrum, C.J., Bold, U., Rose, C.V., Strauss, J.V., Higgins, J.A., 2019. An early diagenetic deglacial origin for basal Ediacaran "cap dolostones". Earth Planet. Sci. Lett. 506, 292–307.

Amato, J.M., Toro, J., Miller, E.L., Gehrels, G.E., Farmer, G.L., Gottlieb, E.S., Till, A.B., 2009. Late Proterozoic-Paleozoic evolution of the Arctic Alaska-Chukotka terrane based on U-Pb igneous and detrital zircon ages: Implications for Neoproterozoic paleogeographic reconstructions, Late Proterozoic-Paleozoic evolution of the Arctic Alaska-Chukotka terrane. Geol. Soc. Am. Bull. 121, 1219–1235.

V.L. Andreichev [Isotope geochronology of intrusive magmatism in the northern Timans]: Russian Academy of Sciences Ural Division, Ekaterinburg 89 1998 p. [in Russian].

Armstrong, H.A., Nakrem, H.A., Ohta, Y., 1986. Ordovician conodonts from the Bulltinden Formation, Motalafjella, central-western Spitsbergen. Polar Res 4, 17–23.

Balašov, J.A., Teben'kov, A.M., Ohta, Y., Larionov, A.N., Sirotkin, A.N., Gannibal, L.F., and Ryungenen, G.I., 1995, Grenvillian U-Pb zircon ages of quartz porphyry and rhyolite clasts in a metaconglomerate at Vimsodden, southwestern Spitsbergen: Polar Research, v. 14, p. 291–302.

Balašov, Y.A., Peucat, J., Teben'Kov, A.M., Ohta, Y., Larionov, A.N., Sirotkin, A.N., and Bjørnerud, M., 1996, Rb-Sr whole rock and U-Pb zircon datings of the granitic-gabbroic rocks from the Skålfjellet Subgroup, southwest Spitsbergen: Polar Research, v. 15, p. 167–181.

Barnes, C.J., and Schneider, D.A., 2019, Late Cretaceous−Paleogene burial and exhumation history of the Southwestern Basement Province, Svalbard, revealed by zircon (U-Th)/He thermochronology, in Piepjohn, K., Strauss, J.V., Reinhardt, L. and McClelland, W.C., eds., Circum-Arctic Structural Events: Tectonic Evolution of the Arctic Margins and Trans-Arctic Links with Adjacent Orogens: Geological Society of America Special Paper 541.

Barnes, C.J., Walczak, K., Janots, E., Schneider, D., and Majka, J., 2020, Timing of Paleozoic exhumation and deformation of the high-pressure Vestgötabreen Complex at the Motalafjella Nunatak, Svalbard: Minerals, v. 123(10), 23 p.

Bazarnik, J., Majka, J., McClelland, W.C., Strauss, J.V., Kósminska, K., Piepjohn, K., Elvevold, S., Czupyt, Z., Mikuš, T., 2019. U-Pb zircon dating of metaigneous rocks from the Nordbreen Nappe of Svalbard's Ny-Friesland terrane suggests their affinity to Northeast Greenland. Terra Nova 31, 518–526.

Beranek, L.P., Pease, V., Hadlari, T., Dewing, K., 2015. Silurian flysch successions of Ellesmere Island, Arctic Canada, and their significance to northern Caledonian palaeogeography and tectonics. J. Geol. Soc. 172 (2), 201–212.

Bergh, S.G., Braathen, A., Andresen, A., 1997. Interaction of basement-involved and thin-skinned tectonism in the Tertiary Fold-Thrust Belt of Central Spitsbergen, Svalbard. AAPG Bull. 81, 637–661.

Bergh, S.G., Maher, H.D., Braathen, A., 2000. Tertiary divergent thrust directions from partitioned transpression, Brøggerhalvøya, Spitsbergen. Norsk Geologisk Tidsskrift 80 (2), 63–81.

Bergh, S.G., Ohta, Y., Andresen, A., Maher Jr., H.D., Braathen, A., and Dallmann, W.K., 2003, Geological map of Svalbard, Sheet B8G, St. Jonsfjorden: Norsk Polarinstitutt, Temakart, v. 47.

Bernard-Griffiths, J., Peucat, J.J., Ohta, Y., 1993. Age and nature of protoliths in the Caledonian blueschist-eclogite complex of western Spitsbergen: a combined approach using U-Pb, Sm-bNd and REE whole-rock systems. Lithos 30, 81–90.

Birkenmajer, K., 1975. Caledonides of Svalbard and Plate Tectonics. Bull. Geol. Soc. Denmark v. 24, 1–19.

Birkenmajer, K., 1978a. Cambrian succession in south Spitsbergen. Studia Geol. Polonica 59, 1–46.
Birkenmajer, K., 1978b. Ordovician succession in southern Spitsbergen. Studia Geol. Polonica 59, 47–82.
Birkenmajer, K. 1981, The geology of Svalbard, the western part of the Barents Sea, and the continental margin of Scandinavia, in Nairn, A.E.M., Churkin, M., and Stehli, F. G., The ocean basins and margins, Vol. 5: The Arctic Ocean: p. 265–329.
Birkenmajer, K., 1991. The Jarlsbergian unconformity (Proterozoic/Cambrian boundary) and the problemm of Varangian tillites in South Spitsbergen: Polish. Polar Res. 12, 269–278.
Birkenmajer, K., 1992. Precambrian Succession at Hornsund, south Spitsbergen: A Lithostratigraphic Guide. Studia Geol. Polonica 98, 7–66.
Birkenmajer, K., 2010. The Kapp Lyell diamictites (Upper Proterozoic) at Bellsund, Spitsbergen: rock-sequence, sedimentological features, palaeoenvironment. Studia Geol. Polonica 133, 7–50.
Birkenmajer, K., and Orłowski, S., 1976, Olenellid fauna from the base of the Lower Cambrian sequence in south Spitsbergen: Norsk Polarinstitutt Årbok, p. 167–180.
Bjørnerud, M., 1990. An Upper Proterozoic unconformity in northern Wedel Jarlsberg Land, southwest Spitsbergen: Lithostratigraphy and tectonic implications. Polar Res. 8, 127–139.
Bjørnerud, M.G., 2010. Stratigraphic record of Neoproterozoic ice sheet collapse: the Kapp Lyell diamictite sequence, SW Spitsbergen, Svalbard. Geol. Magazine 147, 380–390.
Bjørnerud, M., Craddock, C., Wills, C.J., 1990. A major late Proterozoic tectonic event in southwestern Spitsbergen. Precambrian Res. 48, 157–165.
Bjørnerud, M., Decker, P.L., Craddock, C., 1991. Reconsidering Caledonian deformation in southwest Spitsbergen. Tectonics v. 10, 171–190.
Bold, U., Smith, E.F., Rooney, A.D., Bowring, S.A., Buchwaldt, R., Dudas, F., Ramezani, J., Crowley, J.L., Schrag, D.P., Macdonald, F.A., 2016. Neoproterozoic stratigraphy of the Zavkhan terrane of Mongolia: The backbone for Cryogenian and early Ediacaran chemostratigraphic records. Am. J. Sci. 316, 1–63.
Bouvier, A., Vervoort, J.D., and Patchett, P.J., 2008, The Lu–Hf and Sm–Nd isotopic composition of CHUR: constraints from unequilibrated chondrites and implications for the bulk composition of terrestrial planets, Earth Planet. Sci. Lett., v. 273(1-2), p. 48-57.
Braathen, A., Bergh, S.G., Maher, H.D., 1995. Structural outline of a Tertiary basement-cored uplift/inversion structure in western Spitsbergen, Svalbard: Kinematics and controlling factors. Tectonics 14, 95–119.
Brasier, M.D., Shields, G., Kuleshov, V.N., Zhegallo, E.A., 1996. Integrated chemo- and biostratigraphic calibration of early animal evolution: Neoproterozoic -early Cambrian of southwest Mongolia. Geol. Magazine 133 (4), 445–485.
Burzyński, M., Michalski, K., Nejbert, K., Domańska-Siuda, J., Manby, G., 2017. High-resolution mineralogical and rock magnetic study of ferromagnetic phases in metabasites from Oscar II Land, Western Spitsbergen—towards reliable model linking mineralogical and palaeomagnetic data. Geophys. J. Int. 210, 390–405.
Calver, C.R., 2000. Isotope stratigraphy of the Ediacarian (Neoproterozoic III) of the Adelaide Rift Complex, Australia, and the overprint of water column stratification. Precambrian Res. 100, 121–150.
Cawood, P.A., McCausland, P.J., Dunning, G.R., 2001. Opening Iapetus: constraints from the Laurentian margin in Newfoundland. Geol. Soc. Am. Bull. 113 (4), 443–453.
Cawood, P.A., Nemchin, A.A., Strachan, R., Prave, T., Krabbendam, M., 2007. Sedimentary basin and detrital zircon record along East Laurentia and Baltica during assembly and breakup of Rodinia. J. Geol. Soc. 164, 257–275.
Cawood, P.A., Strachan, R., Cutts, K., Kinny, P.D., Hand, M., Pisarevsky, S., 2010. Neoproterozoic orogeny along the margin of Rodinia: Valhalla orogeny, North Atlantic. Geology 38, 99–102.
Cawood, P.A., Strachan, R.A., Pisarevsky, S.A., Gladkochub, D.P., Murphy, J.B., 2016. Linking collisional and accretionary orogens during Rodinia assembly and breakup: implications for models of supercontinent cycles. Earth Planet. Sci. Lett. 449, 118–126.
Cochrane, P.J., 1984, Structure and Stratigraphy of the Hecla Hoek sequence in the Turrsjodalen-Brevassdalen area, Wedel Jarlsberg Land, West Spitsbergen [M.S. thesis]: University of Wisconsin, Madison, 135 p.
Cocks, L.R.M., Torsvik, T.H., 2011. The Palaeozoic geography of Laurentia and western Laurussia: a stable craton with mobile margins. Earth-Sci Rev. 06 (1–2), 1–51.
Colpron, M., Nelson, J.L., 2009, A Palaeozoic Northwest Passage: Incursion of Caledonian, Baltican and Siberian terranes into eastern Panthalassa, and the early evolution of the North American Cordillera: Geological Society of London, Special Publications, v. 318(1), p. 273-307.
Coney, P.J., Jones, D.L., Monger, J.H., 1980. Cordilleran suspect terranes. Nature 288.
Corfu, F., Andersen, T.B., Gasser, D., 2014. The Scandinavian Caledonides: main features, conceptual advances and critical questions. Geol. Soc. London, Special Publications 390 (1), 9–43.
Corfu, F., Heaman, L.M., Rogers, G., 1994. Polymetamorphic evolution of the Lewisian complex, NW Scotland, as recorded by U-Pb isotopic compositions of zircon, titanite and rutile. Contributions Mineral. Petrol. 117, 215–228.
Cowie, J.W., 1974. The Cambrian of Spitzbergen and Scotland: Cambrian of the British Isles, Norden and Spitzbergen: Lower Paleozoic Rocks of the World, v. 2, p. 123-156.
Cox, G.M., Halverson, G.P., Stevenson, R.K., Vokaty, M., Poirier, A., Kunzmann, M., Li, Z. X., Denyszyn, S.W., Strauss, J.V., Macdonald, F.A., 2016. Continental flood basalt weathering as a trigger for Neoproterozoic Snowball Earth. Earth Planet. Sci. Lett. 446, 89–99.
Cui, H., Kaufman, A.J., Xiao, S., Zhu, M., Zhou, C., Liu, X.-M., 2015. Redox architecture of an Ediacaran ocean margin: Integrated chemostratigraphic ($\delta^{13}C$–$\delta^{34}S$–$^{87}Sr/^{86}Sr$–Ce/Ce*) correlation of the Doushantuo Formation, South China. Chem. Geol. 405, 48–62.
Cui, H., Xiao, S., Cai, Y., Peek, S., Plummer, R.E., Kaufman, A.J., 2019. Sedimentology and chemostratigraphy of the terminal Ediacaran Dengying Formation at the Gaojiashan section, South China. Geol. Magazine 156 (11), 1924–1948.
Czerny, J., 1999. Petrogenesis of metavolcanites of the southern part of Wedel Jarlsberg Land (Spitsbergen). Mineral. Trans. 86, 1–88.
Czerny, J., Kieres, A., Manecki, M., Rajchel, J., 1993. Geological map of the SW part of Wedel Jarlsberg Land, Spitsbergen 1:25000. Institute of Geology and Mineral Deposits, University of Mining and Metallurgy.
Czerny, J., Majka, J., Gee, D.G., Manecki, A., Manecki, M., 2010. Torellian Orogeny: evidence of a Late Proterozoic tectonometamorphic event in southwestern Svalbard's Caledonian basement. NGF Abstracts Proc. 1, 35–36.
Dallmann, W.K. (Ed.), 2015a, Geoscience Atlas of Svalbard: Tromsø, Norway, Norwegian Polar Institute, Norwegian Polar Institute Report Series 148, 292 p.
Dallmann, W.K., 2015b, Geological fieldwork in Prins Karls Forland 2014: Internal field report: Norwegian Polar Institute, Project 1411, 60 p.
Dallmann, W.K., Piepjohn, K., 2020. The architecture of Svalbard's Devonian basins and the Svalbardian orogenic event. Geological Survey of Norway Special Publication v. 15, 106 p.
Dallmann, W.K., Hjelle, A., Ohta, Y., Salvigsen, O., Maher, H.D., Bjørnerud, M., Hauser, E.C., and Craddock, C., 1990, Geological map of Svalbard 1:100,000, Sheet B11G Van Keulenfjorden.
Dallmann, W.K., Andresen, A., Bergh, S.G., Maher, H.D., Ohta, Y., 1993a. Tertiary fold-and-thrust belt of Spitsbergen (Svalbard). Norsk Polarinstitutt Meddelelser 128, 26 p.
Dallmann, W.K., Birkenmajer, K., Hjelle, A., Mørk, A., Ohta, Y., Salvigsen, O., Winsnes, T. S., 1993b. Geological map of Svalbard 1:100,000, Sheet C13G Sørkapp. Norsk Polarinstitutt, Temakart 17.
Dallmeyer, R.D., Peucat, J.J., Hirajima, T., Ohta, Y., 1990. Tectonothermal chronology within a blueschist-eclogite complex, west-central Spitsbergen, Svalbard: Evidence from $^{40}Ar/^{39}Ar$ and Rb/Sr mineral ages. Lithos 24, 291–304.
Dhuime, B., Bosch, D., Bruguier, O., Caby, R., Pourtales, S., 2007. Age, provenance and post-deposition metamorphic overprint of detrital zircons from the Nathorst Land group (NE Greenland)—A LA-ICP-MS and SIMS study. Precambrian Res. 155, 24–46.
Dickinson, W.R., Gehrels, G.E., 2009, Use of U–Pb ages of detrital zircons to infer maximum depositional ages of strata: a test against a Colorado Plateau Mesozoic database, Earth Planet. Sci. Lett., 288(1-2), pp.115-125.
Dörr, N., Lisker, F., Jochmann, M., Rainer, T., Schlegel, A., Schubert, K. and Spiegel, C., 2019, Subsidence, rapid inversion, and slow erosion of the Central Tertiary Basin of Svalbard: evidence from the thermal evolution and basin modeling, in Piepjohn, K., Strauss, J.V., Reinhardt, L., and McClelland, W.C. eds., Circum-Arctic Structural Events: Tectonic Evolution of the Arctic Margins and Trans-Arctic Links with Adjacent Orogens: Geological Society of America Special Paper, v. 541.
Edwards, M.B., 1984. Sedimentology of the Upper Proterozoic glacial record, Vestertana Group, Finnmark, North Norway. Norges geologiske undersøkelse 394, 1–76.
Edwards, M.B., Baylis, P., Gibling, M., Goffe, W., Potter, M., Suthren, R.J., 1973. Stratigraphy of the "Older Sandstone Series" (Tanafjord Group) and Vestertana Group north of Stallogaissa, Laksefjord district, Finnmark. Norges geologiske undersøkelse 294, 25–41.
Faehnrich, K., Majka, J., Schneider, D., Mazur, S., Manecki, M., Ziemniak, G., Wala, V.T., Strauss, J.V., 2020. Geochronological constraints on Caledonian strike-slip displacement in Svalbard, with implications for the evolution of the Arctic. Terra Nova 32, 290–299.
Fike, D.A., Grotzinger, J.P., Pratt, L.M., Summons, R.E., 2006. Oxidation of the Ediacaran ocean. Nature 444, 744–747.
Fortey, R.A., Bruton, D.L., 1973. Cambrian-Ordovician rocks adjacent to Hinlopenstretet, north Ny Friesland, Spitsbergen. Geol. Soc. Am. Bull. 84, 2227–2242.
Gasser, D., Andresen, A., 2013. Caledonian terrane amalgamation of Svalbard: detrital zircon provenance of Mesoproterozoic to Carboniferous strata from Oscar II Land, western Spitsbergen. Geol. Magazine 150, 1103–1126.
Gee, D.G., Beliakova, L., Pease, V., Larionov, A., Dovshikova, L., 2000. New, single zircon (Pb-evaporation) ages from Vendian intrustions in the basement beneath the Pechora Basin, northeastern Baltica. Polarforschung 161–170.
Gee, D.G., Page, L.M., 1994. Caledonian terrane assembly on Svalbard; new evidence from $^{40}Ar/^{39}Ar$ dating in Ny Friesland. Am. J. Sci. 294, 1166–1186.
Gee, D.G., Pease, V., 2004. The Neoproterozoic Timanide Orogen of eastern Baltica: Introduction. Geol. Soc. London Memoirs 30 (1), 1–3.
Gee, D.G., Stephens, M.B., 2020. Regional context and tectonostratigraphic framework of the early–middle Paleozoic Caledonide orogen, northwestern Sweden. Geol. Soc. London Memoirs 50 (1), 481–494.
Gee, D.G., Teben'kov, A.M., 2004. Svalbard: a fragment of the Laurentian mar- gin, *in* The Neoproterozoic Timanide Orogen of Eastern Baltica, London. Geol. Soc. 30, 191–206.
Gee, D.G., Johansson, Å., Ohta, Y., Tebenkov, A.M., Balashov, Y.A., Larionov, A.N., Gannibal, L.F., and Ryungenen, G.I., 1995, Grenvillian basement and a major unconformity within the Caledonides of Nordaustlandet, Svalbard, Precambrian Res., v. 70(3-4), p. 215-234.
Gee, D.G., Fossen, H., Henriksen, N., Higgins, A.K., 2008. From the Early Paleozoic Platforms of Baltica and Laurentia to the Caledonide Orogen of Scandinavia and Greenland. Episodes 31, 44–51.
Gehrels, G.E., 2014. Detrital zircon U-Pb geochronology applied to tectonics. Annual Rev. Earth Planet. Sci. 42, 127–149.
Gehrels, G.E., Pecha, M., 2014. Detrital zircon U-Pb geochronology and Hf isotope geochemistry of Paleozoic and Triassic passive margin strata of western North America. Geosphere 10, 49–65.

Gehrels, G., Valencia, V., Pullen, A., 2006. Detrital Zircon Geochronology by Laser-Ablation Multicollector ICPMS at the Arizona LaserChron Center. Paleontol. Soc. Papers 12, 67–76.
Gehrels, G.E., Valencia, V.A., Ruiz, J., 2008. Enhanced precision, accuracy, efficiency, and spatial resolution of U-Pb ages by laser ablation–multicollector–inductively coupled plasma–mass spectrometry. Geochem. Geophys. Geosystems 9.
Gibson, T.M., Faehnrich, K., Busch, J.F., McClelland, W.C., Schmitz, M.D., and Strauss, J. V., 2021, A detrital zircon test of large-scale terrane displacement along the Arctic margin of North America: Geology, v. xx, p. xxx.
Gilotti, J.A., McClelland, W.C., van Staal, C.R., and Petrie, M.B., 2017. Detrital zircon evidence for eclogite formation by basal subduction erosion—An example from the Yukon-Tanana composite arc, Canadian Cordillera, in Bianchini, G., Bodinier, J-L, Braga, R., and Wilson, M., eds., The Crust-Mantle and Lithosphere-Asthenosphere Boundaries: Insights from Xenoliths, Orogenic Deep Sections, and Geophysical Studies: Geological Society of America Special Paper 526, p. 173-189.
Gołuchowska, K., Barker, A.K., Majka, J., Manecki, M., Czerny, J., Bazarnik, J., 2012. Preservation of magmatic signals in metavolcanics from Wedel Jarlsberg Land, SW Svalbard. Mineralogia Polonica 43, 179–197.
Gołuchowska, K., Barker, A.K., Czerny, J., Majka, J., Manecki, M., Farajewicz, M., Dwornik, M., 2016. Magma storage of an alkali ultramafic igneous suite from Chamberlindalen, SW Svalbard. Mineral. Petrol. 110, 623–638.
Gumsley, A., Manby, G., Domańska-Siuda, J., Nejbert, K., Michalski, K., 2020. Caught between two continents: First identification of the Ediacaran Central Iapetus Magmatic Province in Western Svalbard with palaeogeographic implications during final Rodinia breakup. Precambrian Res. 341, 105622.
Halverson, G.P., Hoffman, P.F., Schrag, D.P., Maloof, A.C., Rice, A.H.N., 2005. Toward a Neoproterozoic composite carbon-isotope record. Geol. Soc. Am. Bull. 117, 1181–1207.
Halverson, G.P., Dudás, F.Ö., Maloof, A.C., Bowring, S.A., 2007. Evolution of the $^{87}Sr/^{86}Sr$ composition of Neoproterozoic seawater. Palaeogeogr. Palaeoclimatol. Palaeoecol. 256, 103–129.
Harland, W.B., 1971. Tectonic transpression in Caledonian Spitsbergen. Geol. Magazine 108, 27–41.
Harland, W.B., 1978. A reconsideration of Late Precambrian stratigraphy of southern Spitsbergen. Polarforschung 48, 44–61.
Harland, W.B., 1997, The Geology of Svalbard: London, Geological Society of London, 529 p.
Harland, W.B., Wright, N.J.R., 1979. Alternative hypothesis for the pre-Carboniferous evolution of Svalbard. Norsk Polarinstitutt Skrifter 167, 89–117.
Harland, W.B., Wallis, R.H., Gayer, R.A., 1966. A revision of the lower Hecla Hoek succession in central North Spitsbergen and correlation elsewhere. Geol. Magazine 103, 70–97.
Harland, W.B., Cutbill, J.L., Friend, P.F., Gobbett, D.J., Holliday, D.W., Maton, P.I., Parker, J.R., Wallis, R.H., 1974. The Billefjorden Fault Zone, Spitsbergen: the long history of a major tectonic lineament. Norsk Polarinstitutt Skrifter 171, 72 p.
Harland, W.B., Horsfield, W.T., Manby, G.M., Morris, A.P., 1979. An outline pre-Carboniferous stratigraphy of central western Spitsbergen. Norsk Polarinstitutt Skrifter 167, 119–143.
Harland, W.B., Hambrey, M.J., Waddams, P., 1993. Vendian geology of Svalbard. Norsk Polarinstitutt Skrifter 193, 145 p.
Harrison, J.C., St-Onge, M.R., Petrov, O.V., Strelnikov, S.I., Lopatin, B.G., Wilson, F.H., Tella, S., Paul, D., Lynds, T., Shokalsky, S.P., and Hults, C.K., 2011, Geological Map of the Arctic: Geological Survey of Canada, "A" Series Map 2159A, 9 Sheets.
Henriksen, N., Higgins, A.K., 2008. Geological research and mapping in the Caledonian orogen of East Greenland, 70°N–82°N, *in* Memoir 202: The Greenland Caledonides: Evolution of the Northeast Margin of Laurentia. Geol. Soc. Am. 202, 1–27.
Hirajima, T., Hiroi, Y., Ohta, Y., 1984. Lawsonite and pumpellyite from the Vestgötabreen Formation in Spitsbergen. Norsk Geologisk Tidsskrift 64, 267–274.
Hirajima, T., Banno, S., Hiroi, Y., Ohta, Y., 1988. Phase petrology of eclogites and related rocks from the Motalafjella high-pressure metamorphic complex in Spitsbergen (Arctic Ocean) and its significance. Lithos 22, 75–97.
Hjelle, A., 1962. Contribution to the geology of the Hecla Hoek Formation in Nordenskiöld Land. Norsk Polarinstitutt Årbok, West Spitsbergen, pp. 83–95.
Hjelle, A., 1969, Stratigraphical correlation of Hecla Hoek successions north and south of Bellsund: Norsk Polarinstitutt Årbok, p. 46–51.
Hjelle, A., Ohta, Y., Winsnes, T.S., 1979. Hecla Hoek rocks of Oscar II Land and Prins Karls Forland, Svalbard. Norsk Polarinstitutt Skrifter 167, 145–169.
Hjelle, A., Salvigsen, O., and Winsnes, T.S., 1986, Geological map of Svalbard, Van Mijenfjorden: Oslo, Norsk Polarinstitutt, Scale 1:100,000, 1 sheet.
Hjelle, A., Piepjohn, K., Saalmann, K., Ohta, Y., Salvigsen, O., Thedig, F., Dallmann, W. K., 1999. Geological map of Svalbard 1:100,000, Sheet A7G Kongsfjorden. Norsk Polarinstitutt, Temakart 22, 56 p.
Hoffman, P.F., 2011. Strange bedfellows: glacial diamictite and cap carbonate from the Marinoan (635 Ma) glaciation in Namibia. Sedimentology 58, 57–119.
Hoffman, P.F., Schrag, D.P., 2002. The snowball Earth hypothesis: testing the limits of global change. Terra Nova 14, 129–155.
Hoffman, P.F., Abbot, D.S., Ashkenazy, Y., Benn, D.I., Brocks, J.J., Cohen, P.A., Cox, G. M., Creveling, J.R., Donnadieu, Y., Erwin, D.H., and Fairchild, I.J., 2017, Snowball Earth climate dynamics and Cryogenian geology-geobiology, Sci. Adv., v. 3(11), p. e1600983.
Högström, A.E.S., Jensen, S., Palacios, T., Ebbestad, J.O.R., 2013. New information on the Ediacaran-Cambrian transition in the Vestertana Group, Finnmark, northern Norway, from trace fossils and organic-walled microfossils. Norsk Geologisk Tidsskrift 93, 95–106.
Hoiland, C.W., Miller, E.L., Pease, V., Hourigan, J.K., 2018. Detrital zircon U-Pb geochronology and Hf isotope geochemistry of metasedimentary strata in the southern Brooks Range: constraints on Neoproterozoic-Cretaceous evolution of Arctic Alaska. Geol. Soc. London, Special Publications 460, 121–158.
Horsfield, W.T., 1972. Glaucophane schists of Caledonian age from Spitsbergen. Geol. Magazine 109, 29–36.
Kalinec, J., 1985, The structure and stratigraphy of the Seljehaugfjellet area, Wedel Jarlsberg Land, Spitsbergen [M.S. thesis]: University of Wisconsin, Madison, 188 p.
Kalsbeek, F., Thrane, K., Nutman, A.P., Jepsen, H.F., 2000. Late Mesoproterozoic to early Neoproterozoic history of the East Greenland Caledonides: evidence for Grenvillian orogenesis? J. Geol. Soc. 157, 1215–1225.
Kalsbeek, F., Higgins, A.K., Jepsen, H.F., Frei, R., Nutman, A.P., 2008. Granites and granites in the East Greenland Caledonides, *in* Memoir 202: The Greenland Caledonides: Evolution of the Northeast Margin of Laurentia. Geol. Soc. Am. 202, 227–249.
Kaufman, A.J., Jacobsen, S.B., Knoll, A.H., 1993. The Vendian record of Sr and C isotopic variations in seawater: implications for tectonics and paleoclimate. Earth Planet. Sci. Lett. 120 (3–4), 409–430.
Kirkland, C.L., Pease, V., Whitehouse, M.J., Ineson, J.R., 2009. Provenance record from Mesoproterozoic-Cambrian sediments of Peary Land, North Greenland: Implications for the ice-covered Greenland Shield and Laurentian palaeogeography. Precambrian Res. 1–2, 43–60.
Kjøll, H.J., Andersen, T.B., Corfu, F., Labrousse, L., Tegner, C., Abdelmalak, M.M., and Planke, S., 2019, Timing of breakup and thermal evolution of a pre-Caledonian Neoproterozoic exhumed magma-rich rifted margin, Tectonics, v. 38(6), p.1843–1862.
Kleinspehn, K.L., Teyssier, C., 1992, Tectonics of the Palaeogene Forlandsundet Basin, Spitsbergen: a preliminary report, Norsk geologisk tidsskrift, v. 72(1), p. 93-104.
Knoll, A.H., Ohta, Y., 1988. Microfossils in metasediments from Prins Karls Forland, western Svalbard. Polar Res. 6, 59–67.
Kośmińska, K., Majka, J., Mazur, S., Krumbholz, M., Klonowska, I., Manecki, M., Czerny, J., Dwornik, M., 2014. Blueschist facies metamorphism in Nordenskiöld Land of west-central Svalbard. Terra Nova 26, 377–386.
Kośmińska, K., Schneider, D.A., Majka, J., Lorenz, H., Gee, D.G., Manecki, M., and Barnes, C., 2015, Detrital zircon U-Pb geochronology of metasediments from southwestern Svalbard's Caledonian Province: EGUGA, p.11805.
Kośmińska, K., Spear, F.S., Majka, J., Faehnrich, K., Manecki, M., Piepjohn, K., Dallmann, W.K., 2020. Deciphering late Devonian–early Carboniferous P-T–t path of mylonitized garnet-mica schists from Prins Karls Forland, Svalbard. J. Metamorphic Geol. 38, 471–493.
Kosteva, N.N., Kuznetsov, N.B., Teben'kov, A.M. and Romanyuk, T.V., 2014, First results of the U-Pb isotopic (LA-ICP-MS) dating of detrital zircons from the Lower Paleozoic of Spitsbergen. Doklady Earth Sci., v. 455, p. 259–265.
Krasil'ščikov, A.A., and Kovaleva, G.A., 1979, Precambrian rock-stratigraphic units of the west coast of Spitsbergen: Norsk Polarinstitutt Skrifter, v. 167, p. 73–79.
Kusiak, M.A., Whitehouse, M.J., Wilde, S.A., Nemchin, A.A., Clark, C., 2015. Mobilization of radiogenic Pb in zircon revealed by ion imaging: Implications for early Earth geochronology. Geology 41, 291–294.
Kuznetsov, N.B., Soboleva, A.A., Udoratina, O.V., Hertseva, M.V., and Andreichev, V.L., 2007, Pre-Ordovician tectonic evolution and volcano–plutonic associations of the Timanides and northern Pre-Uralides, northeast part of the East European Craton: Gondwana Research, v. 12(3), p. 305-323.
Labrousse, L., Elvevold, S., Lepvrier, C., and Agard, P., 2008, Structural analysis of high-pressure metamorphic rocks of Svalbard: Reconstructing the early stages of the Caledonian orogeny: Tectonics, v. 27(5).
Lamb, M.P., Fischer, W.W., Raub, T.D., Perron, J.T., Myrow, P.M., 2012. Origin of giant wave ripples in snowball Earth cap carbonate. Geology 40, 827–830.
Larionov, A.N., Teben'kov, A.M., 2004. New SHRIMP-II U-Pb zircon age data from granitic boulders in Vendian tillites of southern coast of Isfjorden, West Spitsbergen. NGF Abstracts Proc. 2.
Larionov, A.N., Andreichev, V.A., Gee, D.G., 2004. The Vendian alkaline igneous suite of northern Timan: ion microprobe U-Pb zircon ages of gabbros and syenite. Geol. Soc., London, Memoirs 30 (1), 69–74.
Larionov, A.N., Teben'kov, A.M., Gee, D.G., Czerny, J., and Majka, J., 2010, Recognition of Precambrian tectonostratigraphy in Wedel Jarlsberg Land, southwestern Spitsbergen: 29th Nordic Geological Winter Meeting, v. 1, p. 106.
Larsen, R.B., Grant, T., Sørensen, B.E., Tegner, C., McEnroe, S., Pastore, Z., Fichler, C., Nikolaisen, E., Grannes, K.R., Church, N., ter Maat, G.W., 2018. Portrait of a giant deep-seated magmatic conduit system: The Seiland Igneous Province. Lithos 296–299, 600–622.
Leslie, A.G., Nutman, A.P., 2003. Evidence for Neoproterozoic orogenesis and early high temperature Scandian deformation events in the southern East Greenland Caledonides. Geol. Magazine 140, 309–333.
Lorenz, H., Gee, D.G., Larionov, A.N., and Majka, J., 2012, The Grenville–Sveconorwegian orogen in the high Arctic, Geol. Magazine, 149(5), p. 875-891.
Ludwig, K.R., 2003, User's Manual for a Geochronological Toolkit for Microsoft Excel (Isoplot/Ex Version 3.0). Berkeley Geochronology Center Special Publication, 70 p.
Macdonald, F.A., Strauss, J.V., Sperling, E.A., Halverson, G.P., Narbonne, G.M., Johnston, D.T., Kunzmann, M., Schrag, D.P., Higgins, J.A., 2013. The stratigraphic relationship between the Shuram carbon isotope excursion, the oxygenation of Neoproterozoic oceans, and the first appearance of the Ediacara biota and bilaterian trace fossils in northwestern Canada. Chem. Geol. 362, 250–272.
Majka, J., and Kośmińska, K., 2017, Magmatic and metamorphic events recorded within the Southwestern Basement Province of Svalbard: Arktos, v. 3(1), p. 5.
Majka, J., Mazur, S., Manecki, M., Czerny, J., Holm, D.K., 2008. Late Neoproterozoic amphibolite-facies metamorphism of a pre-Caledonian basement block in southwest

Wedel Jarlsberg Land, Spitsbergen: new evidence from U-Th–Pb dating of monazite. Geol. Magazine 145, 822–830.
Majka, J., Czerny, J., Mazur, S., Holm, D.K., Manecki, M., 2010. Neoproterozoic metamorphic evolution of the Isbjørnhamna Group rocks from south-western Svalbard: Neoproterozoic metamorphism in southern Svalbard. Polar Res. 29, 250–264.
Majka, J., Larionov, A., Gee, D.G., Czerny, J., Pršek, J., 2012. Neoproterozoic pegmatite from Skoddefjellet, Wedel Jarlsberg Land, Spitsbergen: Additional evidence for c. 640 Ma tectonothermal event in the Caledonides of Svalbard: Polish. Polar Res. 33, 1–17.
Majka, J., Be'Eri-Shlevin, Y., Gee, D.G., Czerny, J., Frei, D., and Ladenberger, A., 2014, Torellian (c. 640 Ma) metamorphic overprint of Tonian (c. 950 Ma) basement in the Caledonides of southwestern Svalbard, Geol. Magazine, 151, p. 732–748.
Majka, J., Kośmińska, K., Mazur, S., Czerny, J., Piepjohn, K., Dwornik, M., Manecki, M., 2015. Two garnet growth events in polymetamorphic rocks in southwest Spitsbergen, Norway: insight in the history of Neoproterozoic and early Paleozoic metamorphism in the High Arctic. Canadian J. Earth Sci. 52, 1045–1061.
Major, H., Winsnes, T.S., 1955. Cambrian and Ordovician fossils from Sørkapp Land, Spitsbergen. Norsk Polarinstitutt Skrifter 106, 47.
Malone, S.J., McClelland, W.C., von Gosen, W., Piepjohn, K., 2014. Proterozoic Evolution of the North Atlantic-Arctic Caledonides: Insights from Detrital Zircon Analysis of Metasedimentary Rocks from the Pearya Terrane, Canadian High Arctic. J. Geol. 122, 623–647.
Manby, G.M., 1986. Mid-Palaeozoic metamorphism and polyphase deformation of the Forland Complex, Svalbard. Geol. Magazine 123, 651–663.
Manecki, M., Holm, D.K., Czerny, J., Lux, D., 1998. Thermochronological evidence for late Proterozoic (Vendian) cooling in southwest Wedel Jarlsberg Land, Spitsbergen. Geol. Magazine 135, 63–69.
Mattinson, J. M., Graubard, C. M., Parkinson, D. L., and McClelland, W. C., 1996. U-Pb reverse discordance in zircons: the role of fine-scale oscillatory zoning and sub-micron transport of Pb, in Basu, A., and Hart, S., eds., Earth Processes: Reading the Isotopic Code, Geophys. Monograph 95, p. 355–376.
Mazur, S., Czerny, J., Majka, J., Manecki, M., Holm, D., Smyrak, A., Wypych, A., 2009. A strike-slip terrane boundary in Wedel Jarlsberg Land, Svalbard, and its bearing on correlations of SW Spitsbergen with the Pearya terrane and Timanide belt. J. Geol. Soc. 166, 529–544.
McClelland, W.C., von Gosen, W., and Piepjohn, K., 2019, Tonian and Silurian magmatism in Nordaustlandet: Svalbard's place in the Caledonian orogen, in Piepjohn, K., Strauss, J.V., Reinhardt, L. and McClelland, W.C., eds., Circum-Arctic Structural Events: Tectonic Evolution of the Arctic Margins and Trans-Arctic Links with Adjacent Orogens, Geol. Soc. Am. Special Paper 541.
McClelland, W.C., Gilotti, J.A., Ramarao, T., Stemmerik, L., Dalhoff, F., 2016. Carboniferous basin in Holm Land records local exhumation of the North-East Greenland Caledonides: Implications for the detrital zircon signature of a collisional orogen. Geosphere 12, 927–947.
Mezger, K., Krogstad, E.J., 1997. Interpretation of discordant U-Pb zircon ages: An evaluation. J. Metamorphic Geol. 15, 127–140.
Michalski, K., Manby, G., Nejbert, K., Domańska-Siuda, J., Burzyński, M., 2017. Using palaeomagnetic and isotopic data to investigate late to post-Caledonian tectonothermal processes within the Western Terrane of Svalbard. J. Geol. Soc. 174, 572–590.
Miller, E.L., Kuznetsov, N., Soboleva, A., Udoratina, O., Grove, M.J., Gehrels, G.E., 2011. Baltica in the Cordillera? Geology 39, 791–794.
Miller, E.L., Meisling, K.E., Akinin, V.V., Brumley, K., Coakley, B.J., Gottlieb, E.S., Hoiland, C.W., O'Brien, T.M., Soboleva, A., Toro, J., 2018. Circum-Arctic Lithosphere Evolution (CALE) Transect C: displacement of the Arctic Alaska-Chukotka microplate towards the Pacific during opening of the Amerasia Basin of the Arctic. Geol. Soc. London, Special Publications 460 (1), 57–120.
Misi, A., Veizer, J., 1998. Neoproterozoic carbonate sequences of the Una Group, Irecê Basin, Brazil: chemostratigraphy, age and correlations. Precambrian Res. 89, 87–100.
Morris, A.P., 1982. Low grade (greenschist facies) metamorphism in southern Prins Karls Forland. Polar Res. 2, 17–56.
Nania, J., 1987, Structure and stratigraphy along a major Proterozoic unconformity, Dunderdalen to Brevassdalen, Wedel Jarlsberg Land, Spitsbergen [M.S. thesis]: University of Wisconsin, Madison.
Narbonne, G.M., Kaufman, A.J., Knoll, A.H., 1994. Integrated chemostratigraphy and biostratigraphy of the Windermere Supergroup, northwestern Canada: Implications for Neoproterozoic correlations and the early evolution of animals. Geol. Soc. Am. Bull. 106 (10), 1281–1291.
Nystuen, J.P., Andresen, A., Kumpulainen, R.A., Siedlecka, A., 2008. Neoproterozoic basin evolution in Fennoscandia, East Greenland and Svalbard. Episodes 31 (1), 35–43.
O'Brien, T.M., Miller, E.L., Benowitz, J.P., Meisling, K.E., and Dumitru, T.A., 2016, Dredge samples from the Chukchi Borderland: Implications for paleogeographic reconstruction and tectonic evolution of the Amerasia Basin of the Arctic, Am. J. Sci., 316(9), p. 873-924.
Ohta, Y., 1979. Blueschists from Motalafjella, Western Spitsbergen. Norsk Polarinstitutt Skrifter 167, 171–217.
Ohta, Y., 1985. Geochemistry of Precambrian basic igneous rocks between St. Jonsfjorden and Isfjorden, central western Spitsbergen, Svalbard. Polar Res. 3, 49–67.
Ohta, Y., 1994. Caledonian and Precambrian history in Svalbard: a review, and an implication of escape tectonics. Tectonophysics 231, 183–194.
Ohta, Y., Krasil'ščikov, A.A., Lepvrier, C., and Teben'Kov, A.M., 1995, Northern continuation of Caledonian high-pressure metamorphic rocks in central-western Spitsbergen, Polar Res., v. 14, p. 303–315.
Olierook, H.K., Barham, M., Kirkland, C.L., Hollis, J., Vass, A., 2020. Zircon fingerprint of the Neoproterozoic North Atlantic: Perspectives from East Greenland. Precambrian Res. 342, 105653.
Orvin, A.K., 1940. Outline of the geological history of Spitsbergen. Skrifter om Svalbard og Ishavet 78, 1–57.
Pease, V., 2011. Eurasian orogens and Arctic tectonics: an overview. Geol. Soc. London, Memoirs 35, 311–324.
Pease, V., Daly, J.S., Elming, S.Å., Kumpulainen, R., Moczydlowska, M., Puchkov, V., Roberts, D., Saintot, A., and Stephenson, R., 2008, Baltica in the Cryogenian, 850–630 Ma, Precambrian Res., v. 160(1-2), p. 46-65.
Piepjohn, K., 2000. The Svalbardian-Ellesmerian deformation of the Old Red Sandstone and the pre-Devonian basement in NW Spitsbergen (Svalbard). Geol. Soc. London, Special Publications 180 (1), 585–601.
Piepjohn, K., Griem-Klee, S., Post, H., Post, J., Thiedig, F., 2000. Geology and structural evolution of pre-Caledonian rocks and the (?)Devonian Sutorfjella conglomerate, northern Prins Karls Forland (Svalbard). Norsk Geologisk Tidsskrift 80, 83–95.
Piepjohn, K., Thiedig, F., and Manby, G.M., 2001, Nappe stacking on Brøggerhalvøya, NW Spistbergen. In Intra-Continental Fold Belts. CASE 1: West Spitsbergen, F. Tessensohn, ed., Geologisches Jahrbuch (Polar Issue No. 7), B, 91: 83–108.
Pu, J.P., Bowring, S.A., Ramezani, J., Myrow, P., Raub, T.D., Landing, E., Mills, A., Hodgin, E., Macdonald, F.A., 2016. Dodging snowballs: Geochronology of the Gaskiers glaciation and the first appearance of the Ediacaran biota. Geology 44, 955–958.
Rice, A.H.N., 1994. Stratigraphic overlap of the late Proterozoic Vadsø and Barents Sea Groups and correlation across the Trollfjorden-Komagelva Fault, Finnmark, North Norway. Norsk Geologisk Tidsskrift 74, 48–57.
Rice, A.H.N., Edwards, M.B., Hansen, T.A., Arnaud, E., Halverson, G.P., 2011. Glaciogenic rocks of the Neoproterozoic Smalfjord and Mortensnes formations, Vestertana Group, E. Finnmark, Norway. Geol. Soc., London, Memoirs 36, 593–602.
Roberts, R.J., Corfu, F., Torsvik, T.H., Ashwal, L.D., Ramsay, D.M., 2006. Short-lived mafic magmatism at 560–570 Ma in the northern Norwegian Caledonides: U-Pb zircon ages from the Seiland Igneous Province. Geol. Magazine 143, 887–903.
Roberts, D., Siedlecka, A., 2012. Provenance and sediment routing of Neoproterozoic formations on the Varanger, Nordkinn, Rybachi and Sredni peninsulas, North Norway and Northwest Russia: a review. Norges geologiske undersøkelse Bulletin 452, 1–19.
Rooney, A.D., Macdonald, F.A., Strauss, J.V., Dudas, F.O., Hallmann, C., Selby, D., 2014. Re-Os geochronology and coupled Os-Sr isotope constraints on the Sturtian snowball Earth. Proc. Natl. Acad. Sci. 111, 51–56.
Rooney, A.D., Strauss, J.V., Brandon, A.D., Macdonald, F.A., 2015. A Cryogenian chronology: Two long-lasting synchronous Neoproterozoic glaciations. Geology 43, 459–462.
Rooney, A.D., Cantine, M.D., Bergmann, K.D., Gómez-Pérez, I., Baloushi, B., Boag, T.H., Busch, J.F., Sperling, E.A., Strauss, J.V., 2020. Calibrating the co-evolution of Ediacaran life and environment. Proc. Natl. Acad. Sci. 117, 16824–16830.
Rosa, D., Majka, J., Thrane, K., Guarnieri, P., 2016. Evidence for Timanian-age basement rocks in North Greenland as documented through U-Pb zircon dating of igneous xenoliths from the Midtkap volcanic centers. Precambrian Res. 275, 394–405.
Rubatto, D., 2017. Zircon: The Metamorphic Mineral. Rev. Mineral. Geochem. 83, 261–295.
Saalmann, K., Thiedig, F., 2002. Thrust tectonics on Brøggerhalvøya and their relationship to the Tertiary West Spitsbergen Fold-and-Thrust Belt. Geol. Magazine 139 (1), 47–72.
Sawaki, Y., Ohno, T., Tahata, M., Komiya, T., Hirata, T., Maruyama, S., Windley, B.F., Han, J., Shu, D., Li, Y., 2010. The Ediacaran radiogenic Sr isotope excursion in the Doushantuo Formation in the Three Gorges area, South China. Precambrian Res. 176, 46–64.
Schneider, D.A., Faehnrich, K., Majka, J., and Manecki, M., 2019, 40Ar/39Ar geochronologic evidence of Eurekan deformation within the West Spitsbergen Fold and Thrust Belt, in Piepjohn, K., Strauss, J.V., Reinhardt, L. and McClelland, W.C., eds., Circum-Arctic Structural Events: Tectonic Evolution of the Arctic Margins and Trans-Arctic Links with Adjacent Orogens: Geological Society of America Special Paper 541.
Scrutton, C.T., Horsfield, W.T., Harland, W.B., 1976. Silurian fossils from western Spitsbergen. Geol. Magazine 113, 519–523.
Shields, G.A., Braiser, M.D., Stille, P., Dorjnamjaa, D., 2002. Factors contributing to high ^{13}C values in Cryogenian limestones of western Mongolia. Earth Planet. Sci. Lett. 196 (3–4), 99–111.
Siedlecka, A., 1985. Development of the Upper Proterozoic sedimentary basins of the Varanger Peninsula, East Finnmark, North Norway. Bull. Geol. Survey Finland 331, 175–185.
Siedlecka, A., and Roberts, D., 1992, The bedrock geology of Varanger Peninsula, Finnmark, North Norway: an excursion guide: Trondheim, Geological Survey of Norway, Special publication / Norges Geologiske Undersøkelse no. 5, 45 p.
Siedlecka, A., Roberts, D., Nystuen, J.P., Olovyanishnikov, V.G., 2004. Northeastern and northwestern margins of Baltica in Neoproterozoic time: evidence from the Timanian and Caledonian Orogens. Geol. Soc. London, Memoirs 30, 169–190.
Slagstad, T., Saalmann, K., Kirkland, C.L., Høyen, A.B., Storruste, B.K., Coint, N., Pin, C., Marker, M., Bjerkgård, T., Krill, A., and Solli, A., 2020, Late Neoproterozoic–Silurian tectonic evolution of the Rödingsfjället Nappe Complex, orogen-scale correlations and implications for the Scandian suture: Geological Society, London, Special Publications, v. 503.

Slama, J., Walderhaug, O., Fonneland, H., Kosler, J., Pedersen, R.B., 2011. Provenance of Neoproterozoic to upper Cretaceous sedimentary rocks, eastern Greenland: implications for recognizing the sources of sediments in the Norwegian Sea. Sedimentary Geol. 238, 254–267.
Sønderholm, M., Frederiksen, K.S., Smith, M.P., Tirsgaard, H., 2008. Neoproterozoic sedimentary basins with glacigenic deposits of the East Greenland Caledonides. Memoir Geol. Soc. Am. Bull. 202, 99–136.
Stouge, S., Harper, D., Boyce, W., Knight, I., Christiansen, J., 2013. Development of the Lower Cambrian-Middle Ordovician Carbonate Platform: North Atlantic Region. AAPG Memoir 597–626.
Strachan, R.A., Nutman, A.P., Friderichsen, J.D., 1995. SHRIMP U-Pb geochronology and metamorphic history of the Smallefjord sequence, NE Greenland Caledonides. J. Geol. Soc. 152 (5), 779–784.
Strauss, J.V., Macdonald, F.A., Taylor, J.F., Repetski, J.E., McClelland, W.C., 2013. Laurentian origin for the North Slope of Alaska: Implications for the tectonic evolution of the Arctic. Lithosphere 5 (5), 477–482.
Strauss, J.V., Hoiland, C.W., Ward, W.P., Johnson, B.G., Nelson, L.L., McClelland, W.C., 2017. Orogen transplant: Taconic-Caledonian arc magmatism in the central Brooks Range of Alaska. Geological Soc. Am. Bull. 129, 649–676.
Strauss, J.V., Johnson, B.G., Colpron, M., Nelson, L.L., Perez, J., Benowitz, J.A., Ward, W., and McClelland, W.C., 2019, Pre-Mississippian stratigraphy and provenance of the North Slope subterrane of Arctic Alaska II: Basinal rocks of the northeastern Brooks Range and their significance in circum-Arctic evolution, in Piepjohn, K., Strauss, J.V., Reinhardt, L. and McClelland, W.C., eds., Circum-Arctic Structural Events: Tectonic Evolution of the Arctic Margins and Trans-Arctic Links with Adjacent Orogens: Geological Society of America Special Paper 541, p. 525–572.
Swett, K., 1981. Cambro-Ordovician strata in Ny Friesland, Spitsbergen and their palaeotectonic significance. Geol. Magazine 118, 225–250.
Tessensohn, F., ed., 2001, Intra-Continental Fold Belts (CASE 1): West Spitsbergen: Geologisches Jahrbuch (Polar Issue No. 7), B, 91: 733–773.
Till, A.B., Dumoulin, J.A., Ayuso, R.A., Aleinikoff, J.N., Amato, J.M., Slack, J.F., Shanks III, W.P., 2014. Reconstruction of an early Paleozoic continental margin based on the nature of protoliths in the Nome Complex, Seward Peninsula, Alaska. Geol. Soc. Am. Special Paper 506, 1–28.
Trettin, H.P., 1989, The Arctic Islands, in Bally, A.W. and Palmer, A.R. eds., The Geology of North America—An Overview, Geological Society of America, p. 349–370.
Turchenko, S.I., Teben'kov, A.M., Barkhatov, D.B., Barmatenkov, I.I., 1983, Geologicheskoye stroyeniye i magmatizm regiona Chemberlenovoy doliny, Zapadnyy Shpitsbergen (Geological structure and magmatism of the Chamberlain Valley region, western Spitsbergen): Geology of Spitsbergen. PGO "Sevmorgeologiya" Publishing House, Leningrad, pp. 38–48 (in Russian).
Valley, J.W., Cavosie, A.J., Ushikubo, T., Reinhard, D.A., Lawrence, D.F., Larson, D.J., Clifton, P.H., Kelly, T.F., Wilde, S.A., Moser, D.E., Spicuzza, M.J., 2014. Hadean age for a post-magma-ocean zircon confirmed by atom-probe tomography. Nat. Geosci. 7, 219–223.
Vermeesch, P., 2013. Multi-sample comparison of detrital age distributions. Chem. Geol. 341, 140–146.
Vermeesch, P., 2018. IsoplotR: a free and open toolbox for geochronology. Geosci. Front. 9, 1479–1493.
Vervoort, J.D., Blichert-Toft, J., 1999. Evolution of the depleted mantle: Hafnium isotope evidence from juvenile rocks through time. Geochimica et Cosmochimica Acta 63, 533–556.
Vervoort, J.D., Patchett, P.J., 1996. Behavior of hafnium and neodymium isotopes in the crust: Constraints from Precambrian crustally-derived granites. Geochimica et Cosmochimica Acta 60 (19), 3717–3733.
Vervoort, J.D., Patchett, P.J., Blichert-Toft, J., Albarede, F., 1999. Relationships between Lu-Hf and Sm-Nd isotopic systems in the global sedimentary system. Earth Planet. Sci. Lett. 168, 79–99.
von Gosen, W., and Paech, H.J., 2001, Structures in the Tertiary sediments of the Forlandsundet Graben, Geologisches Jahrbuch Reihe B, p. 475-506.
Watt, G.R., Kinny, P.D., Friderichsen, J.D., 2000. U-Pb geochronology of Neoproterozoic and Caledonian tectonothermal events in the East Greenland Caledonides. J. Geol. Soc. 157, 1031–1048.
Wiemer, D., Allen, C.M., Murphy, D.T., Kinaev, I., 2017. Effects of thermal annealing and chemical abrasion on ca. 3.5 Ga metamict zircon and evidence for natural reverse discordance: Insights for U-Pb LA-ICP-MS dating. Chem. Geol. 466, 285–302.
Wetherill, G.W., 1956. Discordant uranium-lead ages, I. Eos Trans. Am. Geophys. Union 37, 320–326.
Williams, I.S., 1998, U-Th-Pb geochronology by ion microprobe. In: McKibben, M.A., Shanks IIIW.C., Ridley, W.I. (Eds.), Applications of Microanalytical Techniques to Understanding Mineralizing Processes. Rev. Econ. Geol., v. 7, p. 1–35.
Williams, I.S., Claesson, S., 1987. Isotopic evidence for the Precambrian provenance and Caledonian metamorphism of high grade paragneisses from the Seve Nappes, Scandinavian Caledonides: II ion microprobe zircon U-Th-Pb. Contrib. Mineral. Petrol. 97, 205–217.
Yoshioka, H., Asahara, Y., Tojo, B., Kawakami, S., 2003. Systematic variations in C, O, and Sr isotopes and elemental concentrations in Neoproterozoic carbonates in Namibia: implications for a glacial to interglacial transition. Precambrian Res. 124 (1), 69–85.
Zhang, W., Roberts, D., Pease, V., 2015. Provenance characteristics and regional implications of Neoproterozoic, Timanian-margin successions and a basal Caledonian nappe in northern Norway. Precambrian Res. 268, 153–167.
Zhu, M., Lu, M., Zhang, J., Zhao, F., Li, G., Aihua, Y., Zhao, X., Zhao, M., 2013. Carbon isotope chemostratigraphy and sedimentary facies evolution of the Ediacaran Doushantuo Formation in western Hubei, South China. Precambrian Res. 225, 7–28.
Ziemniak, G., Kośmińska, K., Schneider, D.A., Majka, J., Lorenz, H., McClelland, W.C., Wala, V.T., and Manecki, M., 2019, Defining tectonic boundaries using detrital zircon signatures of Precambrian metasediments from Svalbard's Southwestern Caledonian Basement Province, in Piepjohn, K., Strauss, J.V., Reinhardt, L., and McClelland, W.C. eds., Circum-Arctic Structural Events: Tectonic Evolution of the Arctic Margins and Trans-Arctic Links with Adjacent Orogens: Geological Society of America Special Paper, v. 541.